AD-A019 321

BALLISTIC IMPACT FLASH RESULTING FROM COMPLETE
PROJECTILE PENETRATION OF TITANIUM TARGETS

Joseph G. Aja

Air Force Institute of Technology
Wright-Patterson Air Force Base, Ohio

December 1975

DISTRIBUTED BY:

NTIS

National Technical Information Service
U. S. DEPARTMENT OF COMMERCE

BALLISTIC IMPACT FLASH RESULTING FROM
COMPLETE PROJECTILE PENETRATION
OF TITANIUM TARGETS

Thesis

GAE/MC/75D-1   Joseph G. Aja
                                     Captain USAF

BALLISTIC IMPACT FLASH RESULTING FROM
COMPLETE PROJECTILE PENETRATION
OF TITANIUM TARGETS

Thesis

GAE/MC/75D-1   Joseph G. Aja
                               Captain   USAF

REPORT DOCUMENTATION PAGE		READ INSTRUCTIONS BEFORE COMPLETING FORM
1. REPORT NUMBER GAE/EC/75D-1	2. GOVT ACCESSION NO.	3. RECIPIENT'S CATALOG NUMBER
4. TITLE (and Subtitle) BALLISTIC IMPACT FLASH RESULTING FROM COMPLETE PROJECTILE PENETRATION OF TITANIUM TARGETS		5. TYPE OF REPORT & PERIOD COVERED MS Thesis
		6. PERFORMING ORG. REPORT NUMBER
7. AUTHOR(s) Joseph G. Aja Captain USAF		8. CONTRACT OR GRANT NUMBER(s)
9. PERFORMING ORGANIZATION NAME AND ADDRESS Air Force Institute of Technology (AFIT-EN) Wright-Patterson AFB, Ohio 45433		10. PROGRAM ELEMENT, PROJECT, TASK AREA & WORK UNIT NUMBERS
11. CONTROLLING OFFICE NAME AND ADDRESS Survivability/Vulnerability Branch (PTS) Air Force Flight Dynamics Laboratory Wright-Patterson AFB, Ohio 45433		12. REPORT DATE December 1975
		13. NUMBER OF PAGES 144
14. MONITORING AGENCY NAME & ADDRESS(if different from Controlling Office)		15. SECURITY CLASS. (of this report) Unclassified
		15a. DECLASSIFICATION/DOWNGRADING SCHEDULE

16. DISTRIBUTION STATEMENT (of this Report)

Approved for public release; distribution unlimited

17. DISTRIBUTION STATEMENT (of the abstract entered in Block 20, if different from Report)

18. SUPPLEMENTARY NOTES   Approved for public release; IAW AFR 190-17

Jerry C. Hix, Captain, USAF
Director of Information

19. KEY WORDS (Continue on reverse side if necessary and identify by block number)

Ballistic Impact
Impact Flash
High Velocity Impact

20. ABSTRACT (Continue on reverse side if necessary and identify by block number)

The down range flash resulting from the perforation of thin titanium plates by high velocity steel spheres was investigated to quantify the magnitude and duration of this flash. The titanium flash was compared with the flash resulting from identical spheres impacting aluminum targets. Visually the titanium flash was significantly larger, but measurement of the spectral irradiance at selected wavelengths found the peak intensities were

DD $_{1\ JAN\ 73}^{FORM}$ 1473   EDITION OF 1 NOV 65 IS OBSOLETE

approximately the same.   The duration time of the titanium flash
was approximately five times as long as the aluminum flash.   The
flash was found to occur as two events, each of which had distinct
flash intensity maxima.   The first maxima occured approximately
10 microseconds after penetration, while the second occured 30 to
80 microseconds later.   Coating the impact surface of the titanium
target with either white polyurethane paint, white barium titanate
silicone paint, or white flurocarbon paint reduced the down range
flash only a small amount.   The flash spectral irradiance was
compared to a blackbody temperature curve.   The titanium flash
was found to radiate approximately as a blackbody source, with the
temperature varing from 2400 to 4000°K over a velocity range of
3000 to 5000 fps.

BALLISTIC IMPACT FLASH RESULTING FROM

COMPLETE PROJECTILE PENETRATION

OF TITANIUM TARGETS

THESIS

Presented to the Faculty of the School of Engineering

of the Air Force Institute of Technology

Air University

in Partial Fulfillment of the

Requirements for the Degree of

Master of Science

by

Joseph G. Aja, BSME

Captain   USAF

Graduate Aeronautical Engineering

December 1975

Approved for public release; distribution unlimited.

Preface

This report is the results of my attempt to expand the knowledge available in the area of ballistic impact flash. My principal concern has been in quantifying ballistic impact flash resulting from steel spheres perforating 6Al-4V titanium targets and in evaluating state-of-the-art coating materials for their effectiveness in reducing this flash.

Contents

List of Figures

List of Tables

xi

Abstract

The down range flash resulting from the perforation of thin titanium plates by high velocity steel spheres was investigated to quantify the magnitude and duration of this flash. For analysis, the titanium flash was compared with the flash resulting from identical steel spheres impacting aluminum targets. Visually the titanium flash was significantly larger than the aluminum flash but measurement of the spectral irradiance at selected wavelengths found the peak intensities were approximately the same. Analysis of the time histories of the two flashes showed that duration time of the titanium flash was approximately five times as long as the aluminum flash. The flash was found to occur as two events, each of which had distinct flash intensity maxima. The first maxima occurred approximately 10 microseconds after penetration, while the second occurred 30 to 80 microseconds later. Both the spectral irradiance of the two maxima and the total flash energy for titanium scaled as approximately the eighth power of the velocity while aluminum scaled as approximately the fifth power of the velocity. Coating the impact surface of the target with either white polyurethane paint, white barium titanate silicone paint, or white flurocarbon paint reduced the down range flash by only a small amount. The flash spectral irradiance for both metals was compared to a blackbody

temperature curve. Both flashes were found to radiate approximately as blackbody sources with the aluminum flash temperature increasing from 2800 to 3500° K over an impact velocity range of 3500 to 5000 fps while the titanium temperature varied from 2400 to 4000° K over a velocity range of 3000 to 5000 fps.

BALLISTIC IMPACT FLASH RESULTING FROM
COMPLETE PROJECTILE PENETRATION
OF TITANIUM TARGETS

I. Introduction

Current combat aircraft incorporate sophisticated electronic systems which aid in the penetration of target defenses. Once its presence has been detected, the aircraft uses its size and speed and tactics to evade the armament directed at it. Even with these evasion factors working for it, the probability of the aircraft taking a hit still remains. The projectile may cause minor damage to the aircraft but at the instant of impact an intense, short duration flash of radiation is generated. When produced in a combustible atmosphere, this flash could lead to fire, explosive detonation, and possible loss of the aircraft.

This ballistic impact flash is a threat to aircraft in combat and is a major concern of weapon systems designers from both an offensive and defensive point of view. Extensive research has been conducted to find means of suppressing fuel tank fires, but very little research has been published in the area of impact flash suppression. A literature search revealed only two published studies of impact flash reduction. The first study, published in 1952, evaluated several state-of-the-art coating materials (Ref 1).

Because of a restriction in time, the second study, published in 1974, evaluated only two state-of-the-art coatings (Ref 2). Both studies found that coating the impact surface reduced the flash at the point of penetration completion. This literature search also revealed that the studies of ballistic impact flash and flash suppression evaluated primarily aluminum targets.

However, current aircraft designs, such as the B-1 bomber, require high strength, low weight materials such as 6A1-4V titanium. Rockwell International, the prime contractor for the B-1, has conducted extensive evaluations of the vulnerability of the materials used in the construction of the B-1. Results of their fragment penetration test indicated that titanium did not produce a hot, incandescent spall as observed with aluminum targets and that the flash duration of aluminum was longer (Ref 3:19). The Air Force Flight Dynamics Laboratory conducted tests which took a "very quick look" at the ballistic impact flash resulting from perforation of titanium targets (Ref 4). The results of these tests were contradictory to those found by Rockwell International.

Because of the disagreement in reports on the impact flash resulting from penetration of titanium and the need for evaluation of state-of-the-art coatings, this investigation had two objectives. First, the duration and magnitude of the ballistic impact flash resulting from projectiles impacting and perforating titanium targets were investigated.

Second, three state-of-the-art coating materials will be evaluated for their effectiveness in flash suppression.

Background

The phenomenon of ballistic impact flash received little study until early in the United States space program. At that time, impact flash was studied as a means for detecting and quantifying meteoroid impacts on space vehicles. The encounter between an earth satellite and a meteoroid in space takes the form of a hypervelocity impact with the meteoroid serving as the projectile and the satellite as the target. The impact velocity may range from nearly zero up to 85 km/sec, depending upon the relative orbit of the satellite and the meteoroid. The size range of the particle is also particularly broad, with the smallest of them being approximately a micron in size. Early studies of the phenomenon of ballistic impact flash were confined to micron sized particles accelerated by electrostatic hypervelocity accelerators to velocities up to 16 km/sec (Ref 5:595). It was assumed that the flash was the result of electrically charged particles emitted from the site of impact. The experiments utilized biased collectors to collect the emitted charge. The resulting data fitted the empirical relationship

$$Q_c = KE_p(V/A) \tag{1}$$

where Q_c is the charge collected, K a constant, E_p the

3

particle energy, A the atomic weight of the particle
material, and V the particle velocity (Ref 5:592). This
gave the first indication that impact flash was dependent
upon material properties and impact velocity.

Larger mass projectiles were fired from guns at
velocities of 0.5 to 2.5 km/sec. Jean (Ref 6) recorded
and analyzed the impact with high speed photography. He
observed that the flash was actually a rapidly expanding
ring of light. Further tests were conducted by Jean and
Rollins (Ref 7) with the addition of photomultiplier tubes
and open shutter cameras to the test instrumentation. Their
analysis of the data indicates that the flash occured in two
pulses. An initial pulse, called a spike, had a half width
of one μsec or smaller and a rise time of less than 0.2 μsec.
The time integrated spectra of this pulse showed an associa-
tion with continuum radiation and with high density, strongly
ionized radiating gas at the point of impact. The second
event was a slow-rising pulse of three to five μsec half
width and spectrosopically characterized by line emissions
of neutral atoms. It was shown that the measured character-
istics of the first event could be related empirically to
the size and the velocity of the impacting projectile.

While the analysis of the impact flash was being
conducted, more accurate methods of meteoroid detection and
quantification were developed, and the impact flash programs
received less attention. However, the program did show that
spectral analysis of flash using photomultiplier tubes and

optical analysis using still and high speed cameras indica-
ted that the flash occurred in two phases and was dependent
on projectile and target properties.

Threat to Combat Aircraft. The experimental evaluation
of impact flash as a threat to combat aircraft was similar
to the meteoroid detection experiments. The threat was
simulated by propelling 1.3 cm projectiles at velocities
up to 1.7 km/sec at sections of aircraft skin. Spectral and
optical analysis were made of the flash at the point of
projectile penetration. The results of Abernathy's work
(Ref 8:32) found that the flash had a temperature of $3400^{\circ}K$
to $4100^{\circ}K$ and a duration of between three and five milli-
seconds. This temperature and duration are significantly
above the spontaneous ignition temperature of current air-
craft fuels (Ref 9:3).

Follow on work by Mansur (Ref 2) and Wingfield (Ref 10)
further verified the magnitude of the threat and also
observed that the exit flash occurred in two events,
similar to Jean's observations (Ref 7:1747). They also
presented an empirical relationship

$$X = KV^n \qquad (2)$$

where X is the intensity of the flash, K is a scaling
constant, V is the projectile velocity, and n is an
empirical parameter which establishes the magnitude of the

5

flash intensity as a function of the relative impact velocity (Ref 2:13).

Mansur and Abernathy also developed physical models of the impact flash process. An extensive physical model of the impact and impact flash process was also found in the work of Wiederhorn and Ehrenfeld (Ref 11:64). The overall physical model of ballistic impact flash can be divided into three phases. At impact, energy is transferred to the target and material is removed from the target in the rupture phase. Next, because of their high velocities, the fragments are heated and their surfaces begin to melt and flow during the ablation phase. Finally, the exposed surface area and oxygen from the atmosphere combine chemically resulting in the burning phase. This physical model was employed by Abernathy, Mansur, and Wingfield in their investigations of the threat of ballistic impact flash to aircraft fuel systems.

Presently there are two basic positions for placement of internal fuel tanks in combat aircraft. They are either buried in the aircraft as shown in Figure 1(a), or they are close to the surface or part of the aircraft's skin as shown in Figure 1(b). As explained in Murrow's evaluation of aircraft fuel subsystems (Ref 9:ii), impact flash is likely to produce a fire in the empty compartments (void areas) adjacent to fuel tanks or in the ullage space of the fuel tank (space above the fuel surface). He also noted that impact flash does not guarantee a fire on impact, but stated

6

(a)

(b)
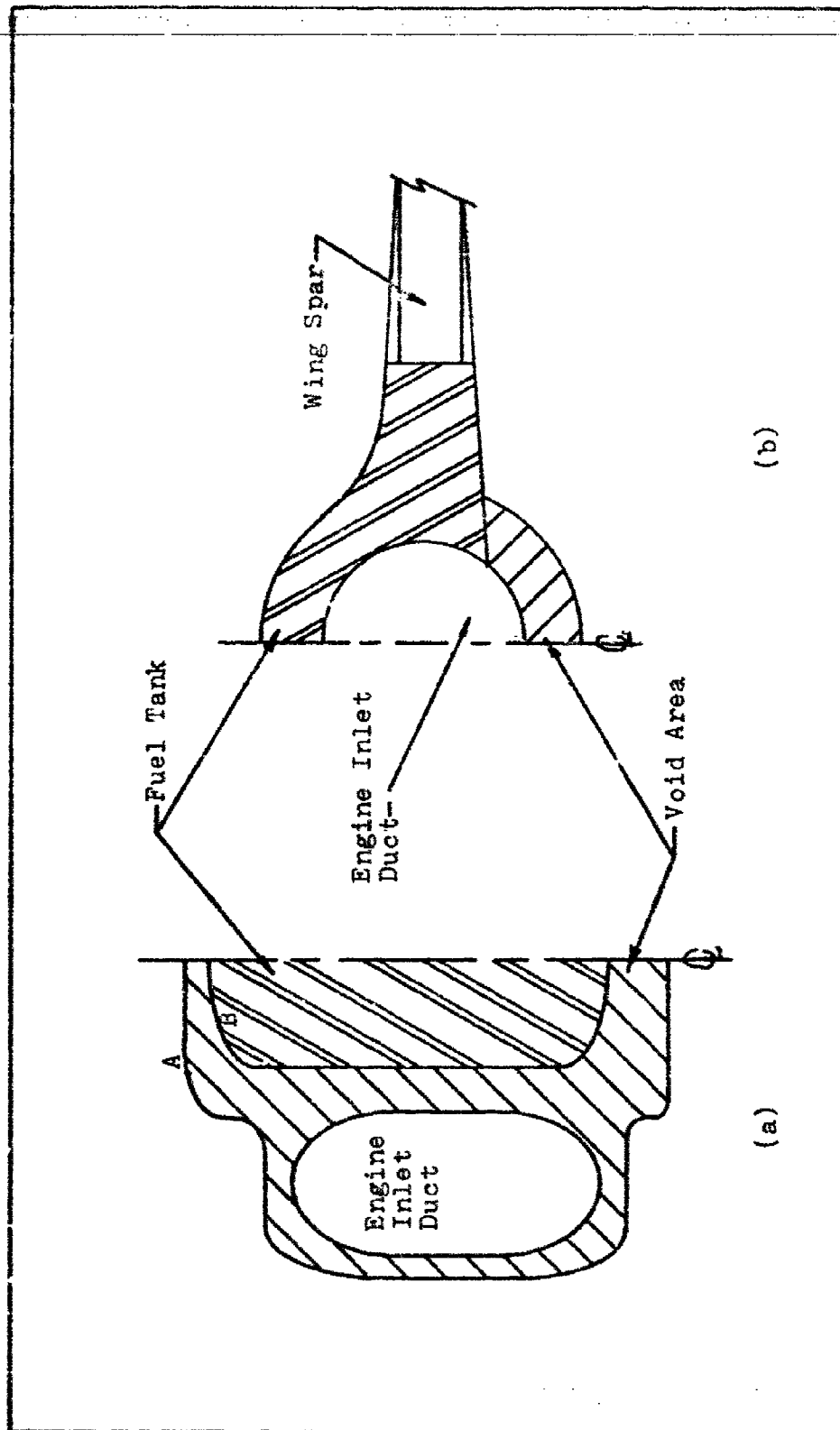
Figure 1. Typical Fuel Tank Positions In Current Aircraft

that the probability of fire is a function of several variables, specifically projectile size, type and impact velocity, and the distance from the skin penetration to fuel tank penetration in the case of void area fires.

Referring to Figure 1(a), a projectile impact at point A on the skin of the aircraft would produce a flash which would not be a threat as a fire ignition source because it is in the free air stream where no fuel vapors are present. However, when the projectile perforates the skin at point A, there will be a flash in the void area. If combustible vapors are present in this area, a fire could start provided the flash was of sufficient duration and intensity to ignite the vapors. As the projectile strikes point B, a flash will occur on the fuel tank surface and will provide an additional ignition source in the void area. When the projectile per-forates the fuel tank, a flash would occur. If the penetra-tion were above the surface of the fuel, the flash could ignite the vapors in the ullage. In the fuel tank, the height of projectile penetration above the fuel surface is also a significant factor (Ref 9:ii). As the projectile passed through the fuel tank and out the other side of the aircraft, one more source of ignition in the ullage and two more in the void area would be generated.

Extensive research has been conducted to find means of containing and suppressing a fire in the fuel tank ullage area. The most effective method for suppression of fuel tank fire and fuel tank vapor explosion is the addition of

8

a polyurethane foam to the fuel tank (Ref 12:5). However, work in the area of ballistic impact flash suppression has been minimal. In 1952, R. L. Kahler (Ref 1) conducted experiments with magnesium alloy and aluminum alloy targets. The targets were coated with state-of-the-art coating materials and the impact flash from projectile perforation was observed. Of all the coating materials tested by Kahler, a 0.050" coating of neopreme sponge and cork was the most effective in reducing, but not eliminating, the flash. A form of this neopreme coating is currently used on B-52 aircraft to reduce thermal flash effects (Ref 13:3). The other published work in flash suppression is by Mansur (Ref 2). He evaluated only two coatings, epoxy based aircraft paint and aircraft fuel cell sealant. Although not comprehensive, his test did indicate that both materials significantly reduced the downstream flash.

Test Material Selection. For this study, 6A1-4V titanium was selected for evaluation because of its use in structural members and surface areas in the void area surrounding the fuel system in the F-15 aircraft and its use as a fuel tank and aircraft skin material in the B-1. After the extent of the threat from impact flash initiated fires had been established, three state-of-the-art coating materials were evaluated for their effectiveness in reducing the intensity and duration of the impact flash.

The first coating evaluated is a white polyurethane aircraft paint. Currently as aircraft receive depot level maintenance, they receive a new coat of this paint. It was selected for evaluation to measure the effectiveness of current inventory paint coatings in reducing impact flash. The second coating evaluated is a barium titanate silicone aircraft paint. This paint is currently under development as an infrared and thermal camouflage coating (Ref 14). It was selected for this test because of its thermal flash resistance and high heat capacity. The final coating material selected for evaluation is a white flurocarbon paint, which is currently being evaluated for its rain erosion protection properties (Ref 15). Rain hitting an aircraft traveling at subsonic speeds reacts in a manner similar to a projectile hitting a target. The purpose of this coating is to break up the rain droplets and dissipate the energy of the impact. This coating was selected for this test because of this energy dissipation property. The targets were impacted with the coated surfaces up and downstream, so that all phases of aircraft penetration could be evaluated.

II. Experimental Method

Steel spheres were fired from a 20 mm smooth bore gun through a velocity measuring system and through test targets as shown in Figure 2. For this report, all directional references are relative to the target. Up range refers to the impact side where the gun was positioned and down range refers to the area behind the target. The targets were one foot squares of 0.070 inch thick 6Al-4V titanium and one foot squares of 0.072 inch thick 2024 T-3 aluminum. Six of the titanium targets were coated on one side with one of the test paints, two were coated with the white polyurethane paint, two with barium titanite silicone paint, and two with flurocarbon paint. The pairs of coated titanium targets were tested in two series; one series with the coating facing up range and one series with the coating facing down range. The target area was screened so that the front face flash and gun muzzle flash were not visible down range. As shown in Figure 3, the back face flash was observed by an impact flash spectrometer and the signal output from the spectrometer was displayed on dual beam oscilloscopes. The back face flash was also recorded by a still camera and an image converter camera.

Projectile

Steel spheres were used as projectiles to reduce the variables as much as possible. Primarily, the steel should

Target

Oscilloscope
Trigger Screen

Light
Barrier

Velocity Screens

Sabot Deflector

20 mm Smooth Bore Gun

Not to Scale
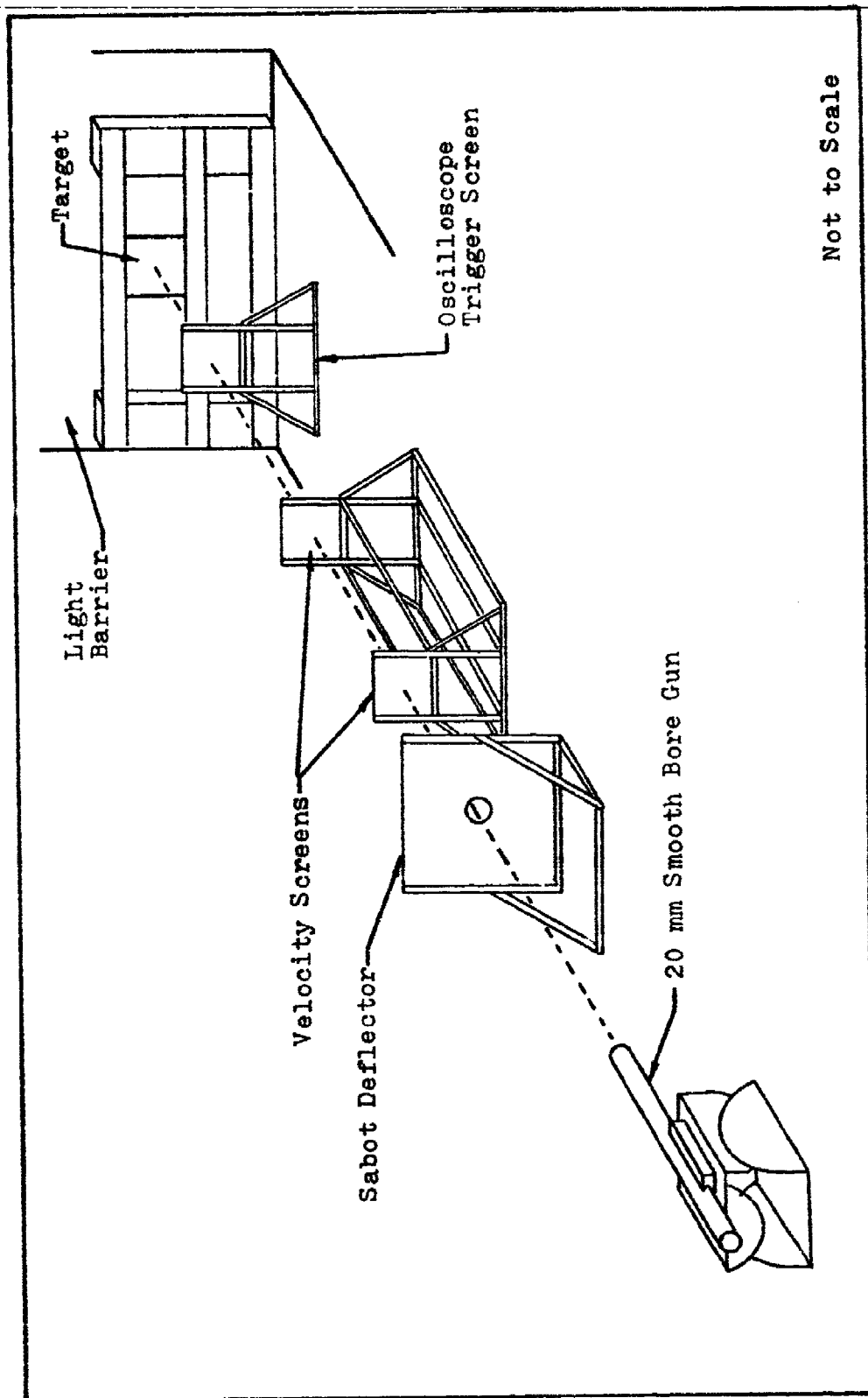
Figure 2. Up Range Test Instrumentation

12
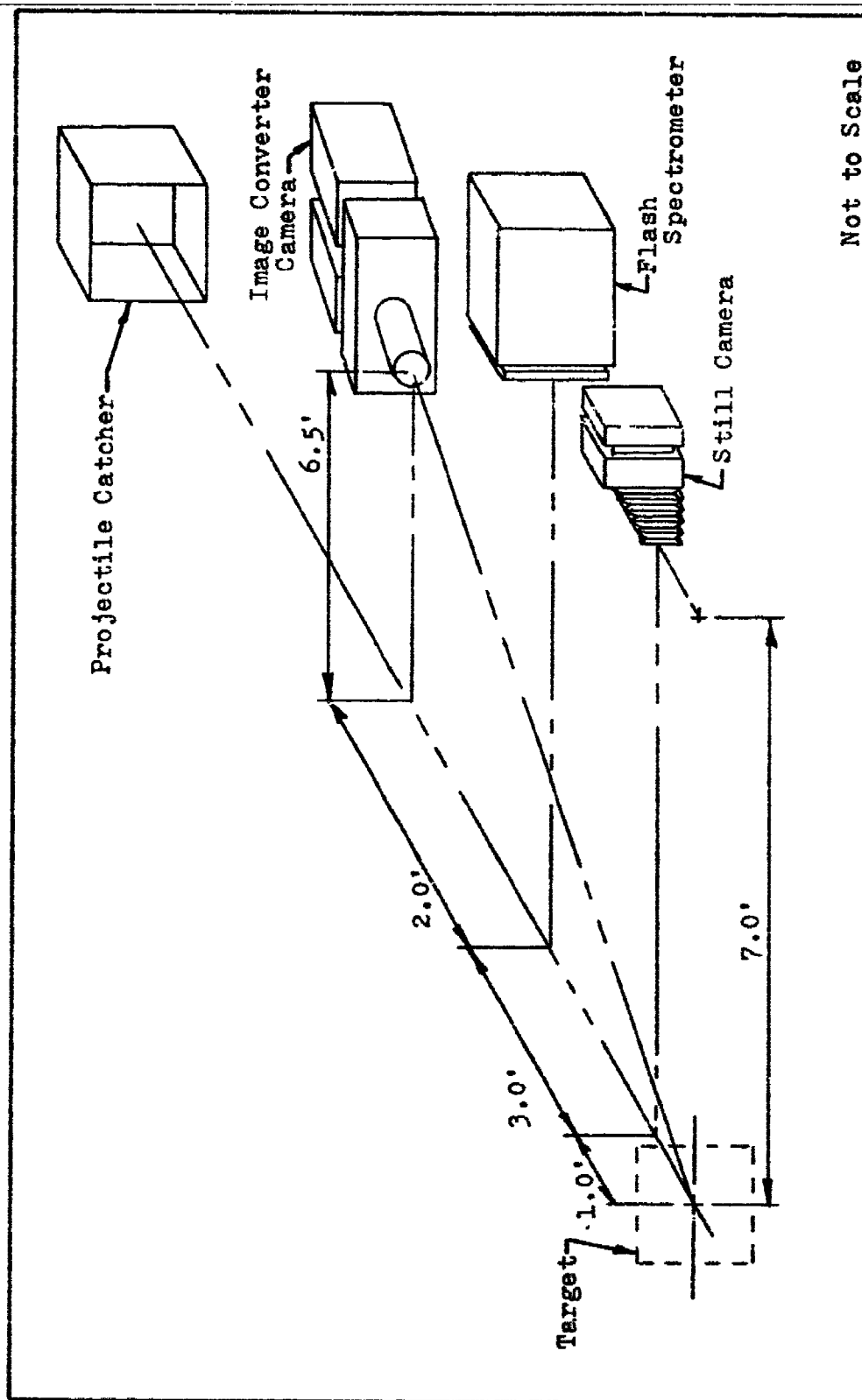
Figure 3. Down Range Test Instrumentation

Projectile Catcher

Image Converter Camera

Flash Spectrometer

Still Camera

Target

6.5'

2.0'

3.0'

1.0'

7.0'

Not to Scale

sustain a minimum of deformation and have a minimum of chemical reaction with the target materials. Also the spherical shape eliminates any concern for small angles of obliquity and position at impact. The projectiles had a diameter of 0.656 inches and weighed 291.7 grains. The spheres were fired from the gun in four section Lexan sabots.

The sabot sections were designed to separate from the projectile upon leaving the gun's eight foot barrel and were deflected from the projectiles path by a sheet of armor plate. This sabot deflector was positioned 18 feet from the gun muzzle and had a three inch diameter hole which allowed the projectile to pass through. The projectile's velocity was varied from approximately 2000 feet per second to approximately 5500 feet per second. The velocities were obtained by varying the amount of powder loaded in the cartridges. The lightest powder load was 70 grains of Hercules 2400 smokeless rifle powder while the maximum load used during this test was 470 grains of the same powder.

Spectrometer

The down range flash was observed by the flash spectrometer. The spectrometer consisted of three photomultipliers which were in line with narrow band by-pass filters. Each filter investigated a distinct area of the visible and near infrared spectrum. The first filter centered at 4008A with a bandwidth of 200A; the second centered at 7010A with a bandwidth of 200A; and the third centered at 9025A with a

bandwidth of 290Å. A standard light source, whose output is known at each wavelength in watts/m^2-nanometer, was used to calibrate the photomultiplier tubes.

The output of the photomultiplier tubes was displayed as a single sweep of dual beam oscilloscopes. The oscilloscopes were triggered prior to impact and the sweep rate was adjusted to allow observation of the entire event. The oscilloscope traces were recorded on Polaroid film for later examination and measurement.

A limitation of photomultiplier tubes is that they are easily saturated. To prevent this from happening, neutral density filters were placed in front of the narrow band by-pass filters. The strength of the filters was increased as the flash intensity increased. These filters were calibrated against the standard light source to determine the amount of light they passed at the three wavelengths.

Still Camera

A 4 x 5 Speed Graphic Camera was positioned perpendicular to the flash line as shown in Figure 3. It was used to record an image of the total flash. The shutter was opened just prior to the shot, and closed after the shot. The image was recorded on Polaroid film.

Image Converter Camera

An image of the down range flash was also recorded by a two camera image converter camera system. The delay circuits which trigger the second camera in this system did not work

properly during this test. However, the camera was positioned as shown in Figure 3, and used as a still camera to give a different view of the flash. As with the still camera, the shutter was opened just prior to the shot, closed after the shot, and the image recorded on Polaroid film.

III. Results and Discussion

Aluminum and Titanium Ballistic Impact Flash

The first objective of this report was to quantify the
magnitude of the ballistic impact flash resulting from a
projectile completely penetrating a titanium target. The
reference base for comparison was data collected in previous
tests conducted on aluminum targets. To validate this data,
11 test shots were fired at aluminum targets on this program.
The down range flash which resulted from a 0.656 inch
diameter steel sphere penetrating a 0.072 inch thick sheet
of 2024 T-3 aluminum is shown in Figure 4. The flash is
approximately 16 inches long and 2.4 inches in diameter,
which is similar to the findings of Mansur (Ref 2:37) and
Abernathy (Ref 8:32). Figure 5 shows the down range flash
which resulted from an identical steel sphere perforating a
0.070 inch thick sheet of 6A1-4V titanium. The camera
position, shutter speed and aperture setting were identical
for the two figures. Also in both photos, measurements can
be made at the scale of one inch equals one foot. Using
this scale, the central fire ball resulting from the steel-
titanium impact is approximately 30 inches long and 16
inches in diameter, with streamers of hot incandescent
particles traveling further down range.

First impressions from these photos would indicate that
the magnitude of the titanium flash is significantly larger
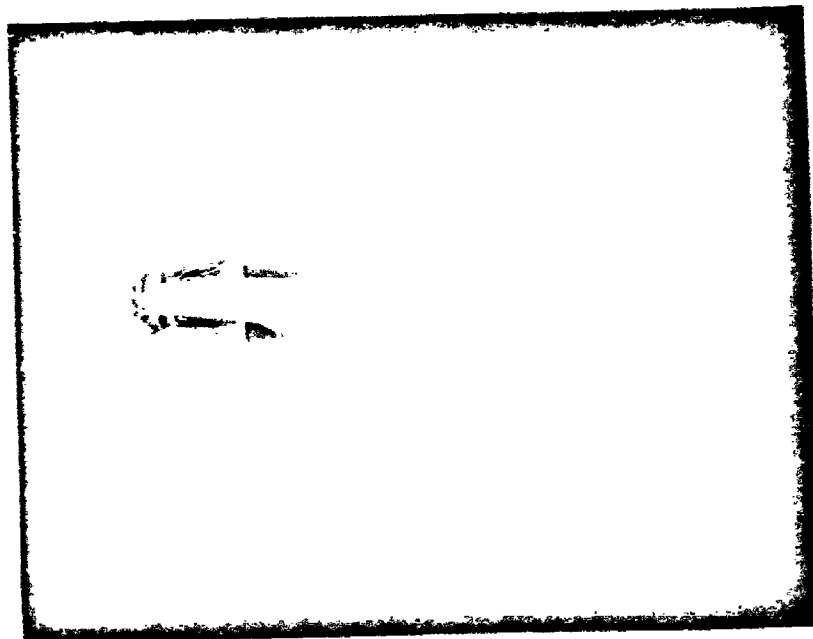
Figure 4.   Down Range Flash Resulting From a
            Steel Sphere (0.656" Dia) Traveling
            at 5465 fps Impacting a 2024 T-3
            Aluminum Target (0.072" Thick)
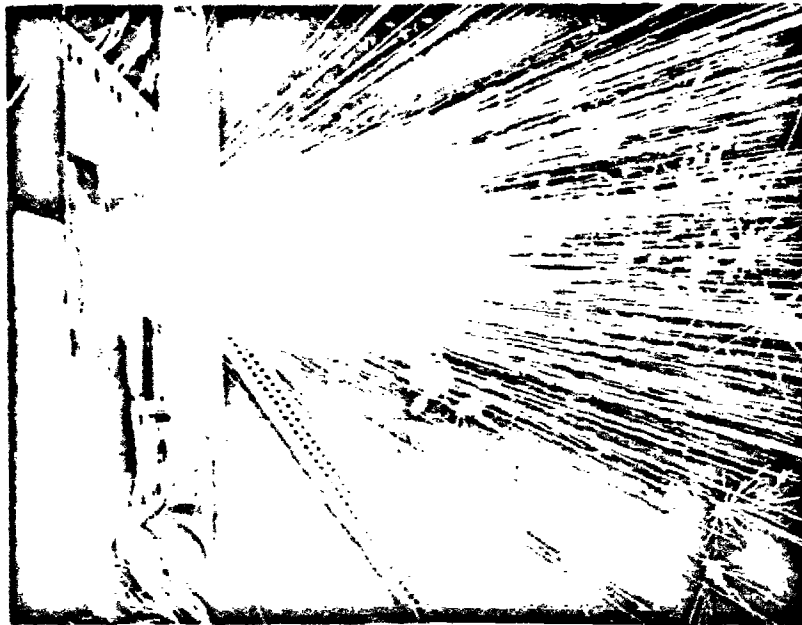
Figure 5.   Down Range Flash Resulting From a
Steel Sphere (0.656" Dia) Traveling
at 5580 fps Impacting a 6Al-4V
Titanium Target (0.070" Thick)

19

than that observed in aluminum. However, analysis of the
oscilloscope traces at selected wavelengths showed that the
peak spectral irradiance was about the same for titanium
and aluminum. A drawing of typical traces for titanium and
aluminum with identical oscilloscope amplitude and sweep
rate settings is shown in Figure 6. Each target displayed
a fast rise to a first maxima, followed by a rapid decrease
in voltage and then a slower rise to a second maxima and a
gradual return to zero voltage. The voltage readings were
converted to spectral irradiance values and plotted for each
of the maxima and wavelength combinations in Figures 7
through 12.

Figures 9 through 12 show that the spectral irradiance
for titanium and aluminum are relatively the same over the
velocity range tested and that the intensity of irradiance
is slightly larger for titanium at higher velocities.
However, Figures 7 and 8 clearly show that the aluminum
spectral irradiance is larger than that of titanium for the
4008A wavelength region of this test. In his analysis of
impact flash, Jean (Ref 7) modeled the first maxima as an
electron flash and the second maxima as irradiance from
neutral atoms. Investigation of the Table of Spectral Lines
of Neutral and Ionized Atoms (Ref 16) and the M.I.T. Wave-
length Tables (Ref 17) revealed that aluminum has a larger
density of neutral and ionized atoms with high intensities
in the 4008A region than titanium which is the probable

20
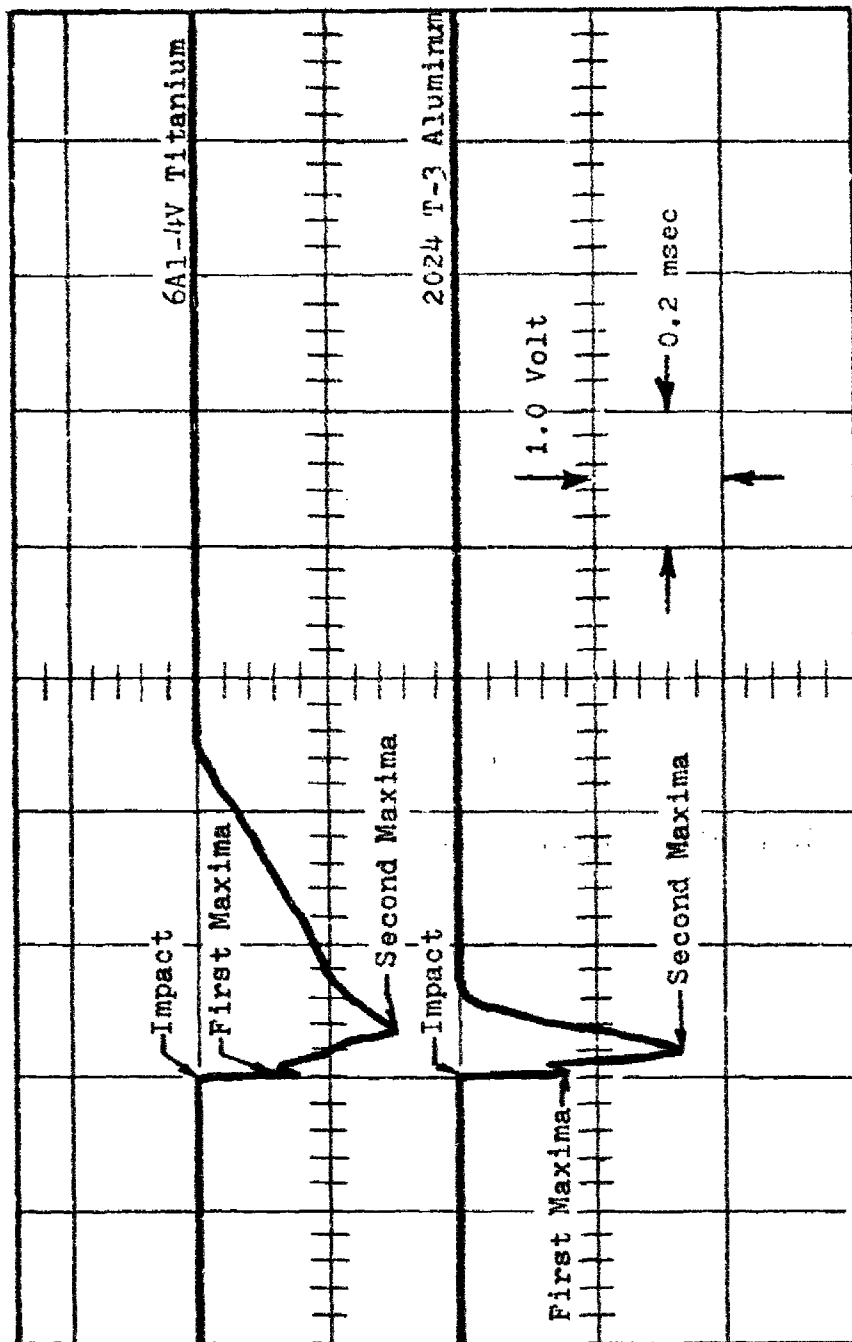
Figure 6. Typical Oscilloscope Traces From Photomultiplier Tubes
Observing Steel Impacts on Titanium and Aluminum Targets

Figure 7. First Maxima of Spectral Irradiance at 4006A as a Function of Velocity

Figure 8.   Second Maxima of Spectral Irradiance
at 4008A as a Function of Velocity

Figure 9. First Maxima of Spectral Irradiance
at 7010A as a Function of Velocity

24

Figure 10. Second Maxima of Spectral Irradiance
at 7010A as a Function of Velocity

Figure 11. First Maxima of Spectral Irradiance at 9025A as a Function of Velocity

Figure 12. Second Maxima of Spectral Irradiance at 9025A as a Function of Velocity

reason for aluminum having a higher intensity of spectral irradiance at this wavelength.

Referring to Figure 6, the difference between the two traces which could account for the difference in observed flash is the duration time of each flash. Table I lists duration times for aluminum and titanium at various velocities. The titanium flash lasts approximately five times as long as the aluminum flash. Integration of the area under the traces gives an indication of the energy released in the form of light as a result of the impact. Figure 13 shows that at 4008A, even though the duration was longer, the flash energy was about the same over the test velocity range. This was the result of titanium having a lower intensity of spectral irradiance and longer duration time. Figure 14 for 7010A and Figure 15 for 9025A indicate that the flash energy for titanium is significantly higher than aluminum as was predicted by Figures 4 and 5. It should be noted that because of difficulties in clearly separating the area under the first maxima from the second maxima, all energy calculations were based on the total area under both curves.

The Bunsen-Roscoe Law states that when the human eye views an event such as a flash, a summing of luminances occurs over a short duration of time (Ref 18:326). This temporal integration last up to approximately 100 msec, thus even though the flash from titanium and aluminum targets have relatively the same intensity, the eye "sees"

28

Table I

Time Duration of Flash

2024 T-3 Aluminum		6A1-4V Titanium	
Velocity (FPS)	Average Duration Time (milliseconds)	Velocity (FPS)	Average Duration Time (milliseconds)
2108.2	0.08	1971.4	0.04
2536.5	0.08	2073.7	0.03
2612.7	0.07	2320.2	0.08
2911.2	0.11	2466.1	0.08
2943.3	0.10	2548.0	0.33
3424.6	0.08	2564.7	0.28
3514.9	0.10	2801.1	0.89
3944.8	0.10	2954.2	0.59
4104.1	0.08	2956.3	0.68
4938.3	0.10	3246.8	0.58
5464.5	0.11	3439.4	0.60
		3508.8	0.72
		3707.1	0.48
		3714.0	0.55
		3964.3	0.52
		4000.0	0.63
		4153.7	0.56
		4454.3	0.58
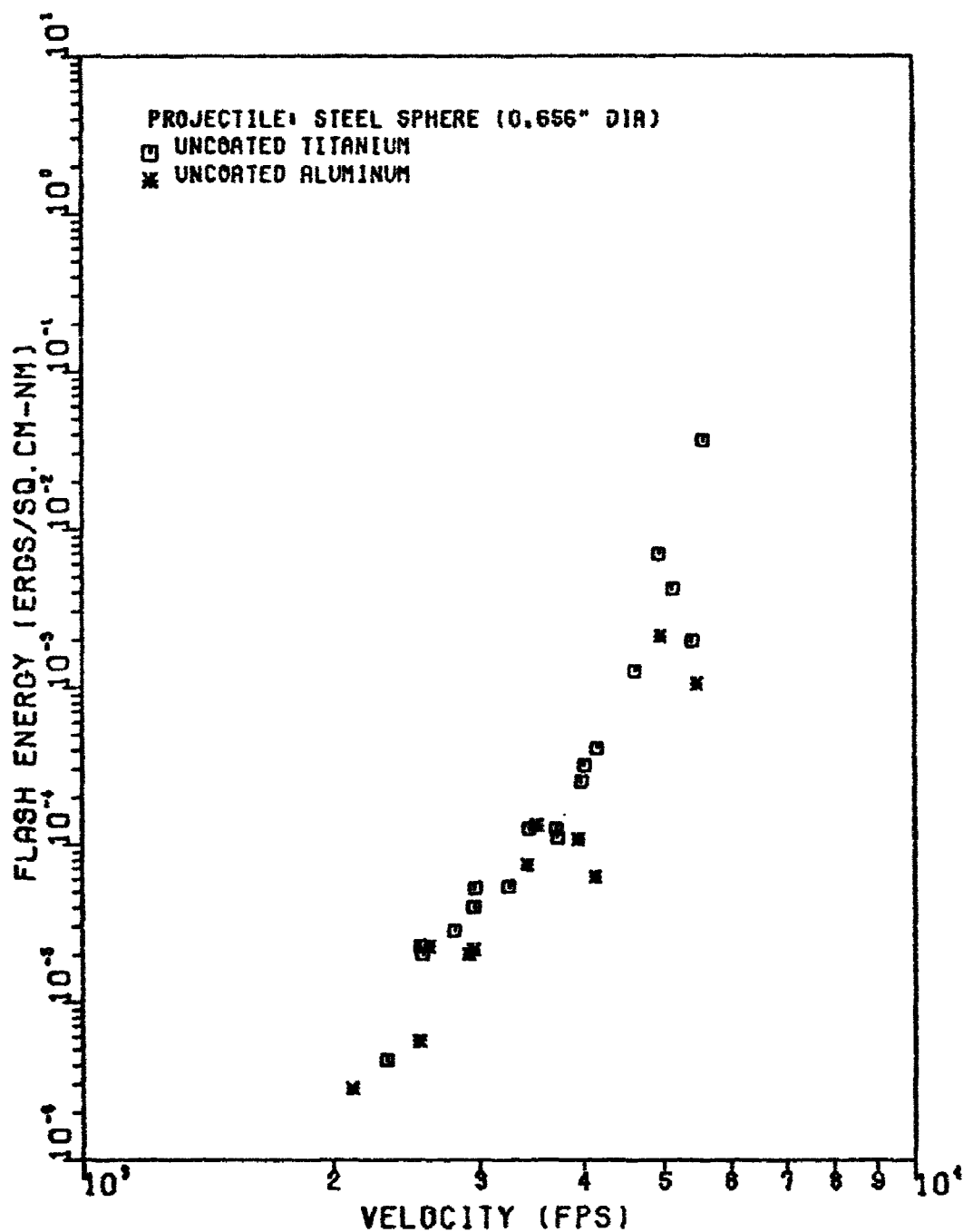
Figure 13. Total Energy at 4008A as a Function of Velocity

Figure 14. Total Energy at 7010A as a
            Function of Velocity

31
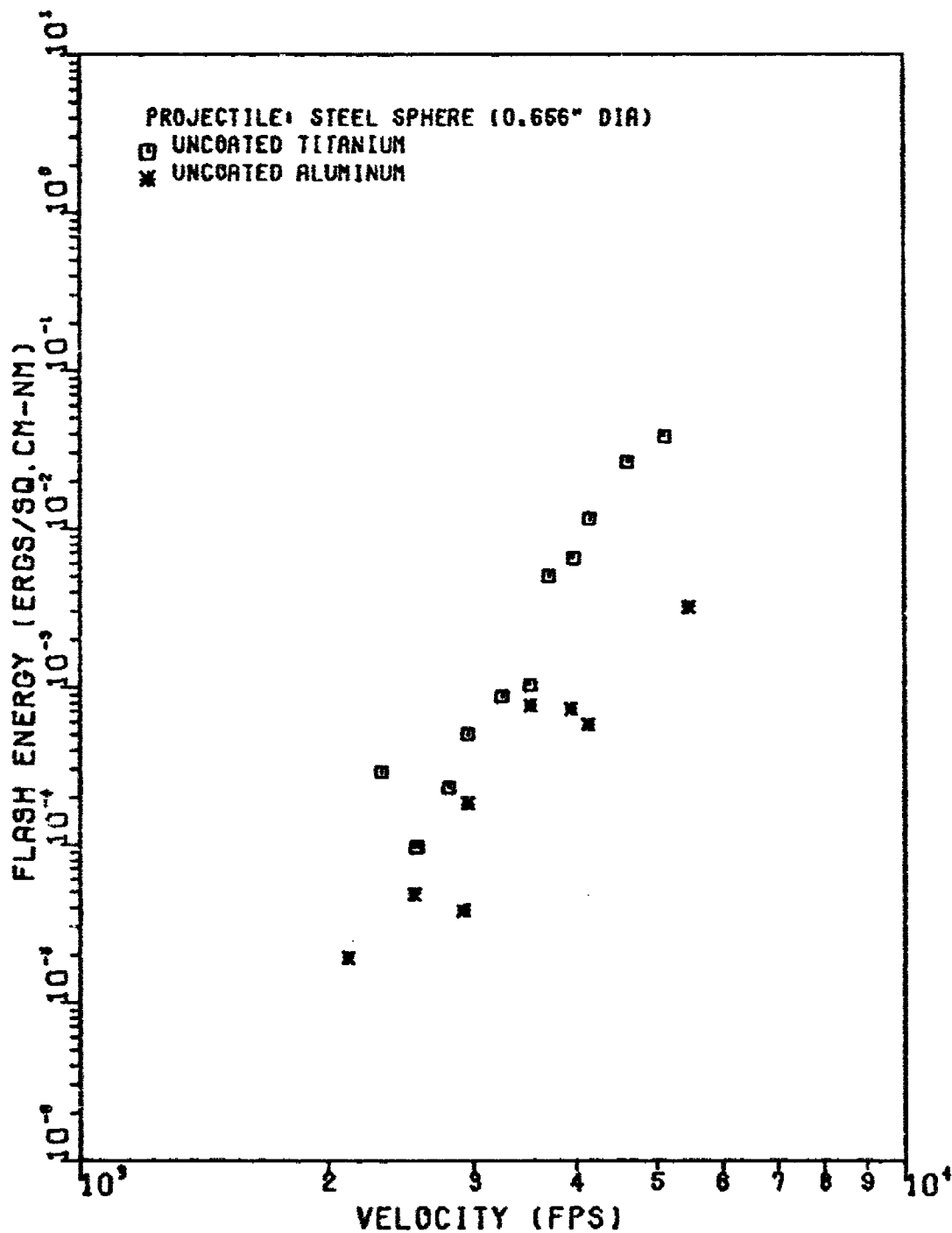
Figure 15. Total Energy at 9025A as a
            Function of Velocity

energy which was found to be of greater magnitude for titanium and sees a "brighter" flash for titanium.

Effect of Test Coatings on Flash Reduction

The second objective of this report was to evaluate state-of-the-art coatings for their effectiveness in reducing the magnitude of ballistic impact flash. Figures 16 through 21 present the first and second maxima of spectral irradiance at the three test wavelengths for titanium targets with a coating on the up range side. Comparison of Figures 16, 18, and 20 show that all three coatings had a negligible effect on the first flash maxima. Comparison of Figures 17, 19, and 21 show that all three coatings reduced the second maxima of spectral irradiance by a small amount. Because of the size of the reduction and the scatter of the data points, a quantitative value for this reduction was not determined. Analysis of the flash energy (Figures 22 through 24) further verifies that coating the up range side of the target reduces the down range flash by only a small amount.

For comparison, targets were impacted with the coated surface down stream. Figures 25 through 30 are plots of the spectral irradiance while Figures 31 through 33 are plots of the flash energy at various wavelengths. In his study, Mansur (Ref 2:34) conducted only a few tests with the coated surface down range and these tests indicated the flash reduction effect of the coating was substantially less than

33

PROJECTILE: STEEL SPHERE (0.656" DIA)
- UNCOATED TITANIUM
- ▲ TI COATED WITH POLYURETHANE PAINT
- ◆ TI COATED WITH BARIUM TITANATE PAINT
- ✱ TI COATED WITH FLUROCARBON PAINT
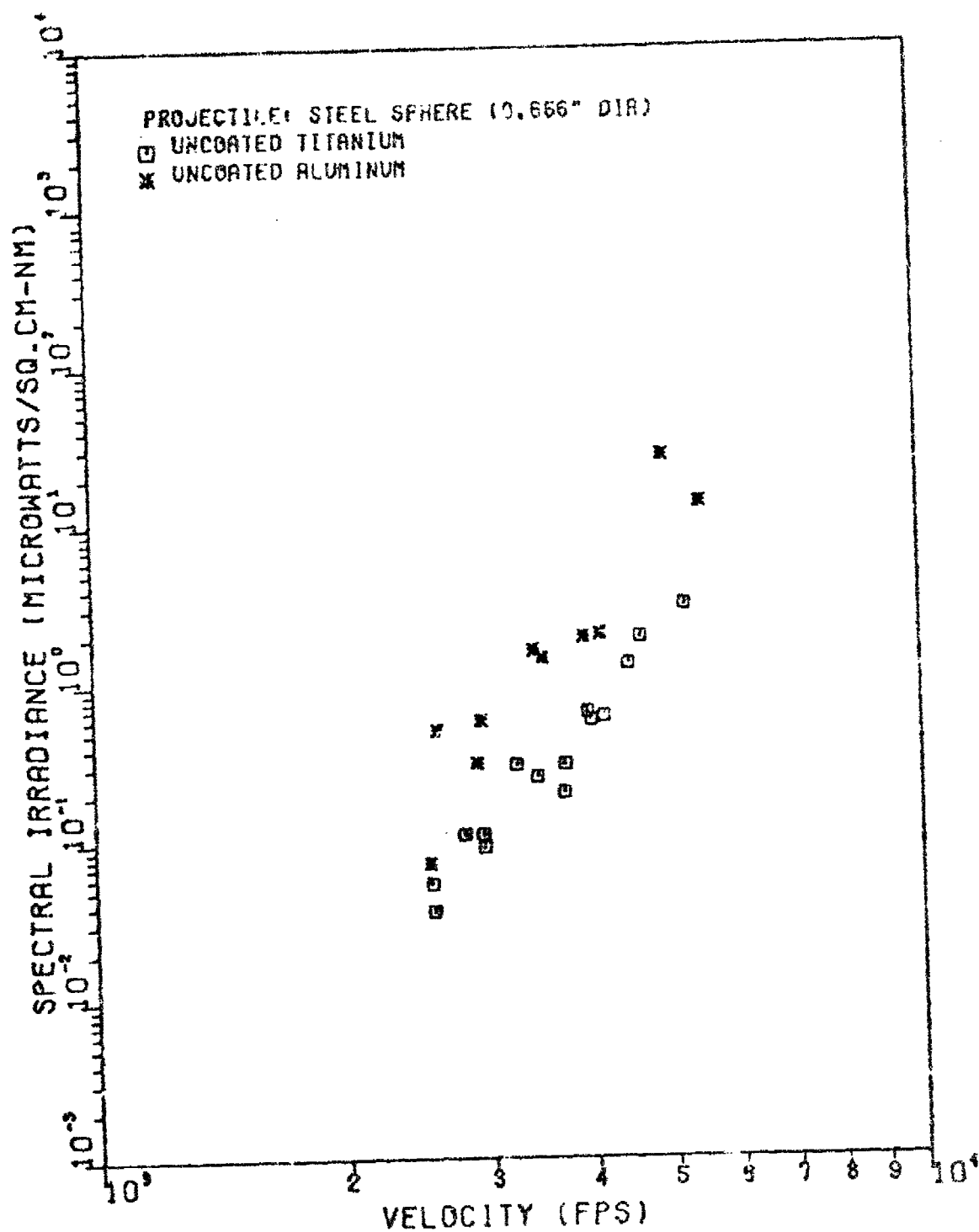 (COATING ON UP RANGE SIDE)
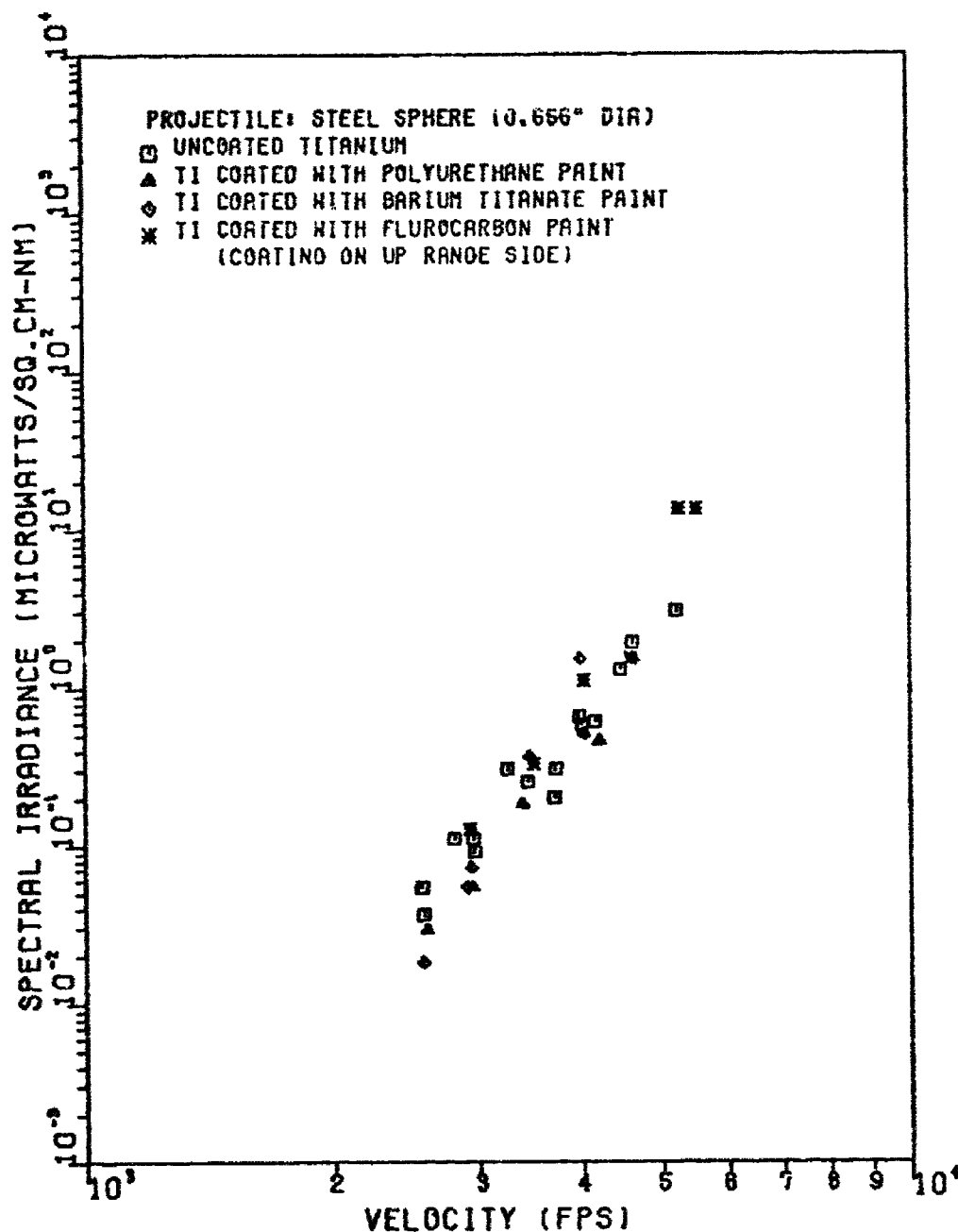
Figure 16. First Maxima of Spectral Irradiance
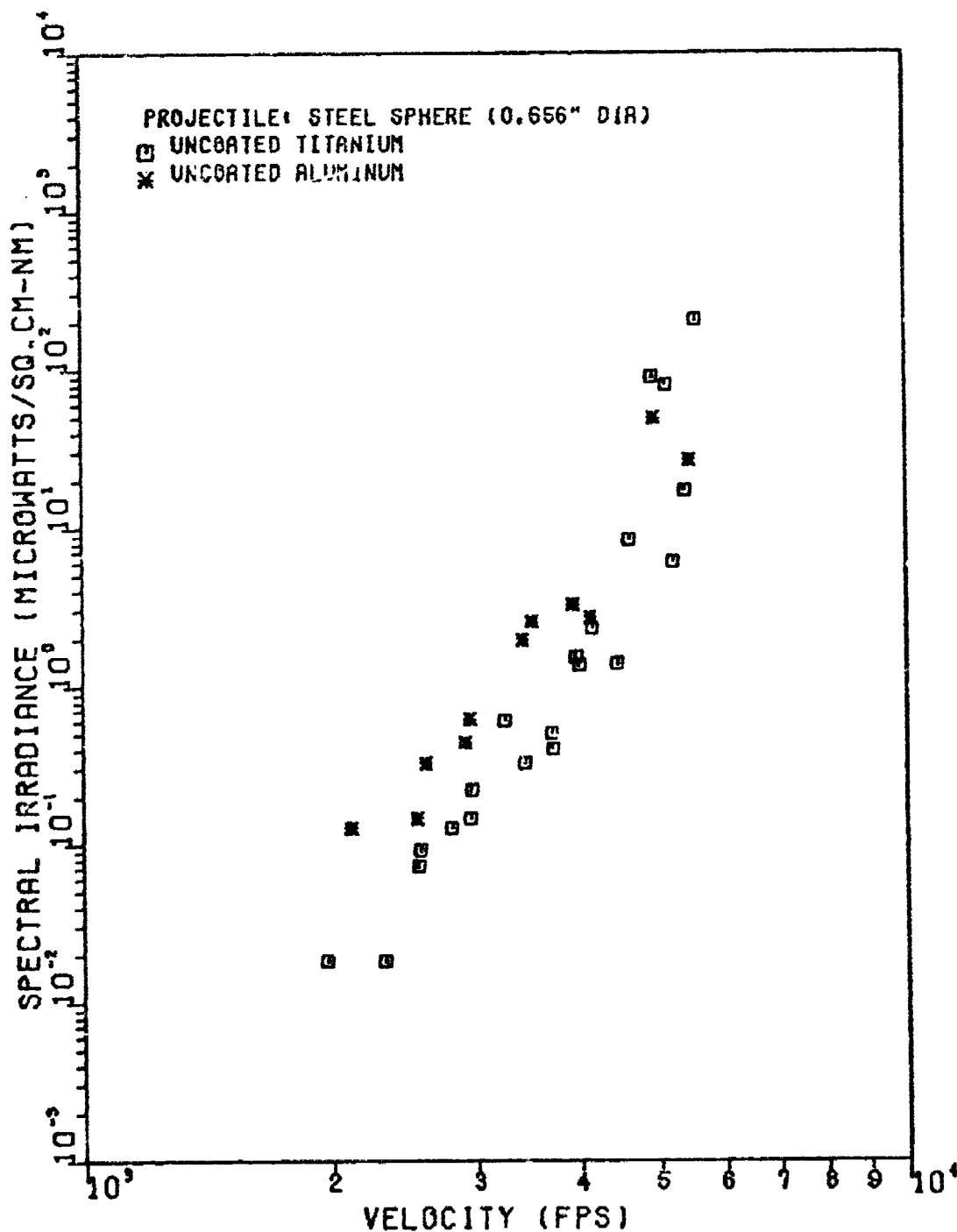at 4008A as a Function of Velocity

34
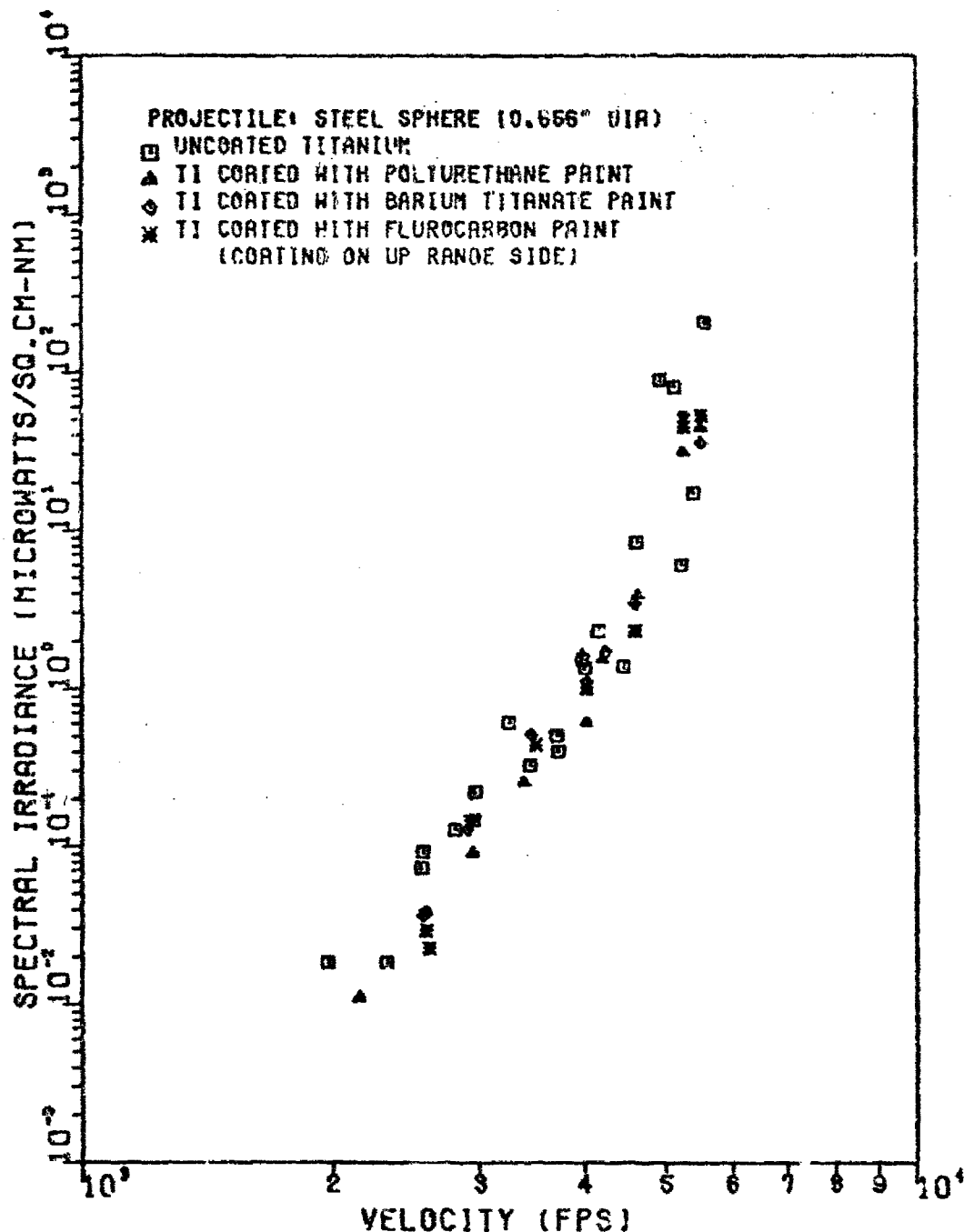
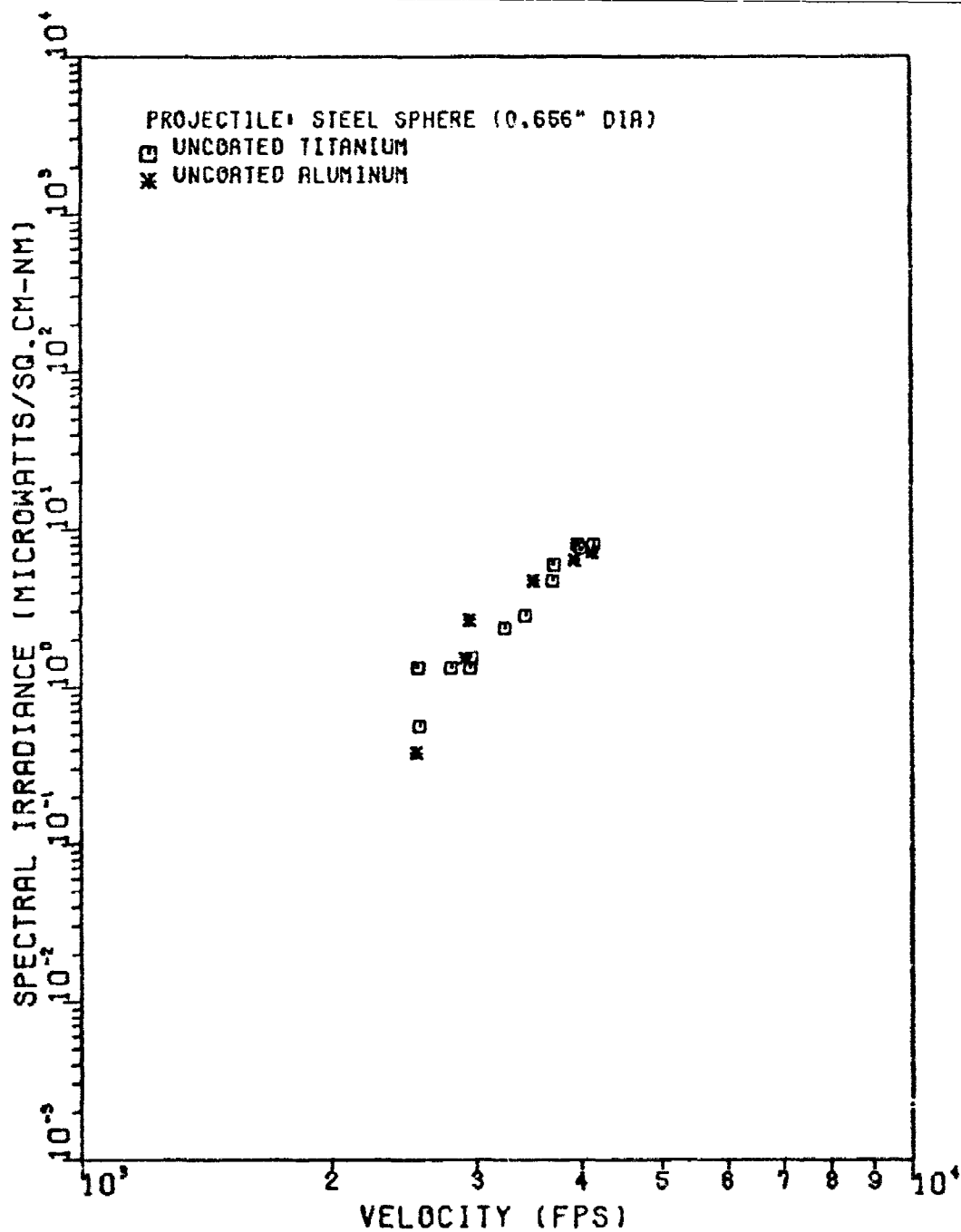Figure 17. Second Maxima of Spectral Irradiance at 4008A as a Function of Velocity
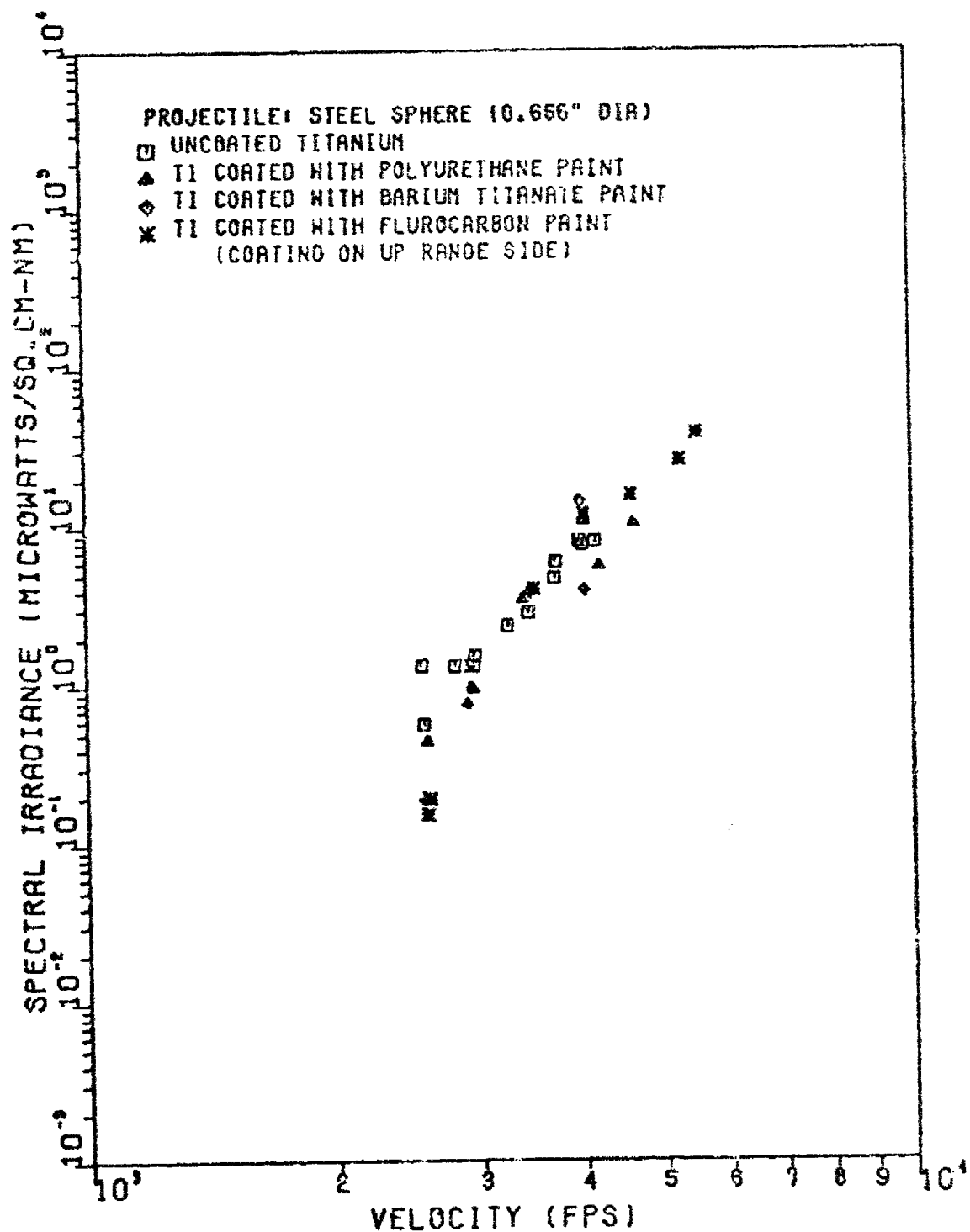
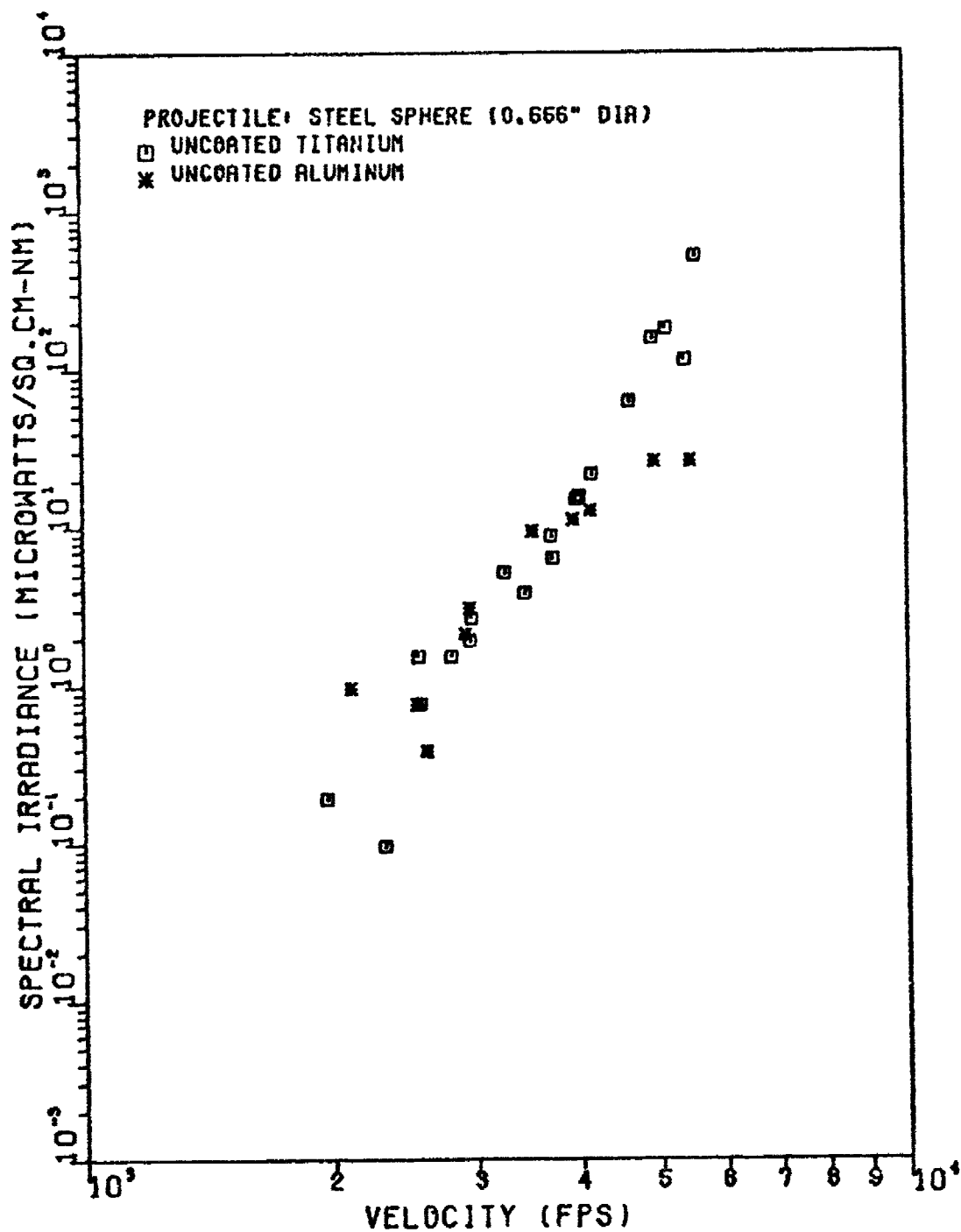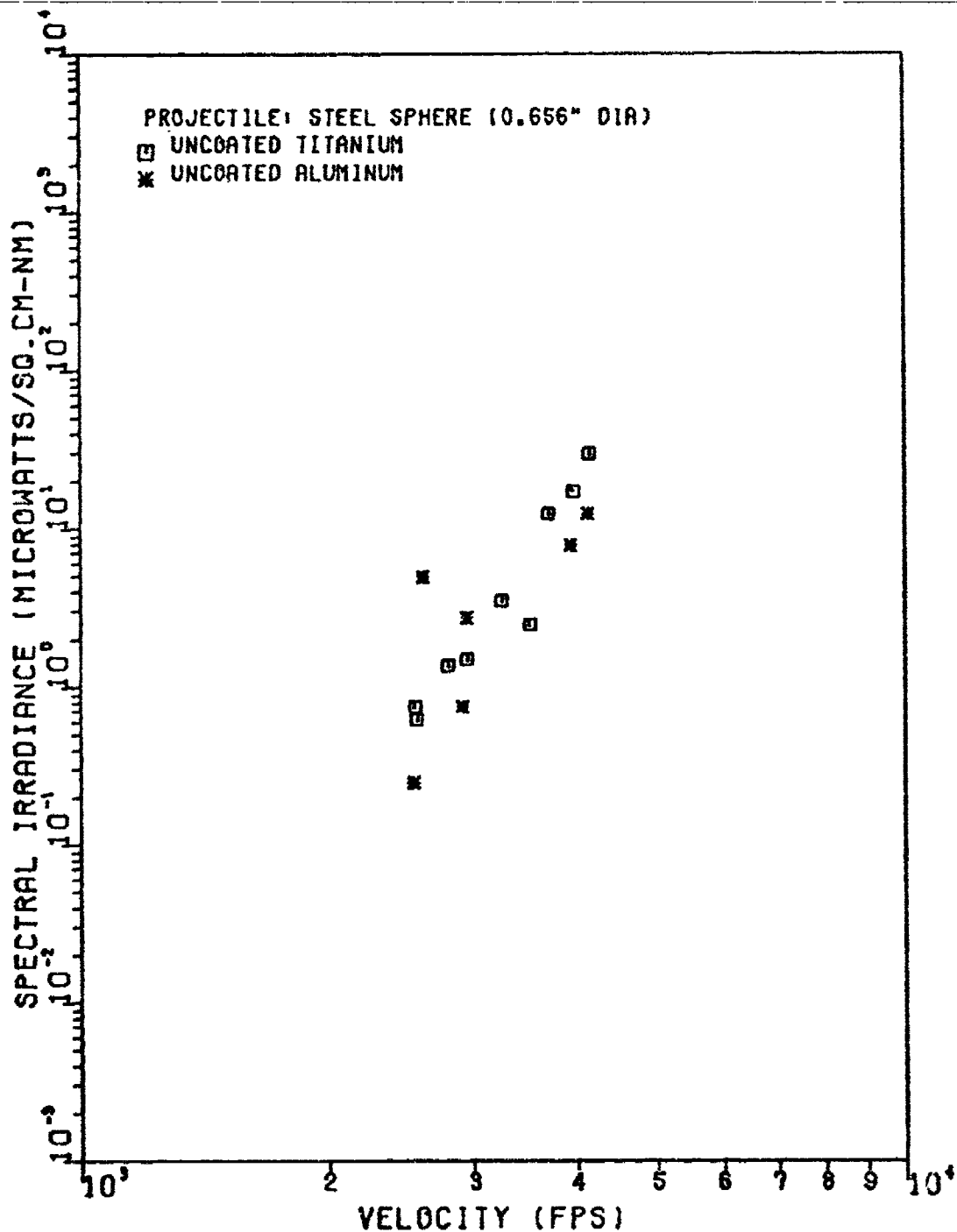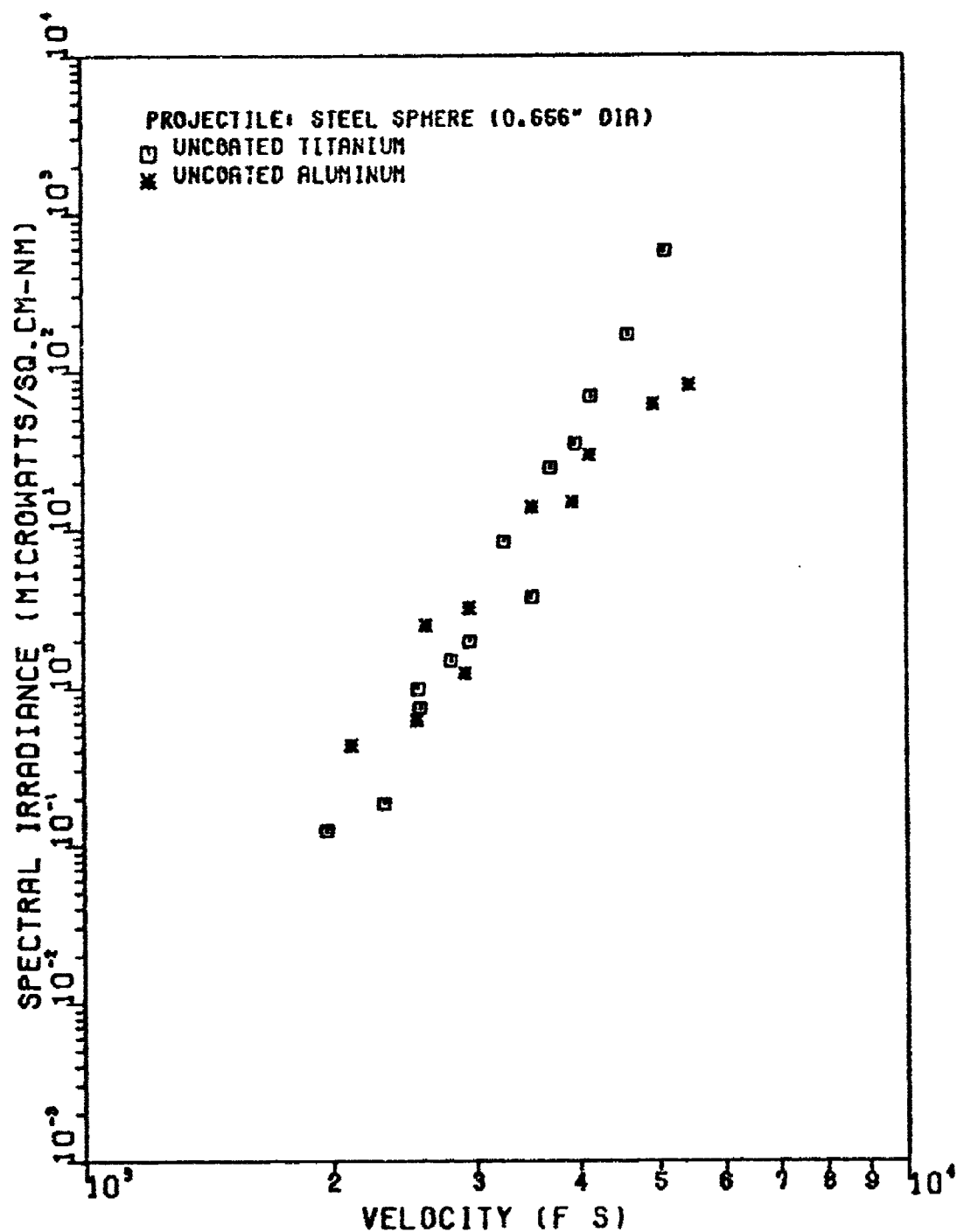Figure 18. First Maxima of Spectral Irradiance
at 7010A as a Function of Velocity

36
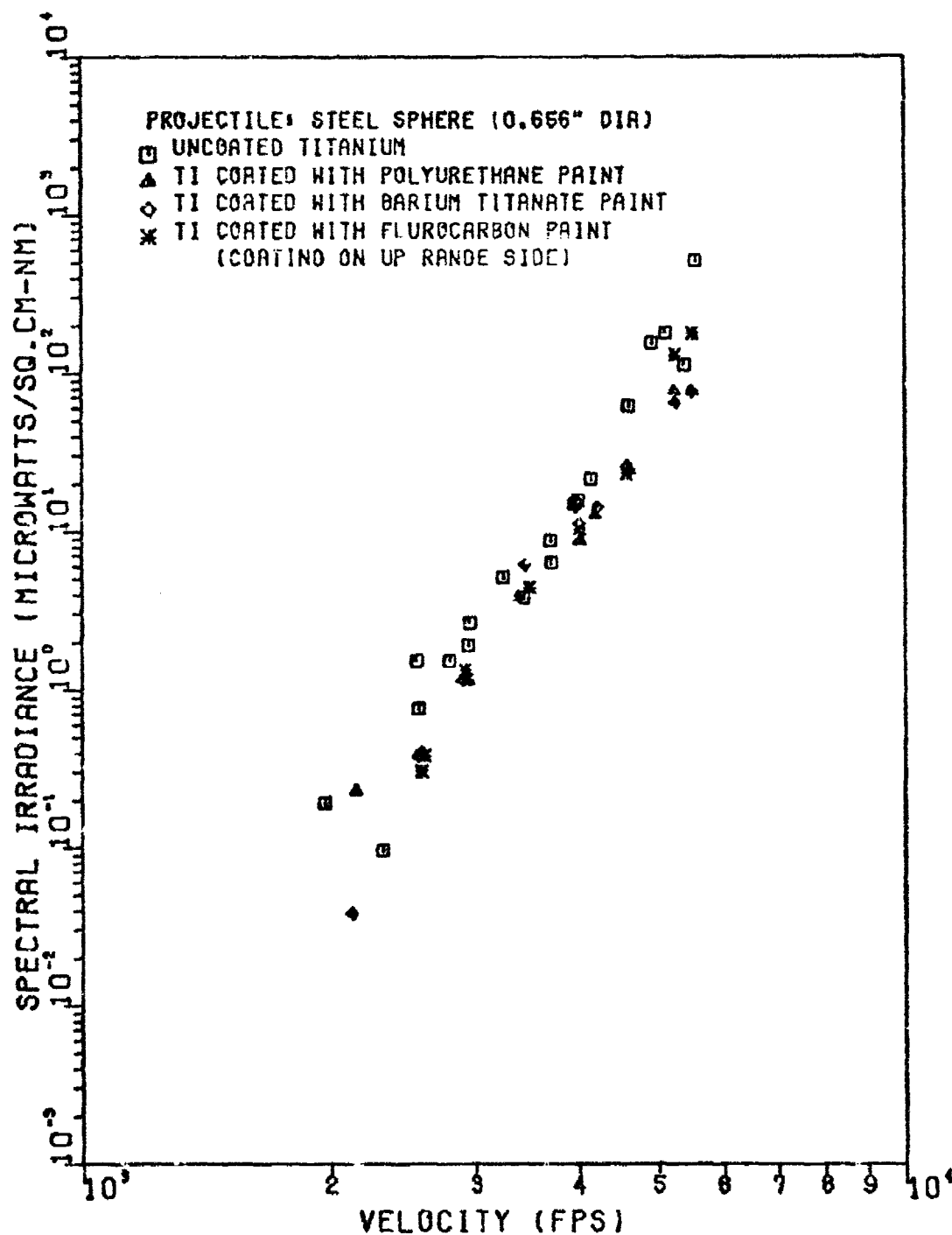
Figure 19. Second Maxima of Spectral Irradiance at 7010A as a Function of Velocity
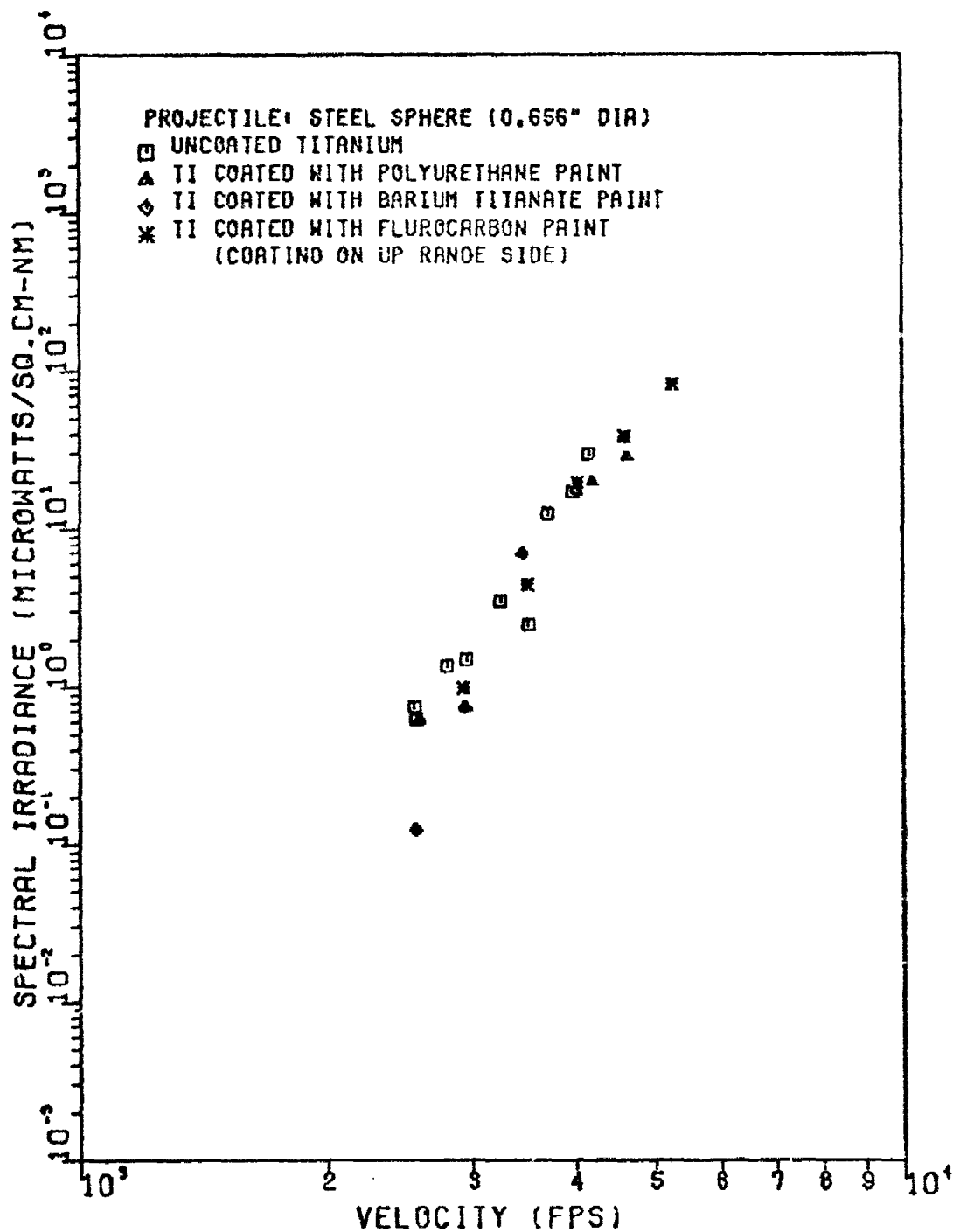
Figure 20. First Maxima of Spectral Irradiance
at 9025A as a Function of Velocity
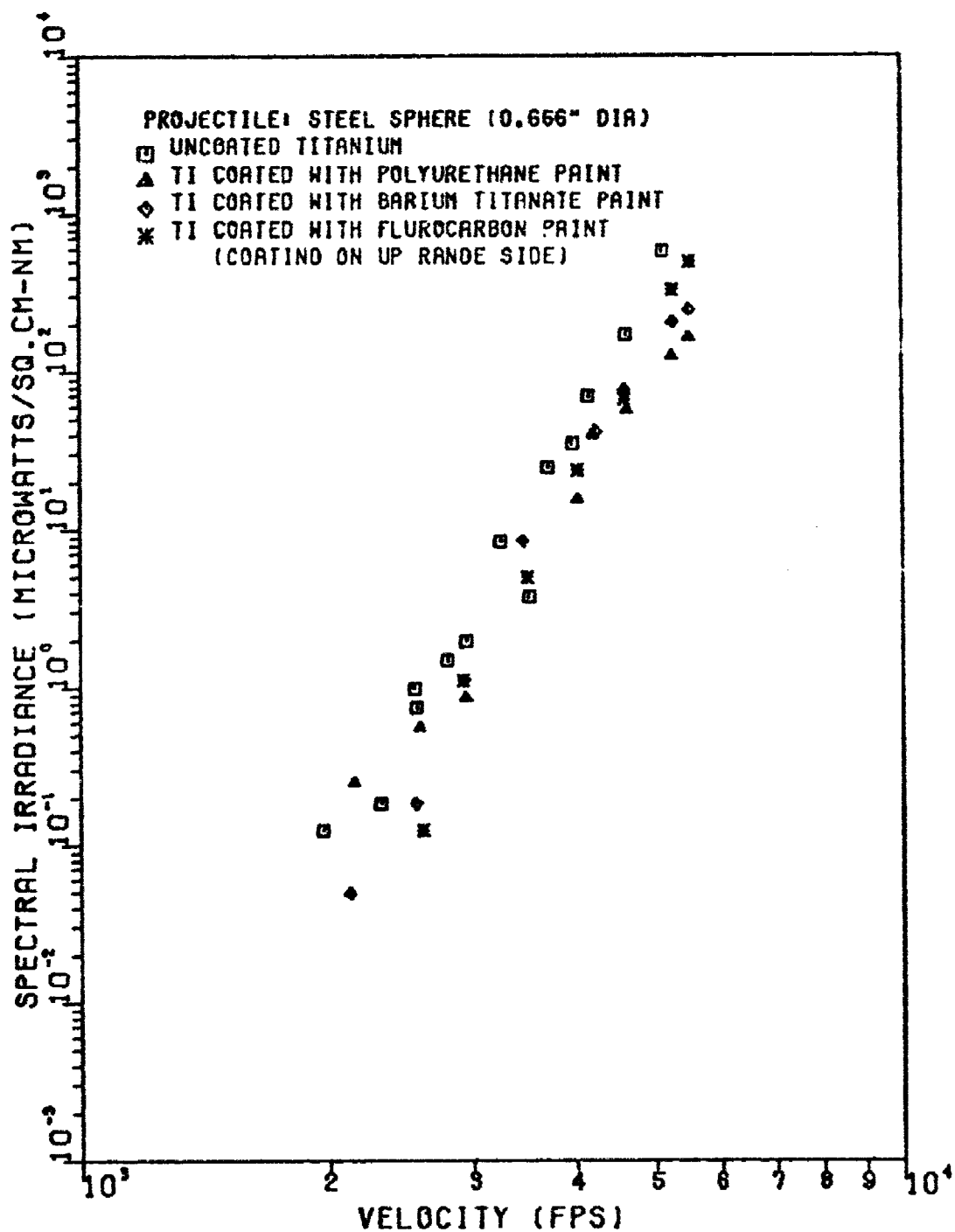
Figure 21. Second Maxima of Spectral Irradiance
at 9025A as a Function of Velocity

39
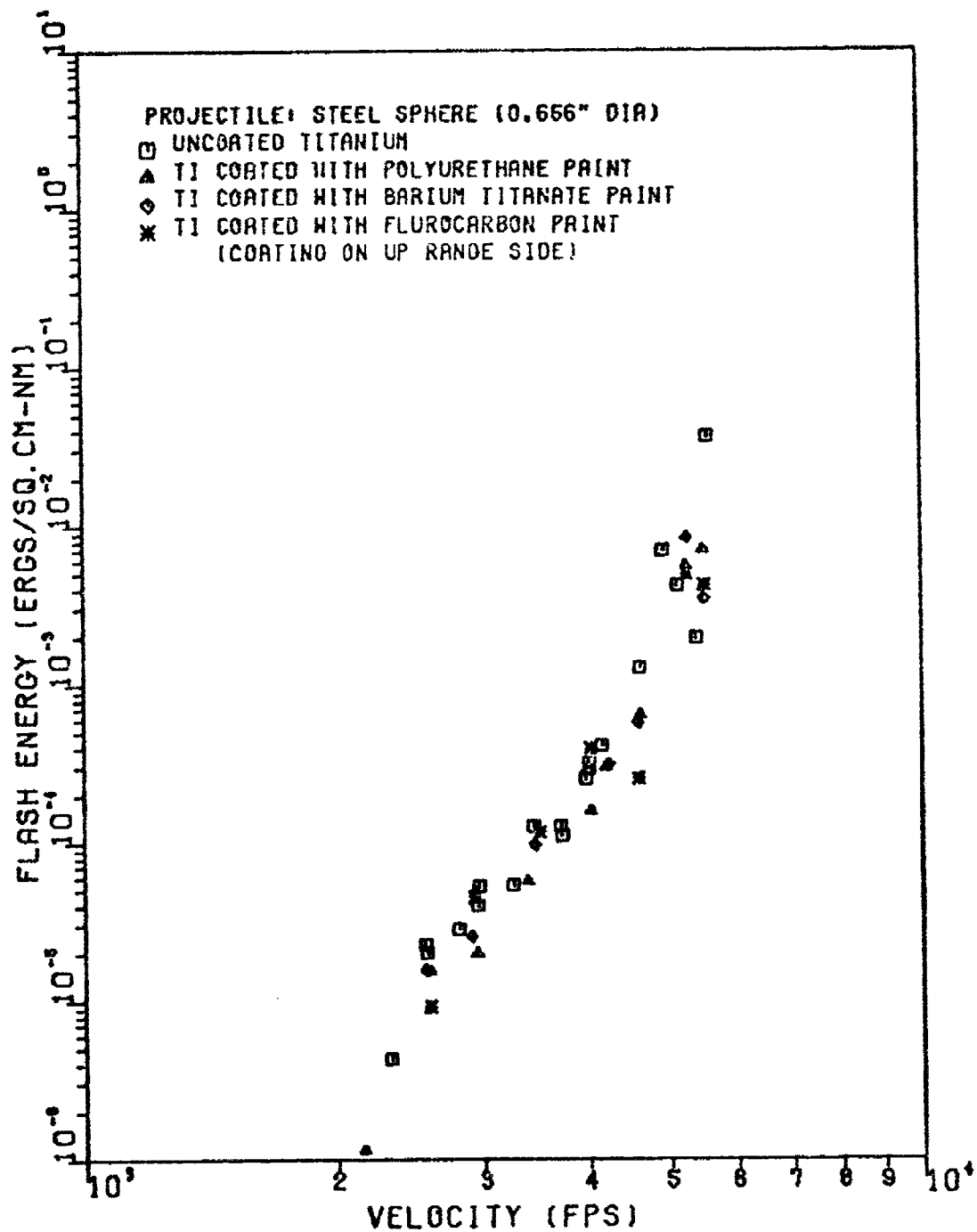
Figure 22. Total Energy at 4008A as a
Function of Velocity

40
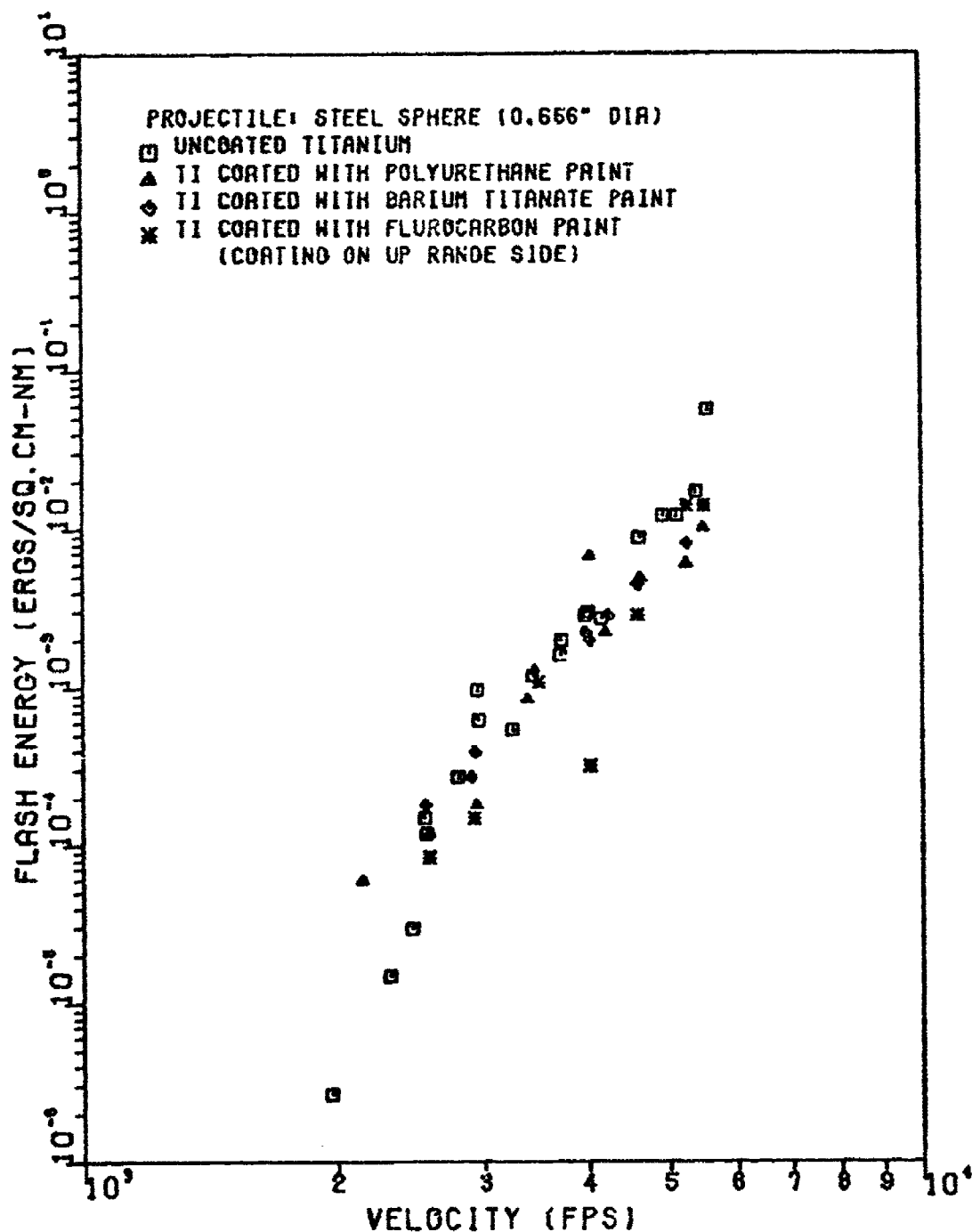
Figure 23. Total Energy at 7010A as a Function of Velocity
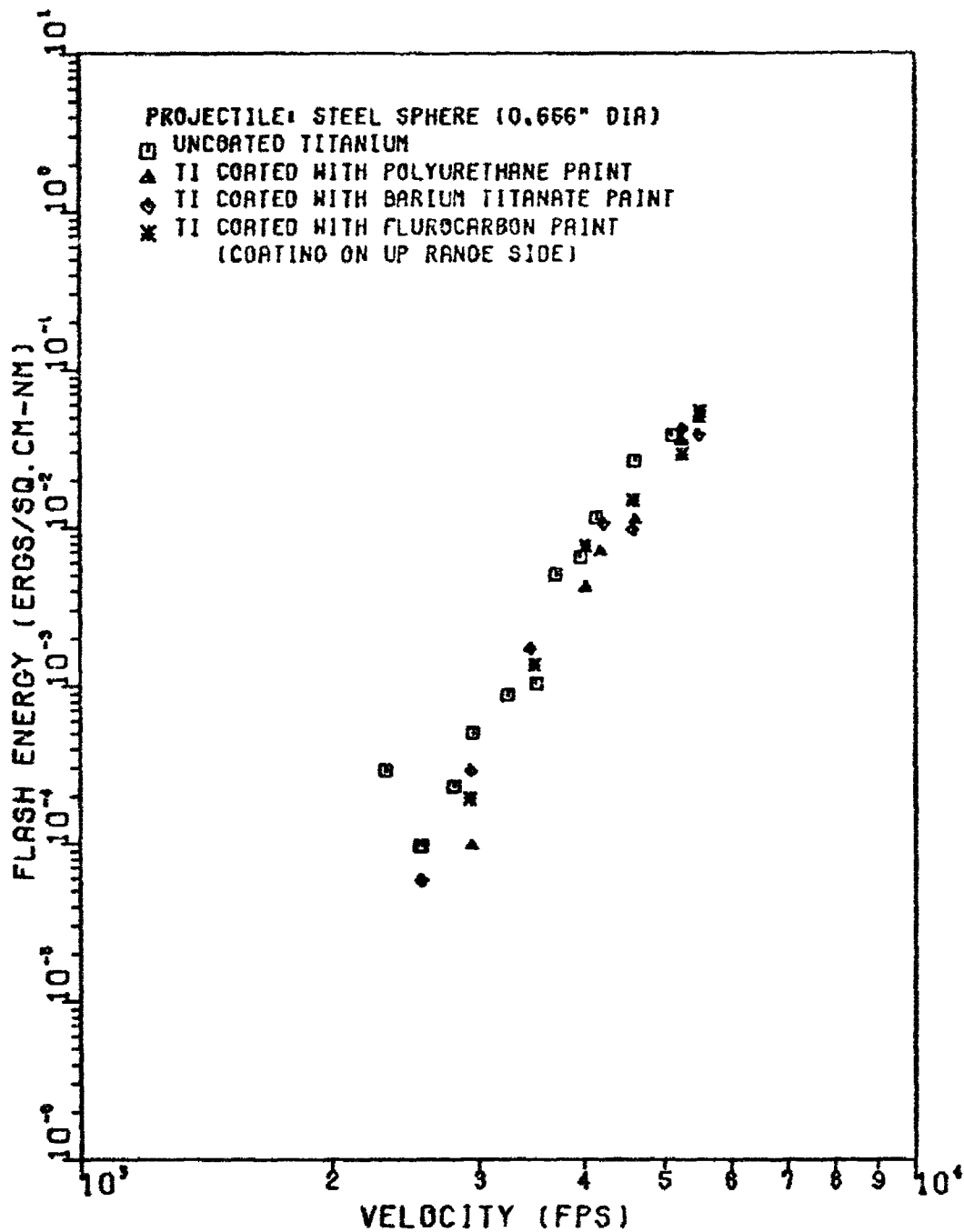
Figure 24. Total Energy at 9025A as a
Function of Velocity
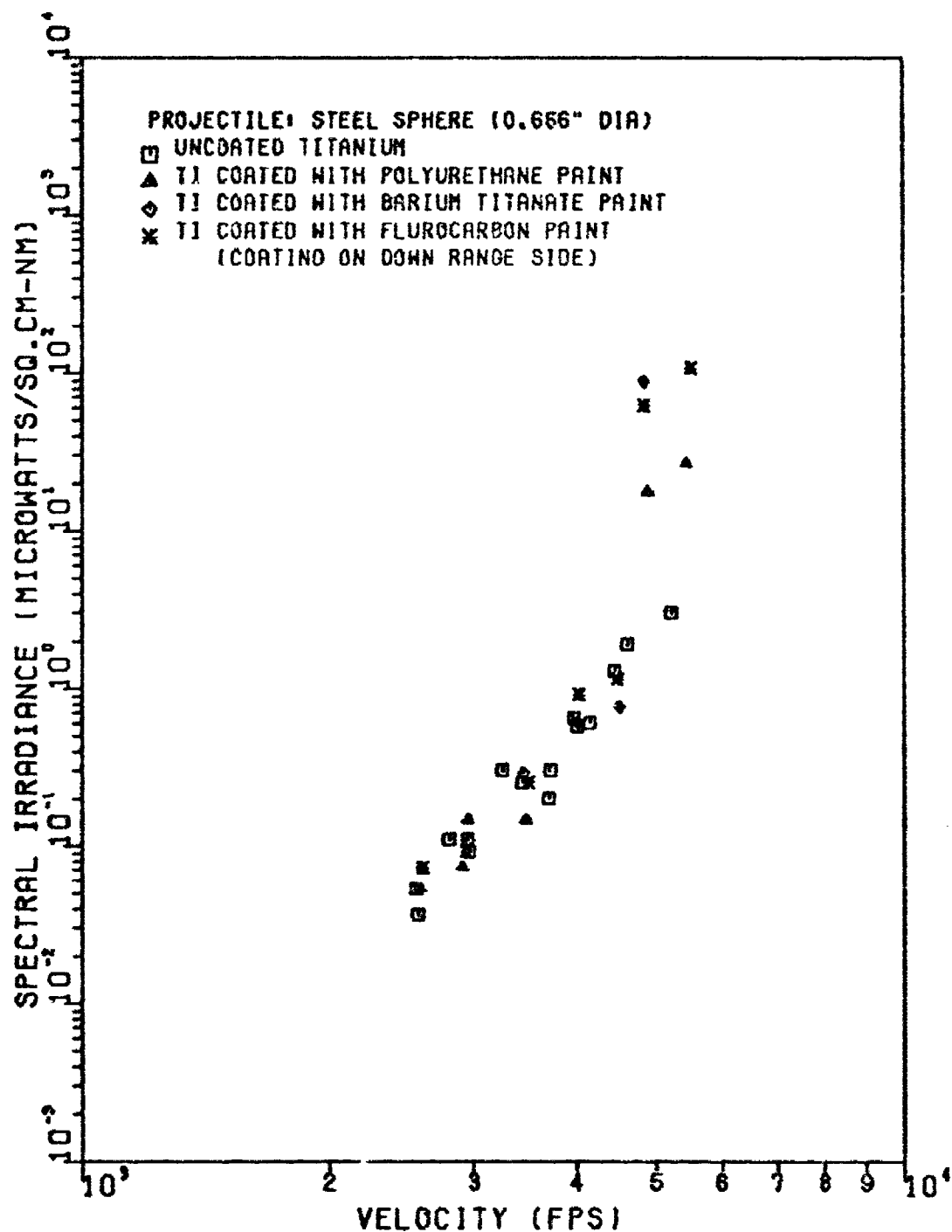
Figure 25. First Maxima of Spectral Irradiance at 4008A as a Function of Velocity

43
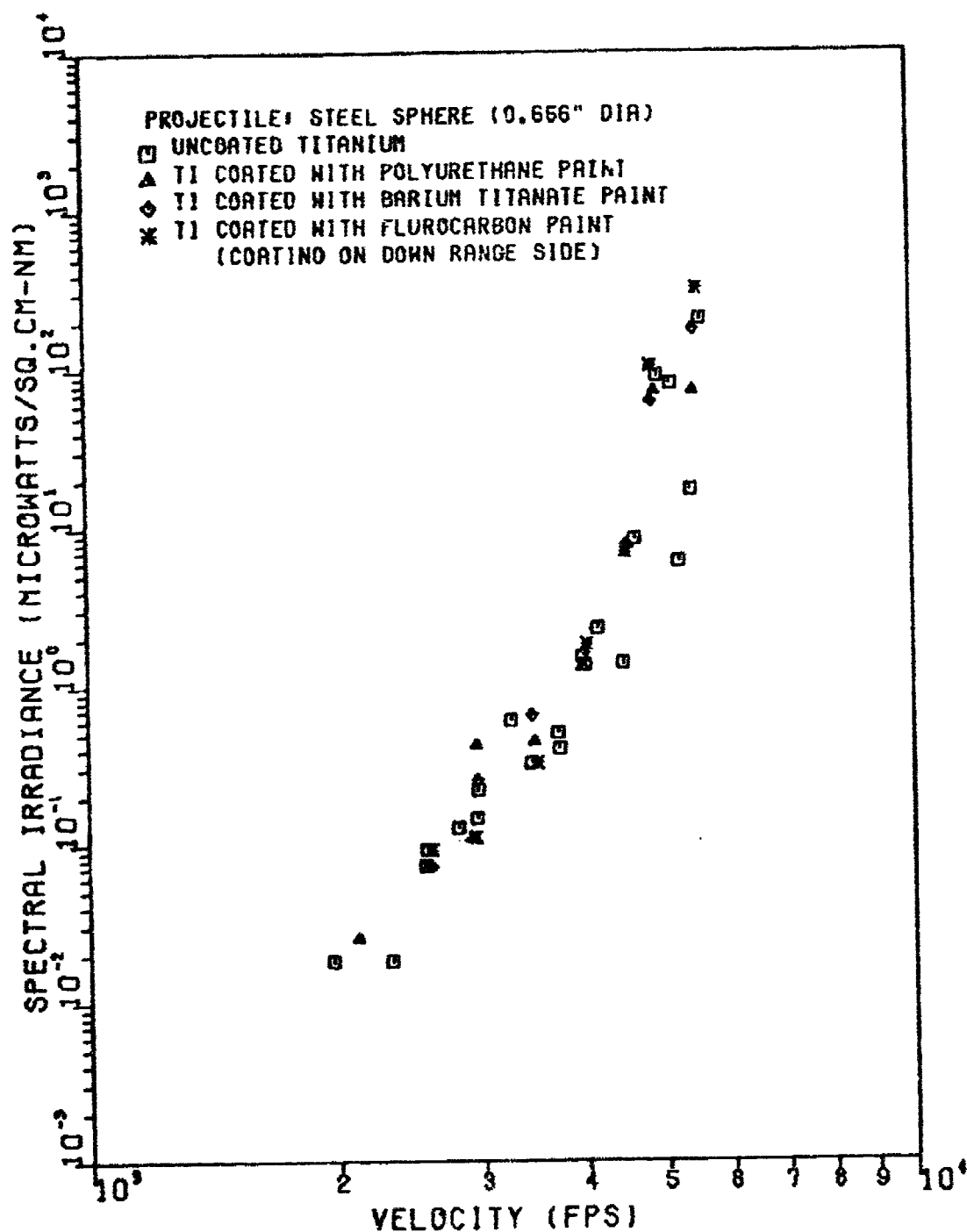
Figure 26. Second Maxima of Spectral Irradiance at 4008A as a Function of Velocity

44
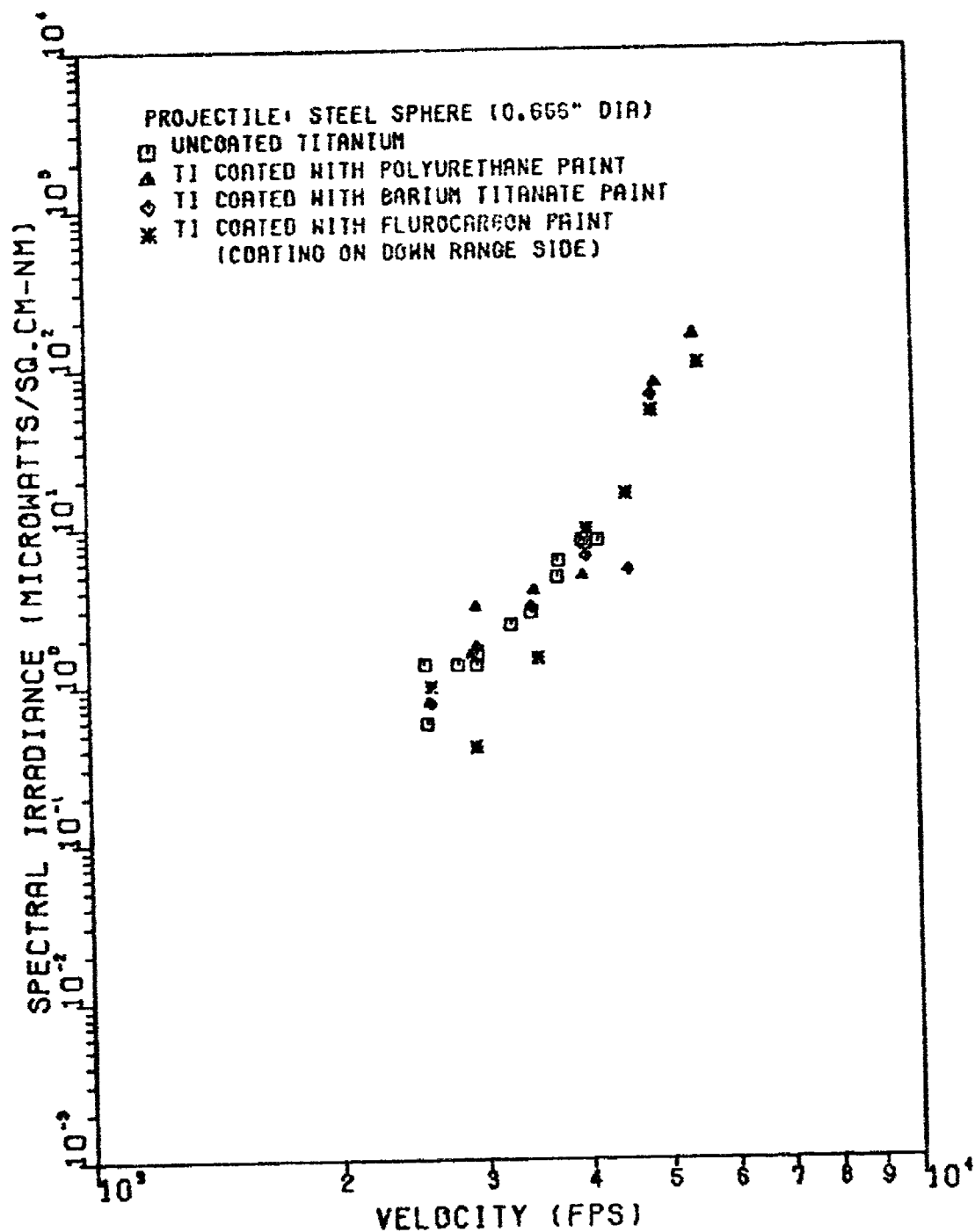
Figure 27. First Maxima of Spectral Irradiance at 7010A as a Function of Velocity
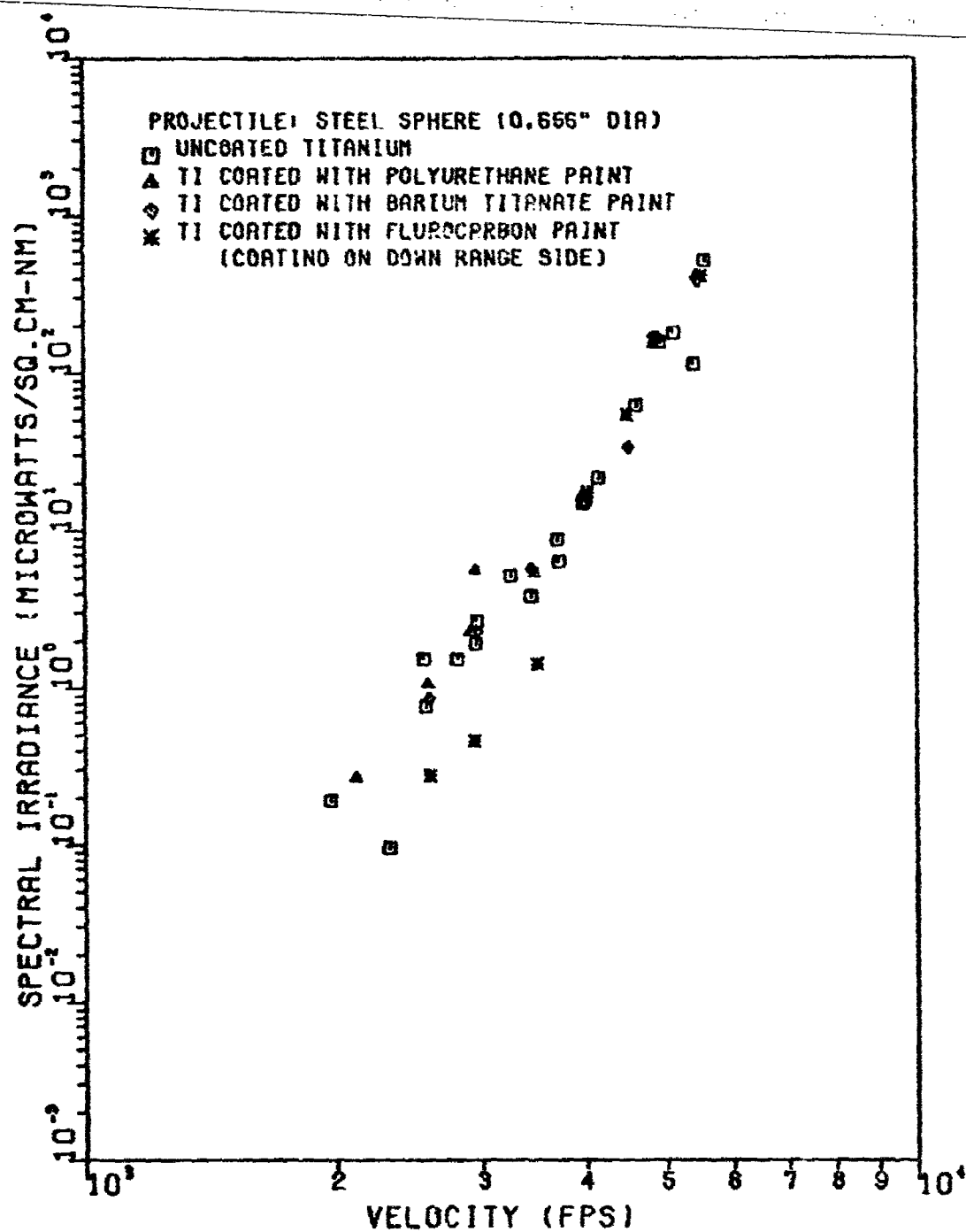
Figure 28. Second Maxima of Spectral Irradiance at 7010A as a Function of Velocity

46
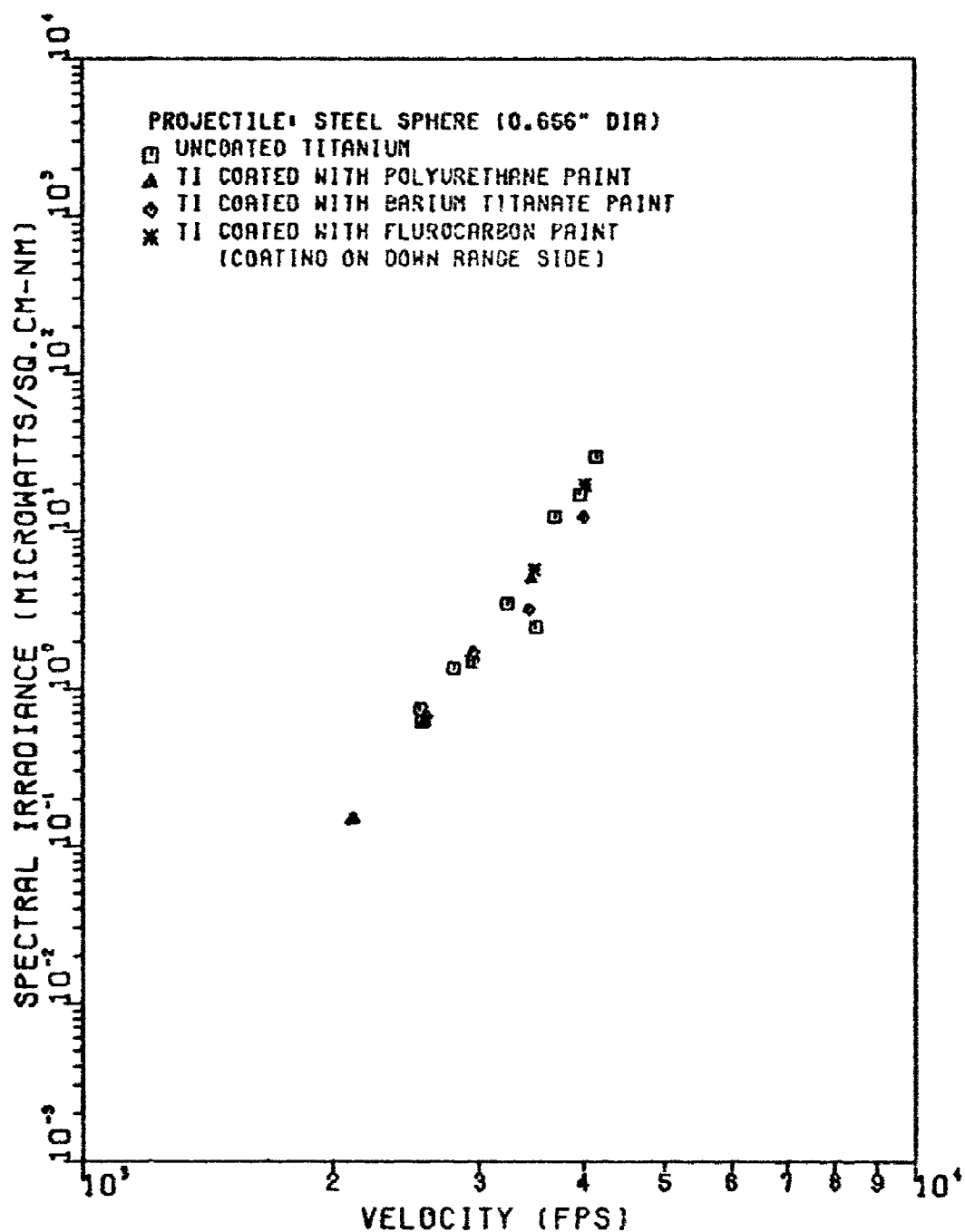
Figure 29. First Maxima of Spectral Irradiance at 9025A as a Function of Velocity
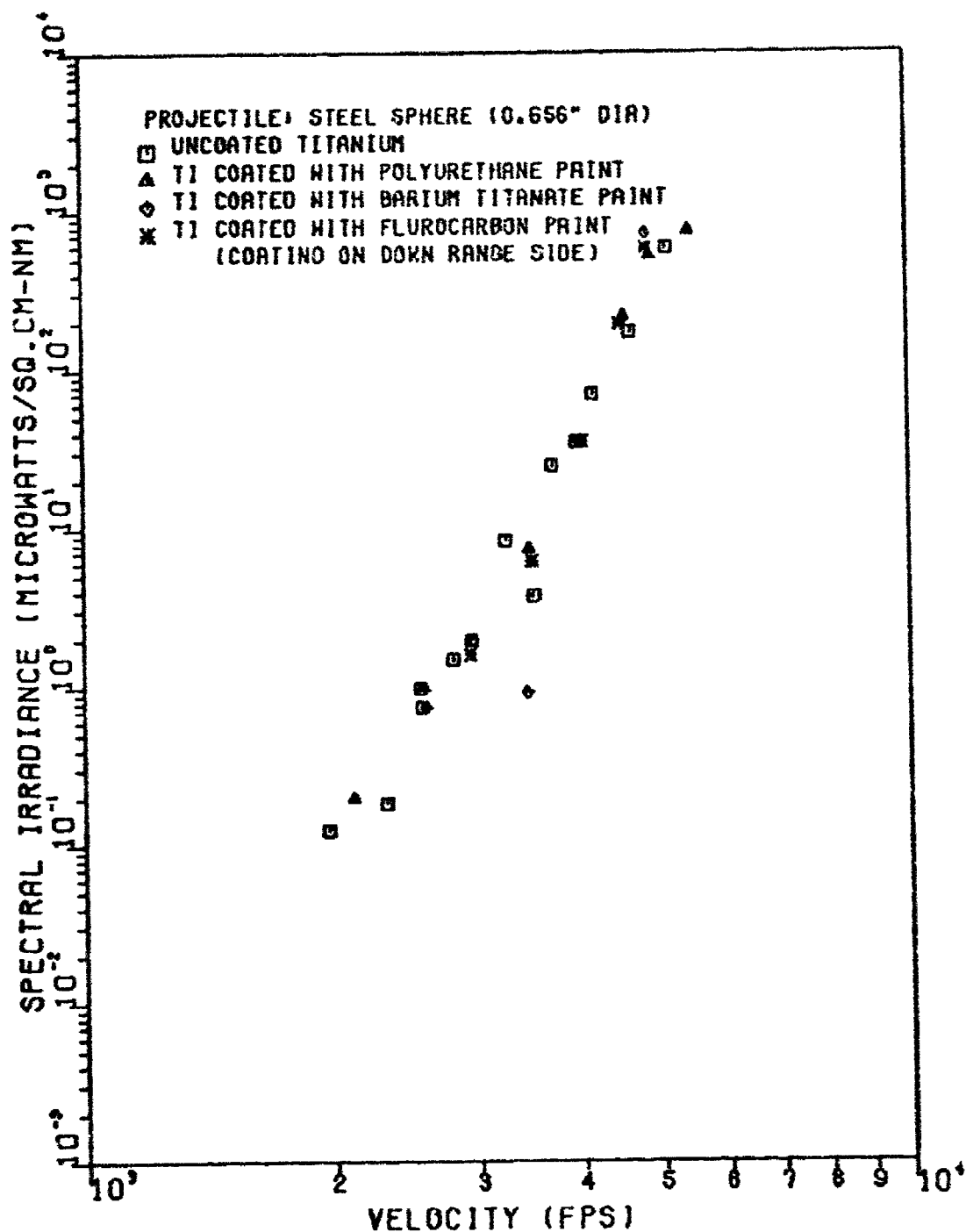
Figure 30. Second Maxima of Spectral Irradiance at 9025A as a Function of Velocity
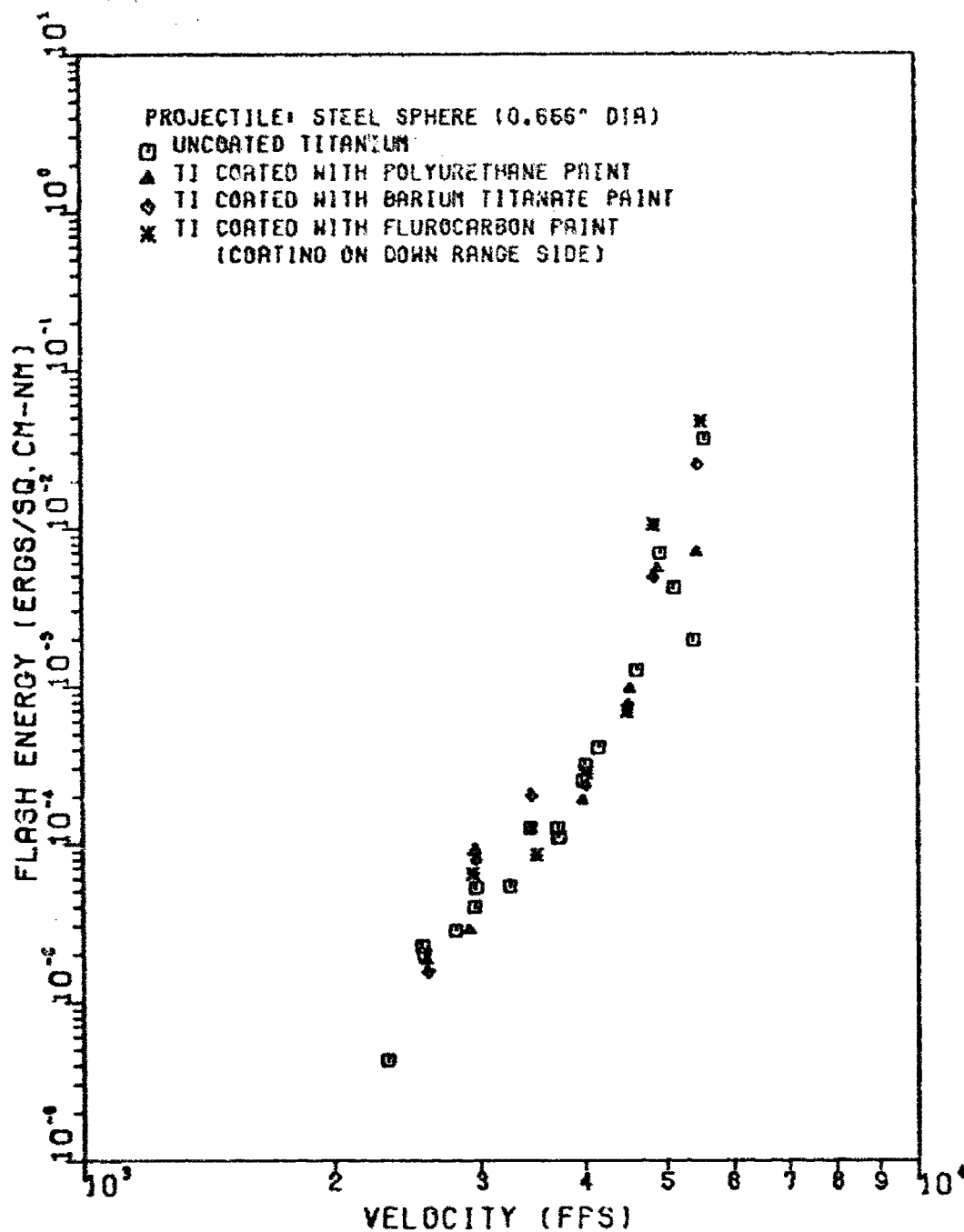
Figure 31. Total Energy at 4008Å as a
Function of Velocity

49

PROJECTILE: STEEL SPHERE (0.666" DIA)
- □ UNCOATED TITANIUM
- ▲ TI COATED WITH POLYURETHANE PAINT
- ◇ TI COATED WITH BARIUM TITANATE PAINT
- ✱ TI COATED WITH FLUROCARBON PAINT
   (COATING ON DOWN RANGE SIDE)

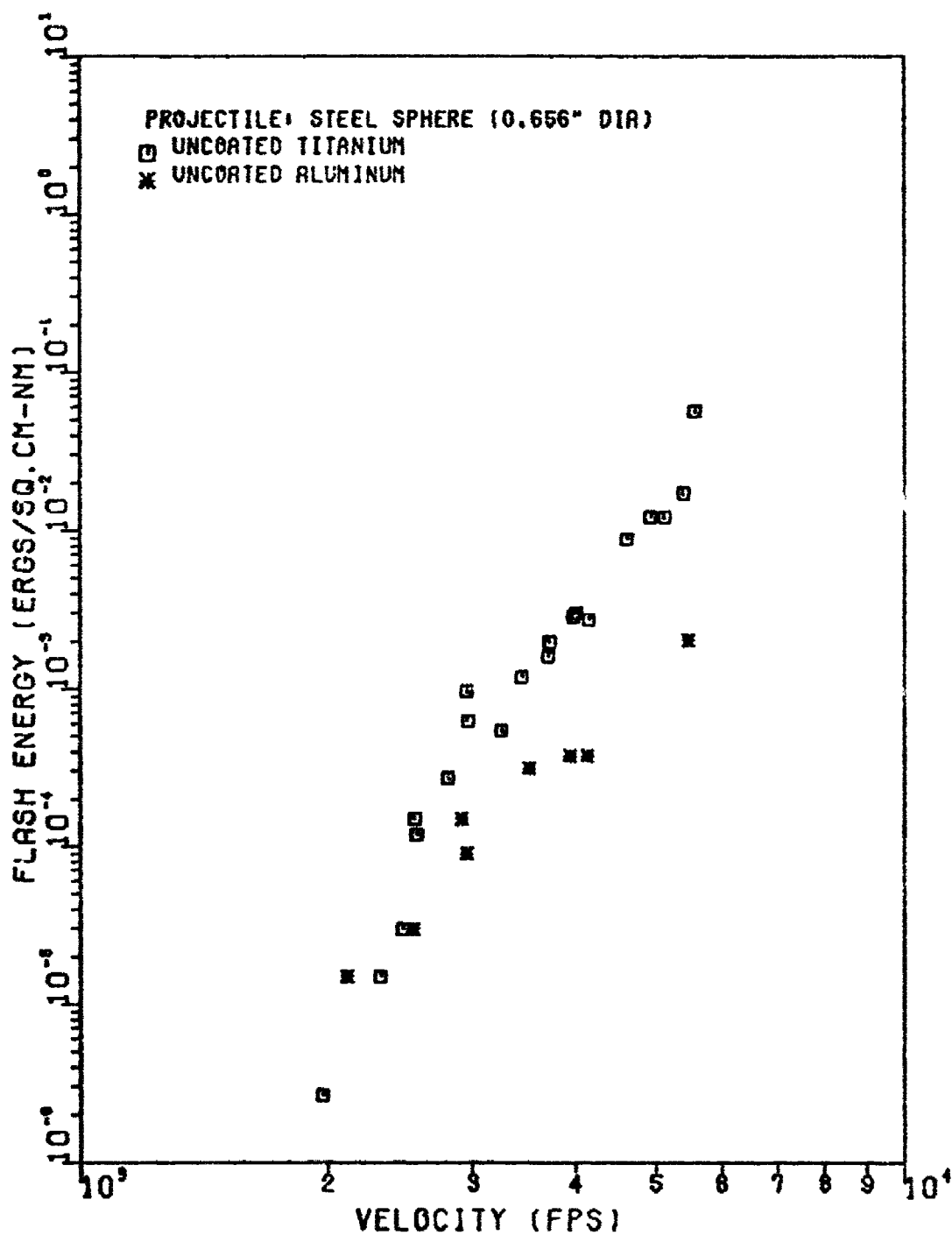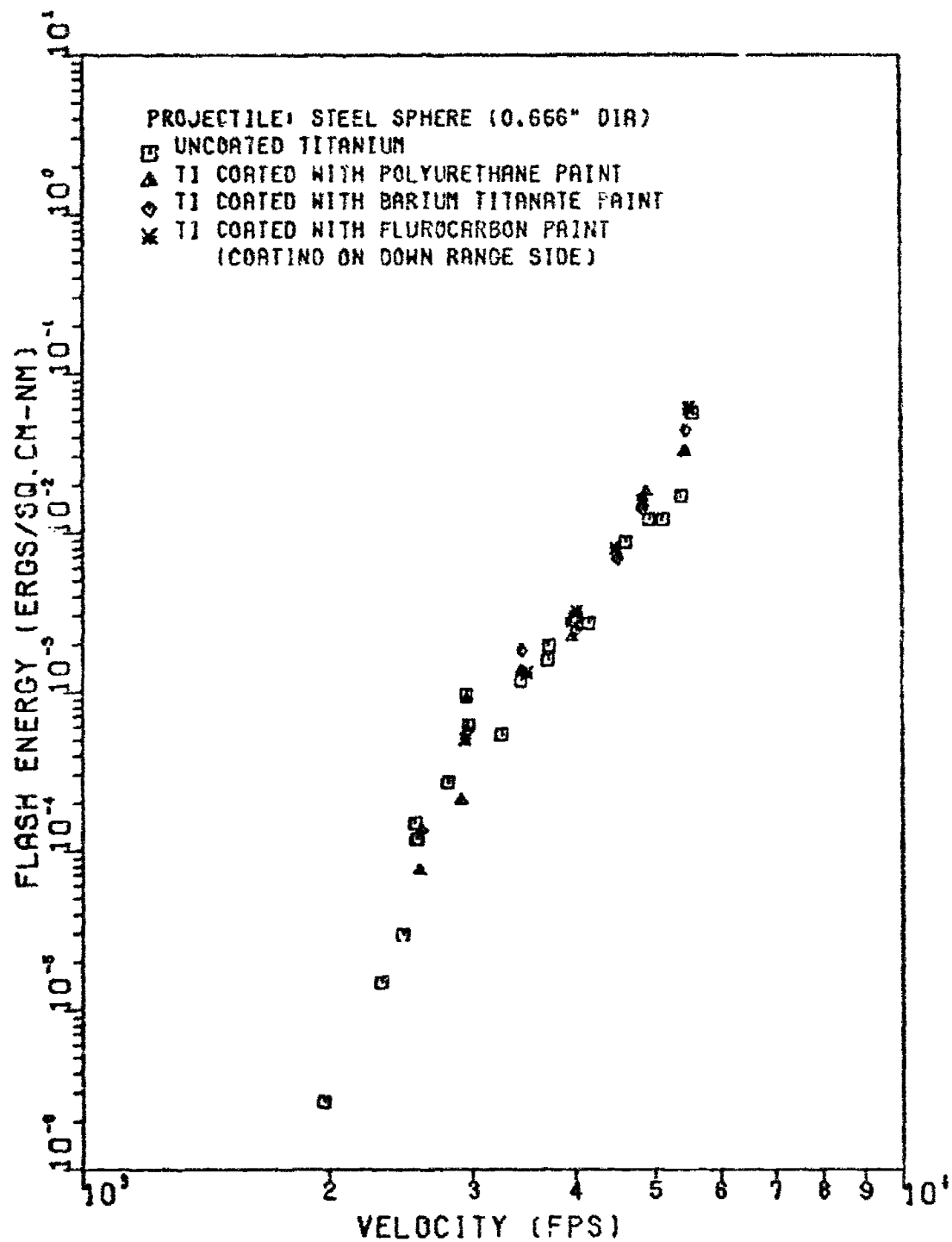Figure 32.   Total Energy at 7010A as a
             Function of Velocity

50
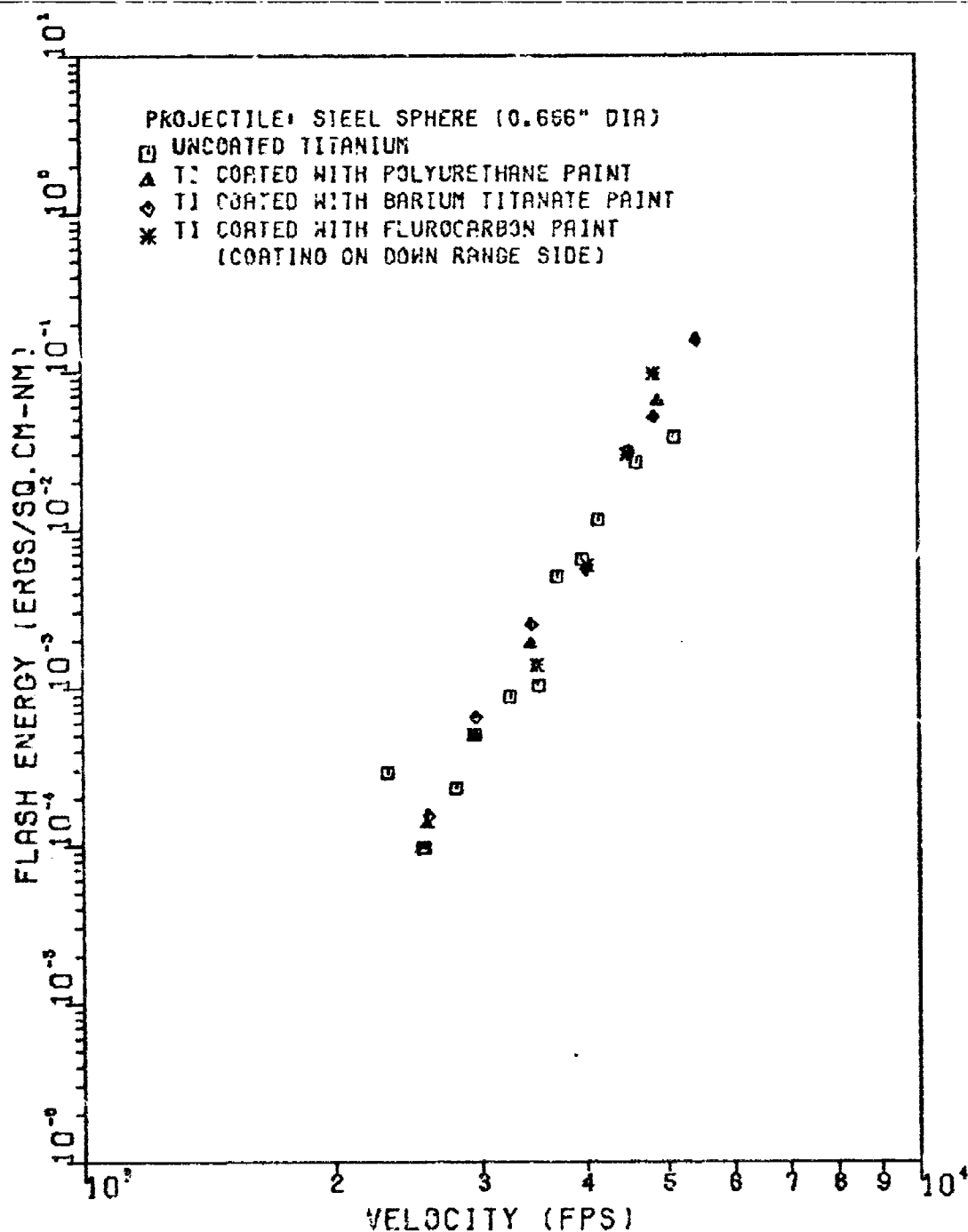
Figure 33.   Total Energy at 9025A as a
              Function of Velocity

51

with the coating up ranges. From Figures 25 through 33, it appears that the coating on the down range side of the target had a minimal effect on the reduction of impact flash.

Velocity Scaling

In his attempt to model impact flash, Mansur arrived at a scaling rule which was presented as Eq (2) of the introduction to this report. He deduced that spectral irradiance and flash energy of the first and second maxima scaled approximately to the fourth power of the velocity (Ref 2:29). Closer analysis of his data (Ref 2:28) reveals that the spectral irradiance scaled to the fourth power of the velocity but that the energy was closer to the fifth power of the velocity.

When the individual plots of this study's test data were generated (Appendix C), a least squares curve fit was also accomplished. The curves were fitted to

$$X = KV^n \qquad (2)$$

and the power to which the velocity is raised appears on each plot, where the logarithm of the irradiance is plotted vs the logarithm of the velocity, as the slope of the least squares curve fit line. The values of the constants K and n are listed in Tables II through V. It was determined from the data generated in this test that the spectral irradiance of the aluminum impacts scaled to an average of

Table II

Empirical Constants for Uncoated Targets

Spectral Irradiance $I = KV^n$

	Wavelength(A)	K	n
6Al-4V Titanium			
First Maxima	4008	1.116E-21	5.758
	7010	1.661E-17	4.896
	9025	3.702E-26	7.398
Second Maxima	4008	2.646E-30	8.313
	7010	1.113E-26	7.567
	9025	1.003E-31	9.054
2024 T-3 Aluminum			
First Maxima	4008	1.386E-22	6.199
	7010	3.359E-19	5.374
	9025	5.995E-19	5.328
Second Maxima	4008	2.941E-23	6.439
	7010	2.715E-16	4.589
	9025	6.119E-21	5.956

Total Flash Energy $E = KV^n$

	Wavelength(A)	K	n
6Al-4V Titanium	4008	7.232E-34	8.274
	7010	2.463E-32	8.072
	9025	3.752E-32	3.110
2024 T-3 Aluminum	4008	8.816E-28	6.468
	7010	2.664E-22	5.054
	9025	4.093E-34	5.609

Table III

Emperical Constants For Titanium Targets Coated
With White Polyurethane Paint

Spectral Irradiance $I = KV^n$

	Wavelength(A)	K	n
Coating on Up Range Side			
First Maxima	4008	1.222E-24	6.548
	7010	4.777E-20	5.579
	9025	1.450E-26	7.474
Second Maxima	4008	5.605E-32	8.721
	7010	1.898E-23	6.583
	9025	1.964E-26	7.476
Coating on Down Range Side			
First Maxima	4008	3.959E-33	9.057
	7010	3.427E-24	6.830
	9025	4.621E-25	7.070
Second Maxima	4008	4.856E-32	8.846
	7010	1.579E-26	9.139
	9025	6.434E-32	9.139

Total Flash Energy $E = KV^n$

Coating on Up Range Side			
	4008	2.545E-35	8.621
	7010	2.196E-24	5.813
	9025	1.314E-38	9.806
Coating on Down Range Side			
	4008	8.735E-33	7.986
	7010	1.542E-30	7.592
	9025	2.466E-37	9.592

Table IV

Empirical Constants for Titanium Targets Coated With White Polyurethane Paint

Spectral Irradiance $I = KV^n$

Wavelength(A)	K	n
Coating on Up Range Side		
First Maxima		
4008	9.931E-32	8.601
7010	7.873E-28	7.784
9025	1.664E-47	13.457
Second Maxima		
4008	1.555E-32	8.901
7010	5.613E-27	7.567
9025	6.368E-33	9.291
Coating on Down Range Side		
First Maxima		
4008	8.114E-32	8.684
7010	9.876E-20	5.522
9025	9.491E-23	6.400
Second Maxima		
4008	3.161E-37	10.307
7010	1.865E-28	8.074
9025	1.807E-39	11.200

Total Flash Energy $E = KV^n$

Wavelength(A)	K	n
Coating on Up Range Side		
4008	2.192E-31	7.549
7010	1.869E-23	5.566
9025	1.367E-33	8.453
Coating on Down Range Side		
4008	1.026E-35	8.831
7010	6.998E-29	7.141
9025	1.112E-35	9.132

55

Table V

Empirical Constants for Titanium Targets Coated
With Flurocarbon Paint

Spectral Irradiance $I = KV^n$

	Wavelength(A)	K	n
Coating on Up Range Side			
First Maxima	4008	4.769E-28	7.592
	7010	1.062E-24	6.869
	9025	3.395E-27	7.656
Second Maxima	4008	4.775E-35	9.589
	7010	1.877E-28	7.995
	9025	2.591E-37	10.508
Coating on Down Range Side			
First Maxima	4008	2.182E-36	9.985
	7010	3.312E-26	7.329
	9025	4.359E-29	8.224
Second Maxima	4008	3.143E-41	11.416
	7010	1.772E-37	10.526
	9025	4.839E-42	11.928

Total Flash Energy $E = KV^n$

	Wavelength(A)	K	n
Coating on Up Range Side			
	4008	1.267E-31	7.605
	7010	5.584E-28	6.765
	9025	9.791E-34	8.497
Coating on Down Range Side			
	4008	4.038E-43	10.883
	7010	2.934E-30	7.533
	9025	7.796E-41	10.562

the fifth power of the velocity as did the total energy. It was determined from the least squares curve fit of the data from the titanium test that the spectral irradiance and flash energy scaled to approximately the eighth power of the velocity.

Mansur tried to relate the magnitude of the impact flash to the energy or momentum of the projectile (Ref 2:29). If such a relationship exists, it could be identified through the power to which the mass and velocity were raised. The fact that this study determined a different value of the power to which the velocity was raised for each target material gives support to Mansur's statement that the flash cannot be modeled as a simple relationship of target and projectile mass and impact velocity (Ref 2:31).

Steel-Titanium Impacts at Velocities Under 2500 fps

Analysis of the oscilloscope traces for impact velocities under 2500 fps revealed a phenomena peculiar to steel-titanium impacts. Figure 34 is a sketch of typical traces for this velocity range. Every trace for titanium in this velocity range revealed a third and fourth maxima of spectral irradiance. The third flash maxima typically occurred 0.2 to 0.5 milliseconds after impact and was larger than the second maxima by a factor of approximately four. It was always larger than the fourth maxima but not by a consistent factor. Evaluation of the targets revealed that the failure was a combination of petal and plug type failures, while
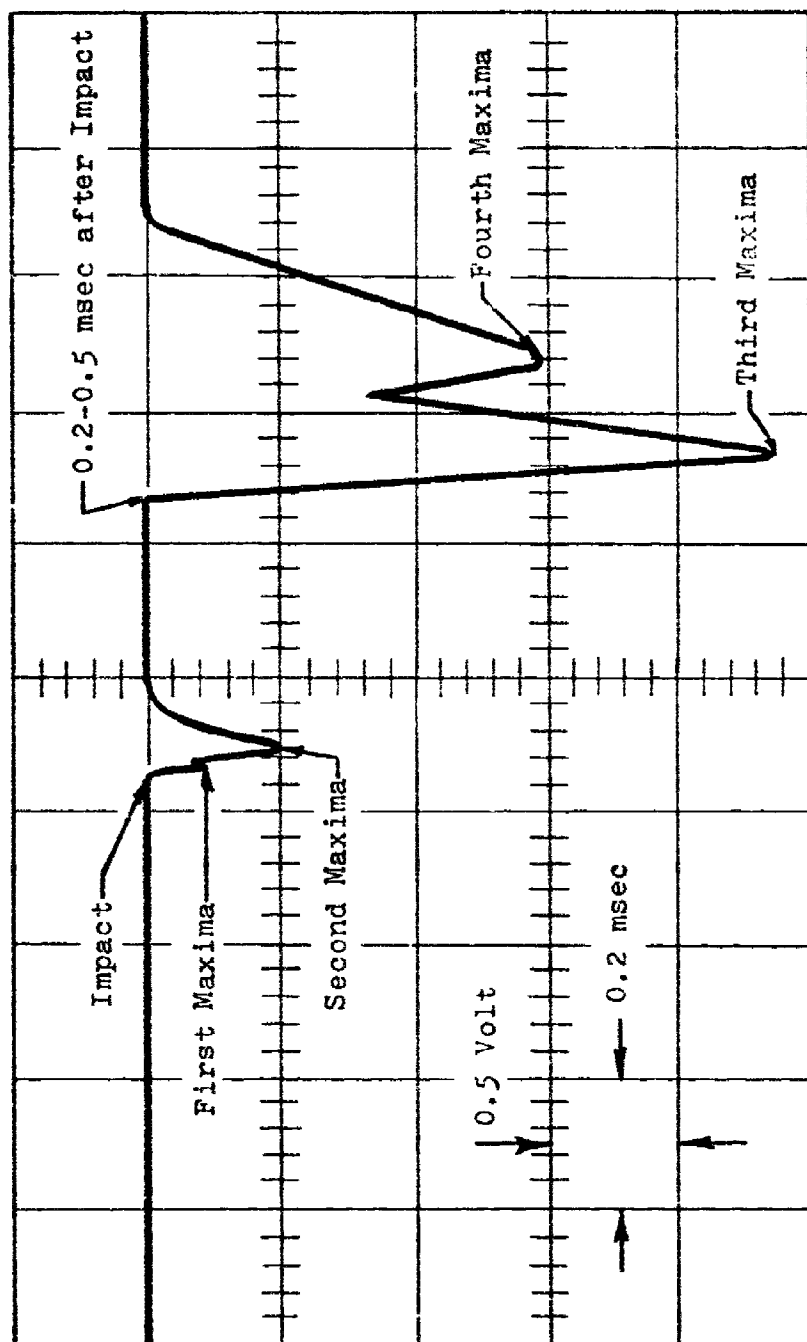
Figure 34. Typical Oscilloscope Trace for Steel-Titanium Impact with Impact Velocity Under 2500 fps

above 2500 fps impact velocity, the failures were all plug type. Analysis of the still photographs of the down range flash for all impact velocities indicate that there is a definite possibility of delayed ignition of the titanium fragments. Figure 5 shows streamers of burning titanium fragments whose ignition is recorded away from the back face of the target. These streamers start in free flight and terminate in a "star," from which new streamers appear. Figure 35 is a still photo of an impact velocity of 2115 fps. The primary flash in this photo is located six inches away from the rear face of the target. The most probable cause for the third and fourth maxima is delayed ignition of large titanium fragments. When ignition does occur, the flame covers the maximum surface area which includes the stress cracks induced by the impact. The surface burning and oxidation along the cracks probably causes a build-up of pressure between the crack surfaces causing the fragment to fly apart releasing the large flash. The delayed ignition of titanium particles which was so pronounced at impact velocities under 2500 fps was also the probable cause of the random "bumps" which were observed on the final return to zero leg of oscilloscope traces for titanium impacts above 2500 fps.

Temperature Analysis

Previous studies of impact flash, the most recent by Mansur (Ref 2), have assumed that the flash radiates as a blackbody. When a light source radiates as a blackbody, it
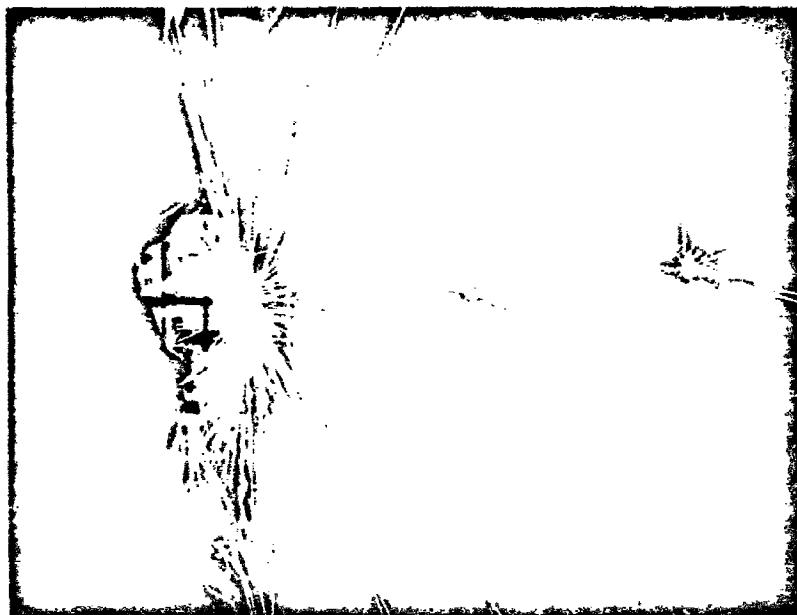
Figure 35.   Flash Located Six Inches Down
Range From The Target

is possible to determine the temperature of the source from Planck's equation.

$$J_\lambda = C_1 \lambda^{-5}/(EXP(C_2/\lambda T)-1) \qquad (3)$$

where J_λ is the spectral irradiance in watts/cm^2-A or similar units, C_1 and C_2 are constants, λ is the wavelength in question, and T is the temperature of the blackbody. Calculations of J_λ can be found in a set of blackbody tables (Ref 19:79). These values were plotted as solid lines representing a constant temperature in Figures 36 and 37. For comparison with Mansur's work, the spectral irradiance for 3000, 3500, 4000, and 5000 fps impacts in aluminum were plotted in Figure 36. The temperature for the 3500 through 5000 fps velocity range was found to vary from 2800° K to 3500° K. These values compare very closely with the work of Mansur (Ref 2:37) and Abernathy (Ref 8:30). Figure 37 depicts the spectral irradiance of titanium for impact velocities between 3000 and 5000 fps. For the velocity range of 3000 fps to 3500 fps, the experimental data agrees fairly well with the blackbody curves. For the 4000 to 4500 fps velocity range, the experimental data approximates a straight line while the 5000 fps data approximates a curve with a slope opposite to the blackbody curves.

Several assumptions are made in the application of Planck's equation. One of the basic assumptions is that the blackbody has a known constant surface area. In the

61
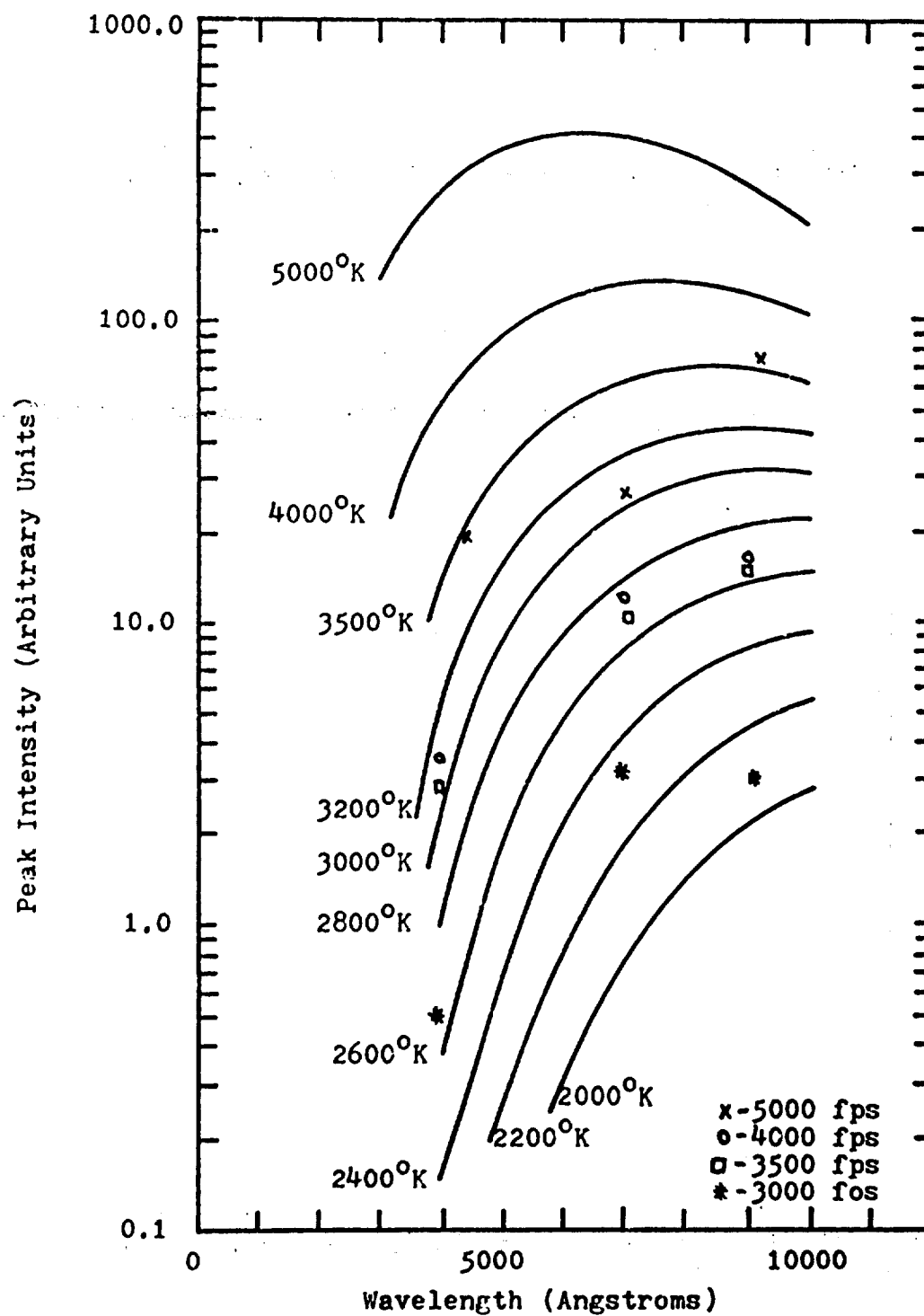
Figure 36. Spectral Distribution of Peak Flash
Intensity as a Function of Velocity
for 2024 T-3 Aluminum
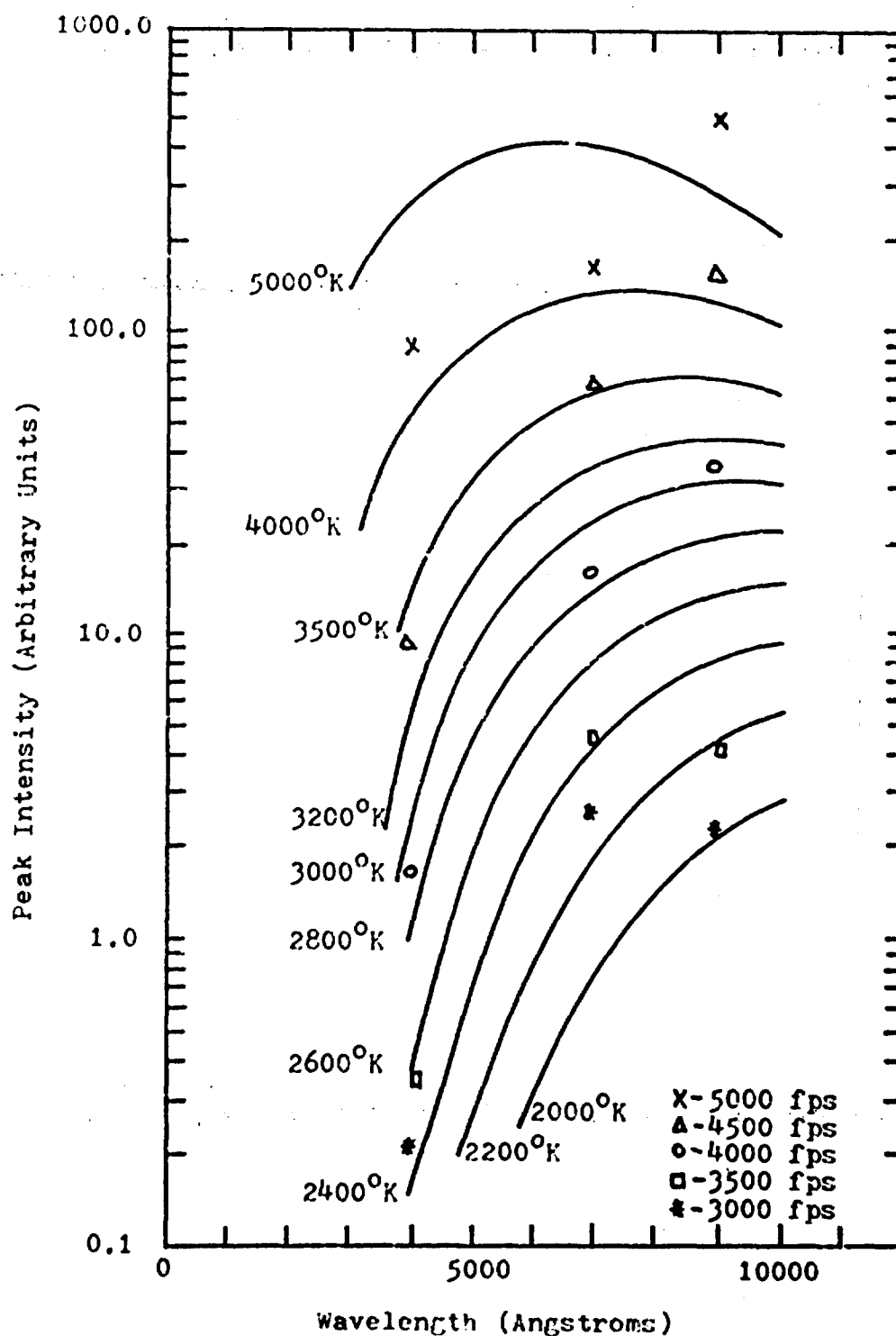
Figure 37. Spectral Distribution of Peak Flash
Intensity as a Function of Velocity
for 6Al-4V Titanium

63

case of a flash, it starts at a point, grows to a maximum surface area and returns to zero surface area. Extensive analysis of this topic was conducted by Mansur (Ref 2:36). Photographic analysis of the flash shows that the maximum surface area increased as the impact velocity increased. Another factor which effects the accuracy of the blackbody approximation is the variation of the emissivity of the heat source under evaluation. Emissivity will vary with the degree of oxidation and thus will be a function of the time of heating. For oxides, the emissivity generally increases with temperature while the reverse occurs with metals (Ref 20:851). Values of emissivity are tabulated for wavelengths of 5500A and 6500A in several handbooks and are found to be relatively constant for these wavelengths (Ref 19:98). Because the combustion of titanium is associated with a molten mixture of oxide and metal and the reaction takes place at the surface of this molten mixture (Ref 21:360), and because the exact effect of the surface area variations and value of emissivity at 9025A are not known, the experimental data points at this wavelength were given less weight in this analysis. From Figure 37, the data for 4008A and 7010A shows that the titanium flas approximates a blackbody and the temperature varies from 2400 to 4000° K over a velocity range of 3000 to 5000 fps.

IV. Conclusions

Visually the down range flash generated by the impact
of a high velocity projectile with a titanium target is
significantly greater than the flash from the impact of a
similar projectile with an aluminum target. Experimental
analysis showed that this flash was characterized by two
intense maxima. As with high velocity impacts in aluminum
targets, the first maxima occurs simultaneously or nearly
simultaneously with perforation of the target. The second
maxima occurs 30 to 80 microseconds later. The intensity of
the spectral irradiance of these maxima is approximately the
same for aluminum and titanium at wavelengths of 7010A and
9025A, but the intensity of the aluminum flash was greater
at 4008A probably as a result of a denser population of
aluminum ion transformations in this region of the spectrum.
The visual difference in intensities between the two target
materials was the result of the differences in duration time
of the flash. The aluminum flash lasted approximately 0.10
milliseconds while the titanium flash was approximately 0.56
milliseconds.

Scaling the intensity of the spectral irradiance and
total energy of the flash as an exact function of measurable
properties could not be accomplished. However, the intensi-
ty and energy of the titanium flash were found to scale to
the eighth power of the relative impact velocity and the

65

aluminum flash to the fifth power of the relative velocity.

While flash in aluminum targets occurred as a single event of two intensity maxima, titanium was characterized by an event of two intensity maxima at impact with the possibility of delayed ignitions and minor pulses of spectral irradiance as the titanium fragments traveled down range. This delayed ignition is most evident at impact velocities under 2500 fps. In this velocity range, a third maxima, which is larger than the previously recorded maxima by a factor of four, occurs 0.2 to 0.5 milliseconds after impact.

Coating the impact surface with polyurethane paint, barium titanate silicone paint, and flurocarbon paint reduced the flash by only a small amount. Coating the down range surface of the target with these paints had negligible effect on reducing flash over the range of impact velocities and wavelengths investigated during this test.

The spectral irradiance of the aluminum and titanium impact flashes were analyzed as approximations to blackbody radiation sources. From this analysis, the aluminum flash temperature was found to vary from 2800 to 2500° K over a velocity range of 3500 to 5000 fps, while the titanium flash temperature varied from approximately 2400 to approximately 4000° K over a velocity range of 3000 to 5000 fps.

In summary, the spectral irradiance and energy of the flash from titanium increases as the eighth power of the

velocity while the temperature ranges 2400 to 4000° K over
a velocity range of 3000 to 5000 fps. These values estab-
lish hypervelocity particles from sources such as surface-
to-air missiles, air-to-air missiles, and aircraft gun
systems as important kill mechanism to aircraft which
incorporate titanium in their design. This phenomena needs
much more investigation to determine its cause and to
develop more effective flash suppression materials.

V. Recommendations

The results of this investigation revealed three areas which require further study. First the delayed ignition characteristic of titanium should be investigated further. Particularly, the cause of the third and fourth flash maxima which occurs under 2500 fps should be determined. A delayed ignition of the magnitude observed in this investigation away from the impact surface would be a definite ignition source for aircraft fires.

Secondly, further work should be conducted in the area of flash temperature measurement. Studies should be conducted to determine the actual surface area of the flash viewed by the sensors at each wavelength and the effective emissivity at these wavelengths should be established. This data could be used to refine the blackbody approximation used in this study. Checks of this approximation could be accomplished by adding optical pyrometers to the test instrumentation.

Finally, further work should be done in the area of coating evaluation. Paints did not produce the desired results on titanium, but Mansur (Ref 2) found that fuel tank sealant was more effective in reducing impact flash from aluminum. This lead should be followed and expanded to include other state-of-the-art fuel cell additives, in particular foams and a fuel cell damage control system

(Ref 22) which consist of layers of ballistic nylon and reticulated rigidized foam. These studies, and all future studies in the area of ballistic impact flash, should add high speed photographic coverage to the test instrumentation for more detailed analysis of the flash propegation.

Bibliography

1. Kahler, R. L. "Impact Flash Suppression". _Joint United States Air Force-United States Navy Technical Symposium on Aircraft and Missile Vulnerability_. Symposium notes. Wright-Patterson Air Force Base, Ohio: 1952.

2. Mansur, John W. _Measurement of Ballistic Impact Flash_ Unpublished thesis. Wright-Patterson Air Force Base, Ohio: Air Force Institute of Technology, September 1974.

3. Artz, G. D. and H. W. Euker. _Summary Report of Phase II Gunfire Test Activities Conducted During The Period November 1972 Through December 1973_. TFD-74-268. Los Angeles, California: Rockwell International, March 1974.

4. Mangold, Vernon L. _Photographic Study of The Target Flash Produced By a Ballistic Impact_. AFFDL-TM-74-105-PTS. Wright-Patterson Air Force Base, Ohio: Air Force Flight Dynamics Laboratory, February 1974.

5. Friichtenicht, J. F. and J. C. Slattery. "Ionization Associated With Hypervelocity Impact". _Proceedings of The Sixth Symposium on Hypervelocity Impact_, 2: 591-612 (August 1963).

6. Jean, B. "Experimental Observations of Optical Radiation Associated With Hypervelocity Impact". _AIAA Journal_, 4: 1854-1856 (October 1966).

7. Jean, B. and T. L. Rollins. "Radiation From Hypervelocity Impact Generated Plasma". AIAA _Journal_, 8: 1742-1748 (October 1970).

8. Abernathy, John B. _Ballistic Impact Flash_. Unpublished thesis. Wright-Patterson Air Force Base, Ohio: Air Force Institute of Technology, June 1968.

9. Murrow, Charles E. _Vulnerability Study of a Generic Aircraft Fuel Subsystem_. NADC-72039-SD. Warmister, Pa: Naval Air Development Center, May 1972.

10. Wingfield, John R. _The Relationship of Projectile Properties and Downrange Ballistic Flash_. Unpublished thesis. Wright-Patterson Air Force Base, Ohio: Air Force Institute of Technology, December 1974.

11. Wiederhorn, Norman M. and John R. Ehrenfeld. *Project CHEOPS An Investigation of Hypervelocity Impact Flash*. AEDC-TDR-64-270. Bedford, Massachusetts: Geophysics Corporation of America, December 1964.

12. Clow, Douglas J. and Floyd L. Cooper. *Gunfire Test of F-15 No. 1 Fuel Tank Explosion Suppression Foam Configuration*. ASD-TR-74-15. Wright-Patterson Air Force Base, Ohio: Aeronautical Systems Division, April 1974.

13. Schmitt, George F., Jr. *Fluoroelastomer Coatings Resistant to Thermal Flash, High Temperature, and Subsonic Rain Erosion*. AFML-TR-74-25. Wright-Patterson Air Force Base, Ohio: Air Force Material Laboratory, April 1974.

14. Mar, Henry Y. and Paul B. Zimmer. *Infrared Diffuse Reflection/Thermal Camouflage Coatings*. AFML-TR-74-209. Wright-Patterson Air Force Base, Ohio: Air Force Material Laboratory, October 1974.

15. Schmitt, G. F., Jr., L. M. Peterson, and W. R. Griffin, *High Temperature Rain Erosion Resistant Fluoroelastomer Coating*. AFMT-TR-71-196. Wright-Patterson Air Force Base: Air Force Material Laboratory, November 1971.

16. Striganov, A. R. and N. S. Sventitskii. *Table of Spectral Lines of Neutral and Ionized Atoms*. New York: IFI/Plenum Data Corporation, 1968.

17. *Massachusetts Institute of Technology Wavelength Tables*. New York: John Wiley and Sons, Inc., June 1950.

18. Raab, David and Elizabeth Fehrer. "Supplementary Report: The Effect of Stimulus Duration and Luminance on Visual Reaction Time." *Journal of Experimental Psychology*, 64: 326-327 (1962).

19. *Smithsonian Physical Tables* (Ninth Revised Edition). Washington, D.C.: Smithsonian Institute Press, 1969.

20. *Encyclopedic Dictionary of Physics*, edited by J. Thewlis. New York: Pergomon Press, 1961.

21. Harrison, P. L. and A. D. Yoffe. "The Burning of Metals" in *Proceedings of the Royal Society of London*, Series A, Vol 261. London: The Royal Society, Burlington House, 23 May 1961.

22. Heitz, R. M. *Protection of Aircraft Fuel Systems Against Small Arms Fire*. NB-74-407. Hawthorne, California: Northrop Corporation, October 1974.

23. Brockert, P. E. and W. C. Cooley. <u>Development of an Impact Flash Spectrometer</u>. Project No. 7844. Eglin Air Force Base, Florida: Directorate of Armament Development, November 1965.

Appendix A

Description of Equipment

The experimental portion of this investigation was conducted in Ballistic Impact Test Facility Range Number One, Building 45, Area B, Wright-Patterson Air Force Base, Ohio. An overview of the test set up can be obtained from Figures 2, 3 and A-1. Using the target as a reference point, Figure 2 shows the up range test instrumentation while Figure 3 shows the down range instrumentation. Figure A-1 depicts the connections between range and control room instrumentation. The test equipment can be described in two general categories, the gun and instrumentation.

20 mm Smooth Bore Gun

The Air Force Flight Dynamics Laboratory furnished a 20 mm smooth bore gun. This gun had an eight foot barrel and was chambered to accept a standard military casing. The casings were primed with a standard 20 mm electric primer and the gun was fired electrically. By varying the powder loads from 70 grains to maximum load of 470 grains of Hercules 2400 smokeless rifle powder, projectile velocities ranging from just under 2000 fps to just over 5500 fps were obtained. The casings could have accommodated more powder and thus higher velocities could have been obtained, but range limitations, specifically the high over pressures in a closed range, made velocities above 5500 fps impractical.
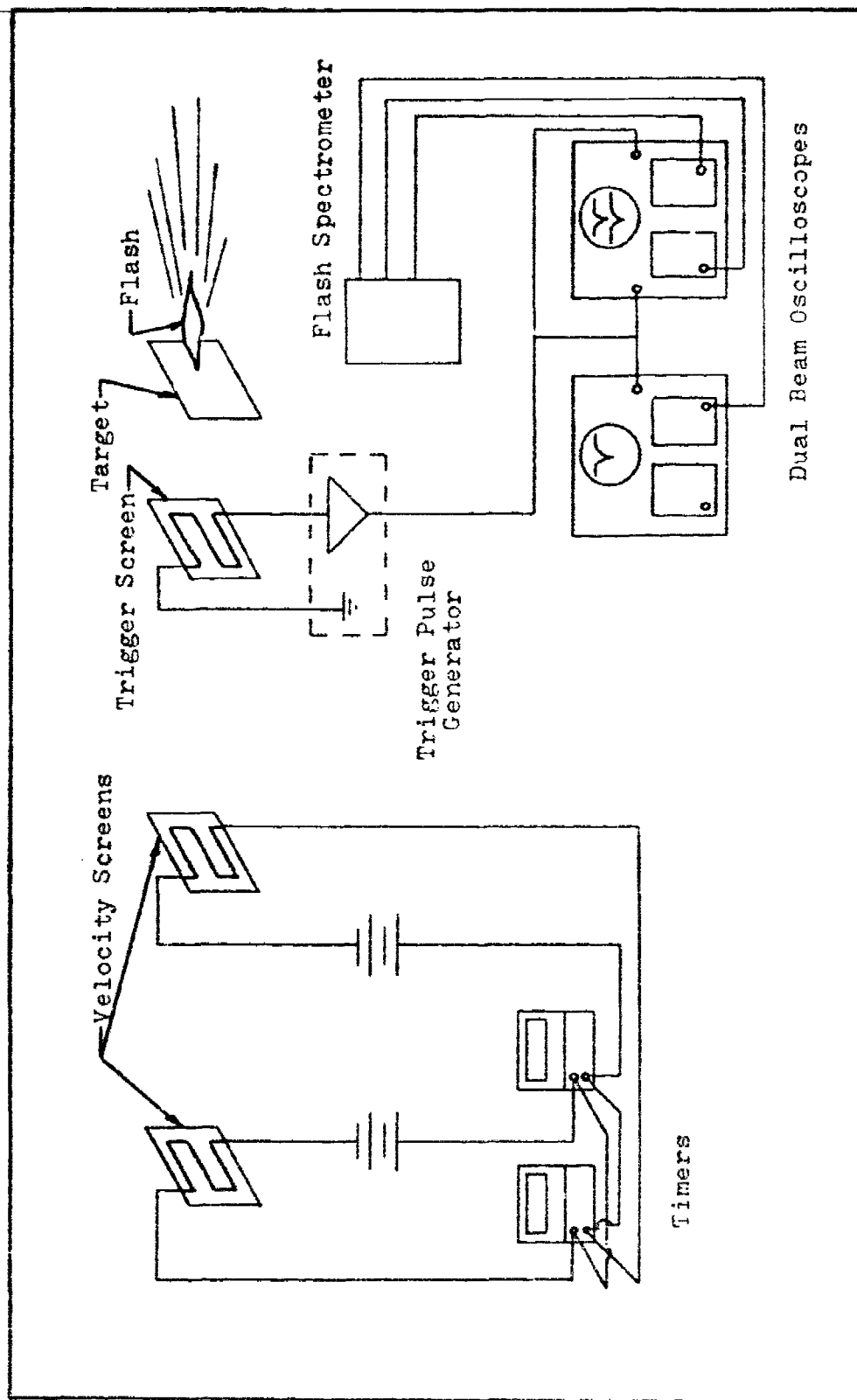
Figure A-1. Typical Instrumentation Setup

74

Instrumentation

This experiment required instrumentation to determine the relative impact velocity and analyze the down range flash. The flash analysis was accomplished through the use of a flash spectrometer, a still camera, and an image converter camera system.

Velocity Measurement. The projectile velocity was measured 29 feet prior to impact over a 4 foot distance. The velocity screens, shown in Figures 2 and A-1 consisted of continuous line printed circuit paper. The velocity screens were connected to two Hewlett-Packard Model 5300A timers as shown in Figure A-1. When a projectile passed through the first screen, both timers were started and perforation of the second velocity screen stopped the timers. The timer read-outs were in microseconds and were converted to velocities calculated to the nearest tenth of a foot per second.

Impact Flash Spectrometer. This system consists of an Exotech three channel spectrometer, low and high voltage power supplies, a Techtronic 556 Dual Beam Oscilloscope, and a Techtronic 565 Dual Beam Oscilloscope. Pretest checks of the spectrometer system revealed several undocumented alterations of the photomultiplier control circuits and defective components. Because the modifications were undocumented and made the systems reliability questionable, they were removed. The spectrometer system also included

three lead selenide sensors which were not used for this test. Analysis of the system circuitry (Ref 23:17) revealed that the control circuits for these sensors could be removed without effecting the photomultiplier tube circuits. This modification was made when the defective components were replaced. The circuitry used for power filtering and distribution is shown in Figure A-2 and the photomultiplier and emitter follower circuitry is shown in Figure A-3.

Each photomultiplier tube consisted of a photocathode, a secondary emission multiplier, and an anode. Photons from the light source strike the photocathode. This releases a number of electrons, which are accelerated onto the first stage or dynode of the multiplier, where they each release additional secondary electrons, which are accelerated onto the next dynode, and so on. A potential gradient is maintained between the successive dynode stages. The electrons released by the last dynode are collected at the anode, which releases an electric pulse as the tube output. The photomultiplier tubes used in this test were two KM2433 visible range tubes and one 6911 infrared tube, all manufactured by DuMont Laboratories Division of Fairchild Camera and Instrument Corporation. The one infrared tube had a type S-1 spectral sensitivity (Figure A-4) and the two visual tubes had a type S-20 spectral sensitivity (Figure A-5). To allow examination of the flash at various wavelengths, narrow band by-pass filters were placed in front of the photomultiplier tubes.
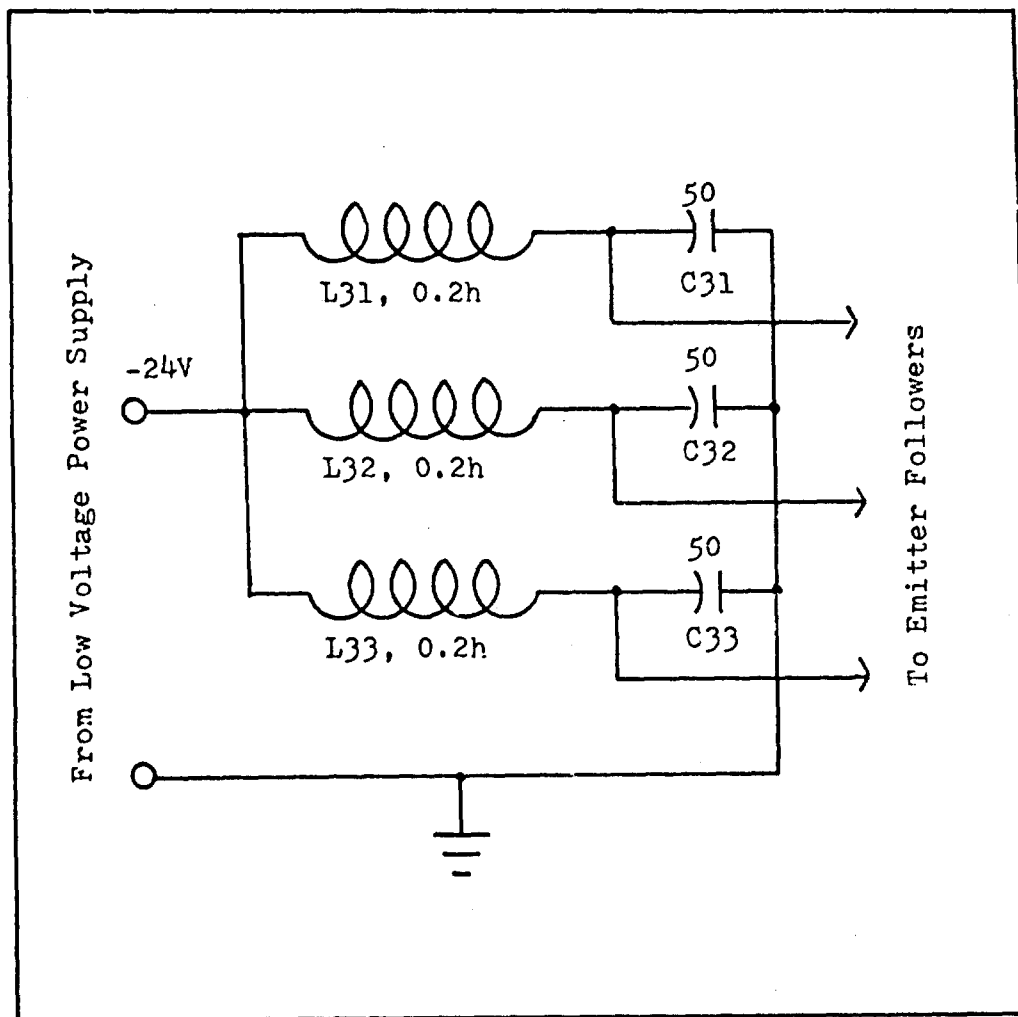
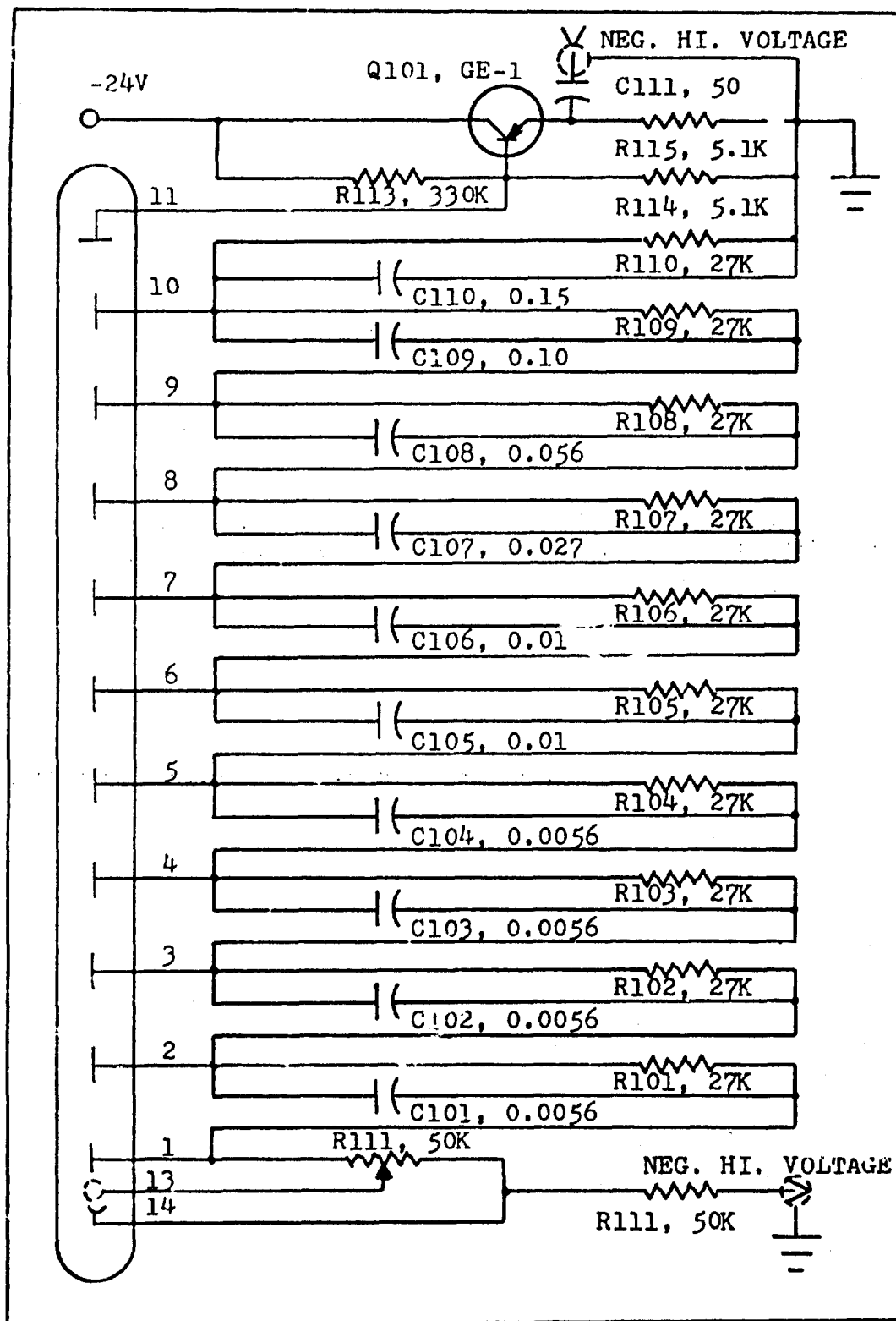Figure A-2. Power Filtering and Distribution Circuitry

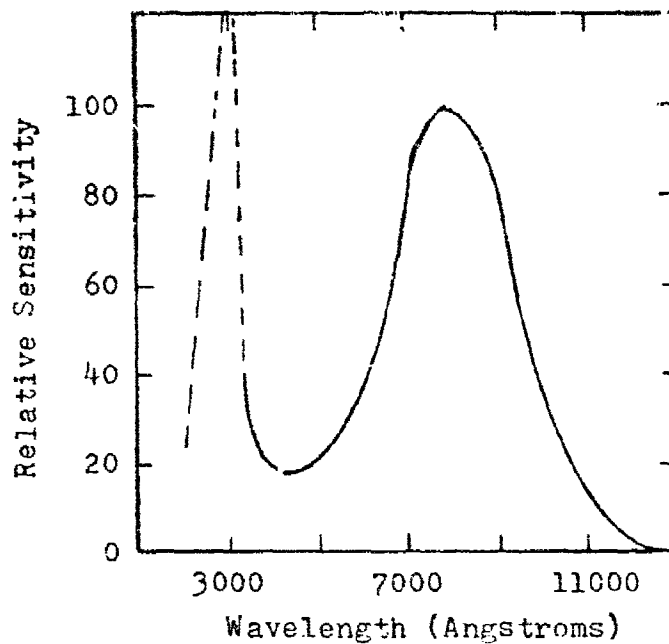Figure A-3. Photomultiplier and Emitter Follower Circuitry

Figure A-4.   Type S-1 Photomultiplier Tube
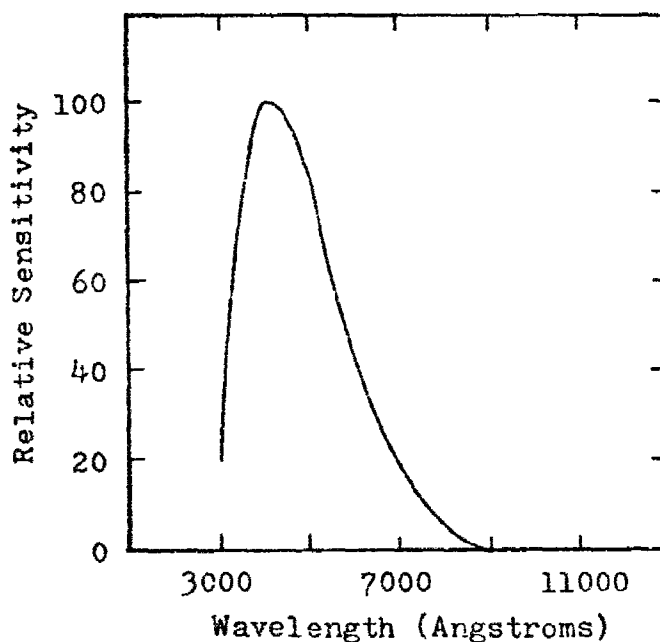Spectral Sensitivity Curve

Figure A-5.   Type S-20 Photomultiplier Tube
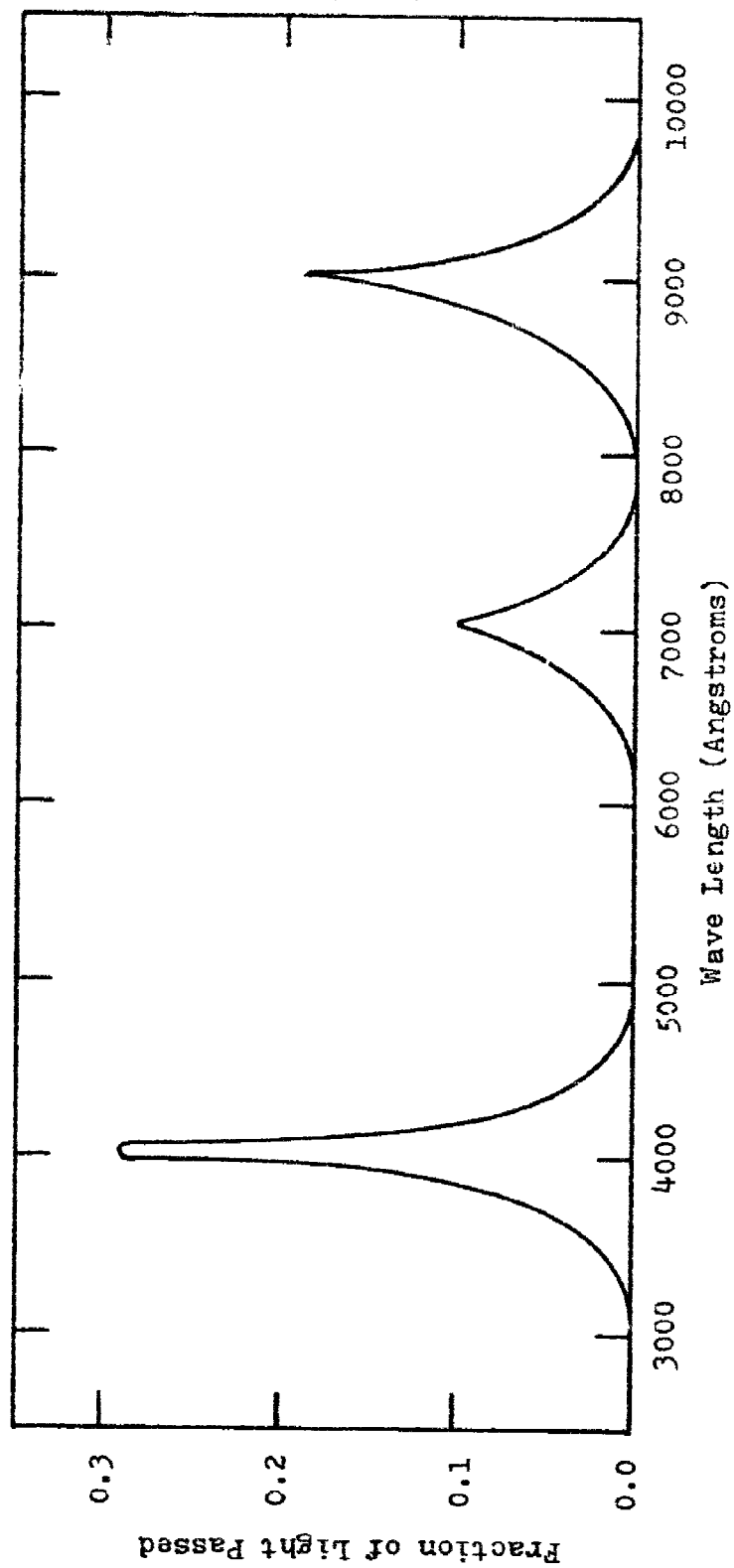Spectral Sensitivity Curve

79

Figure A-6. Spectral Response of Narrow Band By-Pass Filters

To avoid saturating the photomultiplier tubes, Kodak Wratten neutral density filters were used to reduce the number of photons striking the sensors. These filters were calibrated for each combination of photomultiplier tube and narrow band by-pass filter. This data is presented in Appendix B.

The output of the photomultiplier tubes was routed to the two oscilloscopes as shown in Figure A-1. The scope sweeps were triggered by a third sheet of printed circuit paper located two feet in front of the target. Perforation of this sheet of paper activated a Field Emission Corporation Model 1463 Trigger Generator, which insured trace sweep start before Projectile impact.

Still Camera. A 4 x 5 Speed Graphic Camera, which used Polaroid film, was used to obtain one view of the down range flash. The shutter was opened using a remote trigger prior to the shot and closed after the shot.

Image Converter Camera. A Beckman and Whitley X500 Biplanar Image Converter Camera System was used to obtain a different view of the down range flash. This system consisted of two Model 510M camera systems, a Model 5001 Four Channel Time Delay, and two camera heads which use standard Polaroid film. The time delay circuitry did not function properly during this test which resulted in this unit being used only as an open shutter still camera. As with the still camera, the shutter was opened prior to the shot and closed after the shot.

Appendix B

Calibration

The oscilloscope traces were recorded in volts per division and milliseconds per divisions. To convert this data to more usable values, the following calibration conversion calculations were performed.

Calibration of Photomultiplier Tubes

A calibration light source was provided with the spectrometer system. The light source assembly consists of a 1000 watt quartz iodide bulb, a mechanical chopper, and a power supply. The bulb is housed in a 24 inch diameter, 36 inch high cylinder, with aperture allowing a beam of light to pass through the chopper assembly. The chopper consists of an 18 inch diameter disc with a single slot. The disc was turned at a rate of about 3000 rpm by a small motor. The "chopped" light was directed on to the spectrometer sensors for calibration. The light source was calibrated by the National Bureau of Standards (Ref 23:6) in microwatts per cm^2-nanometer at a distance of 50 cm. The calibration values used in this test are present in Table B-I.

Table B-I

Calibration Strengths at 50 cm

Wavelength	Strength
4008A	2.28 μw/cm^2-nm
7010A	21.10 μw/cm^2-nm
9025A	25.28 μw/cm^2-nm

Calibration Procedure. The calibration source was placed at various distances from the spectrometer, and the high voltage power supply was set at 900 volts. The scope output for each narrow band by-pass filter was noted and recorded for each position. Since the light intensity should change by the square of the distance, a constant value of D^2V was expected, where D is the distance between the source and the sensor and V is the recorded voltage. Values of D^2V constant within five percent were obtained. From this an average value of D^2V at the various wavelengths was calculated and recorded in Table B-II.

Table B-II

D^2V Constants for Test Wavelengths

Wavelength	D^2V Constant
4008A	640.0 ft^2 volts
7010A	600.0 ft^2 volts
9025A	36.0 ft^2 volts

The values in Table B-II were used to calculate the conversion factors necessary to convert the flash induced scope output to $\mu w/cm^2$-nm.

Sample Calculation of Conversion Factor. From Table B-1, at 50 cm (1.64 ft) the source produces 2.28 $\mu w/cm^2$-nm for a wavelength of 4008A. Since the D^2V constant for this wavelength is 640.0 ft^2 volts (Table B-II), at a distance of 1.64 ft, an out put of

$$\frac{640.0 \ ft^2 \ volts}{(1.64 \ ft)^2} = 237.95 \ volts \qquad (4)$$

would be expected as a result of 2.28 $\mu w/cm^2$-nm of light irradiance produced by the source. This gives for 1.64 ft

$$\frac{2.28 \ \mu w/cm^2\text{-nm}}{237.95 \ volts} = 0.00958 \ \frac{\mu w/cm^2\text{-nm}}{volt} \qquad (5)$$

At D = 7.0 ft, which was the distance from the flash to the sensors, the scale factor required to convert the scope reading from volts to microwatts/cm^2-nm is

$$Scale \ Factor = \frac{(0.00958 \ \mu w/cm^2\text{-nm/volt})(7.0 \ ft)^2}{(1.64 \ ft)^2} \qquad (6)$$

$$= 0.1745 \ \mu w/cm^2\text{-nm/volt}.$$

Similarly at λ = 7010A

$$Scale \ Factor = 1.72316 \ \mu w/cm^2\text{-nm/volt}$$

and for λ = 9025A

$$Scale \ Factor = 34.408 \ \mu w/cm^2\text{-nm/volt}.$$

Calibration of Kodak Wratten Neutral Density Filters

Kodak Wratten Neutral Density No. 96 filters numbered
at 0.5, 1.0, and 2.0 were used. To determine the amount of
light passed by each filter, scope readings were taken with
and without the filters in place. In addition, combinations
of different strength filters were used to insure the read-
ings remained valid. The results of this are shown in Table
B-III.

Table B-III

Fraction of Light Passed at Selected Wavelengths
by Kodak Wratten Neutral Density No. 96 Filters

| | Amount of Light Passed | | |
Filter No.	4008A	7010A	9025A
0.5	0.3607	0.4814	0.5000
1.0	0.0950	0.1480	0.2600
2.0	0.0041	0.0148	0.0600

The raw data from the neutral density filter evaluation
was processed in the same manner as the photomultiplier tube
calibration. The results from these calculations are
presented in Table B-IV which lists all the conversion
factors used for data reduction in this report.

Scale Factors for All Test Filters

Filter No.	Conversion Factor ($\mu w/cm^2$-nm/volt)		
	4008A	7010A	9025A
0.0 (none)	0.183	1.915	12.387
0.5	0.508	3.977	24.774
1.0	1.926	12.928	47.643
2.0	44.688	128.238	206.453

Appendix C

Test Data

Over 100 test shots were conducted during this
investigation. Compiled in this appendix are the tables
of the results of these shots and graphs of the data from
each series of shots at each of the three wavelengths
investigated. The converted test data was processed by
the Air Force Aeronautical System Division's Control Data
Corporation 6600 computer located at Wright-Patterson Air
Force Base, Ohio. This computer facility was used to
compute the least squares curve approximation to the test
data and generate Figures 7 through 33 and Figures C-1
through C-20.

Table C-I

Spectral Irradiance of First Flash Maxima for Uncoated Titanium Target Impacts

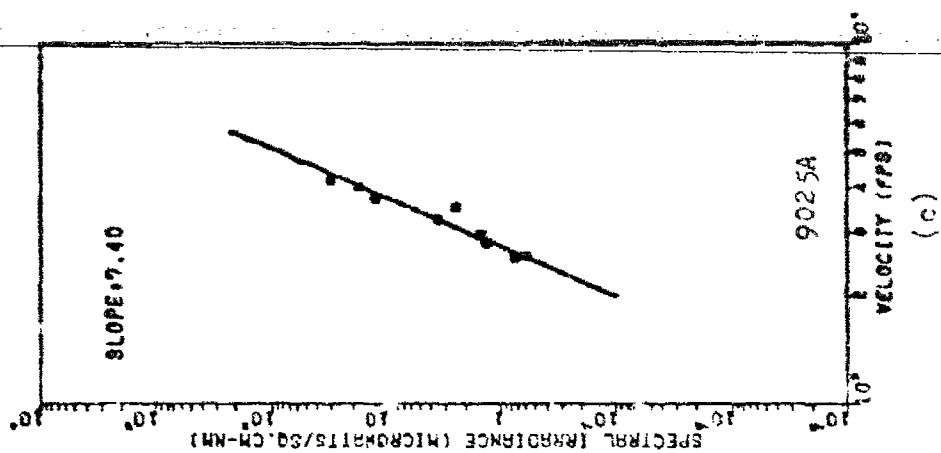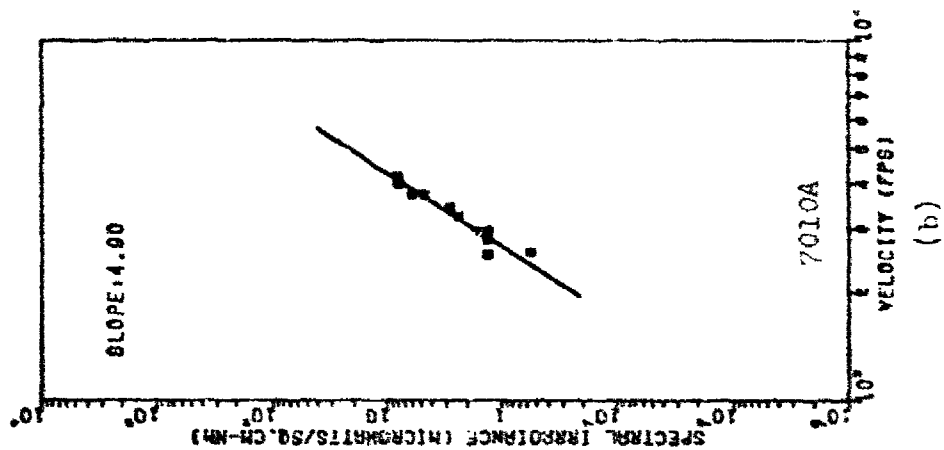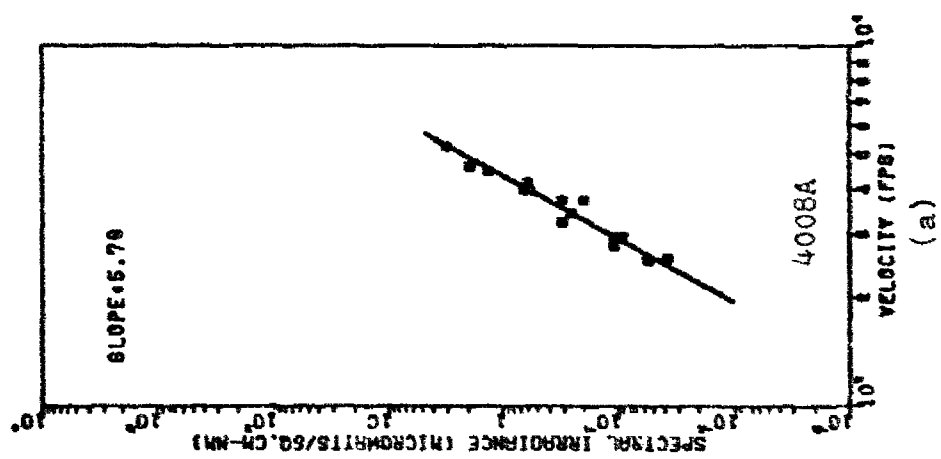| Velocity (FPS)	Spectral Irradiance (Microwatts/cm^2-nm)		
	4008A	7010A	9025A
2548.0	0.0549	1.3405	0.7432
2564.7	0.0366	0.5745	0.6194
2801.1	0.1098	1.3405	1.3626
2954.0	0.1098	1.3405	1.4864
2956.3	0.0915	1.5320	n
3246.8	0.3048	2.3862	3.4684
3439.4	0.2562	2.8725	n
3508.8	n	n	2.4774
3707.1	0.2032	4.7724	12.3870
3714.0	0.3048	5.9655	n
3964.3	0.6604	7.9540	17.3418
4000.0	0.5856	7.6600	n
4153.7	0.6096	7.9540	29.7288
4454.3	1.3176	n	n
4618.9	1.9260	n	n
5221.9	3.0480	n	n

n - no data

88

Figure C-1. Uncoated Titanium First Flash Maxima vs Velocity

Table C-II

Spectral Irradiance of Second Flash Maxima
for Uncoated Titanium Target Impacts

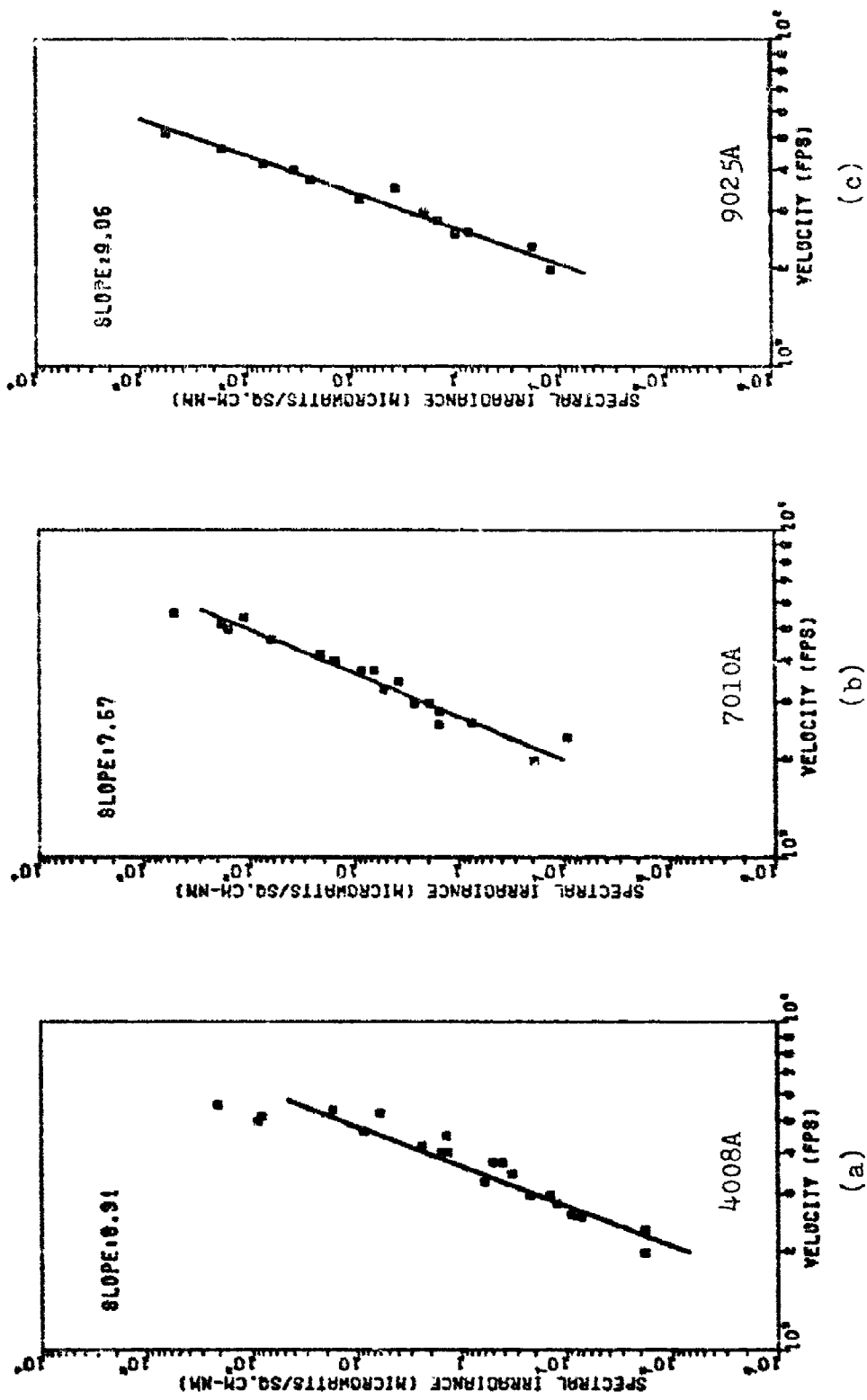| Velocity (FPS)	Spectral Irradiance (Microwatts/cm^2-nm)		
	4008A	7010A	9025A
1971.4	0.0183	0.1915	0.1239
2320.2	0.0183	0.0958	0.1858
2548.0	0.0732	1.5320	0.9909
2564.7	0.0915	0.7660	0.7432
2801.1	0.1281	1.5320	1.4864
2954.0	0.1464	1.9150	1.9819
2956.3	0.2196	2.6810	n
3246.8	0.6096	5.1701	8.4232
3439.4	0.3294	3.8300	n
3508.8	n	n	3.7161
3707.1	0.5080	8.7494	24.7740
3714.0	0.4064	6.3632	n
3964.3	1.5240	15.1126	34.6836
4000.0	1.3542	15.7030	n
4153.7	2.3368	21.4758	69.3672
4454.3	1.3908	n	n
4618.9	8.4744	62.1024	171.5148
4926.1	89.3760	155.0856	n
5115.1	80.4384	180.9332	578.0684
5221.9	6.0960	n	n
5390.8	17.7192	113.7664	n
5578.8	205.2528	516.9520	n

n - no data

Figure C-2. Uncoated Titanium Second Flash Maxima vs Velocity
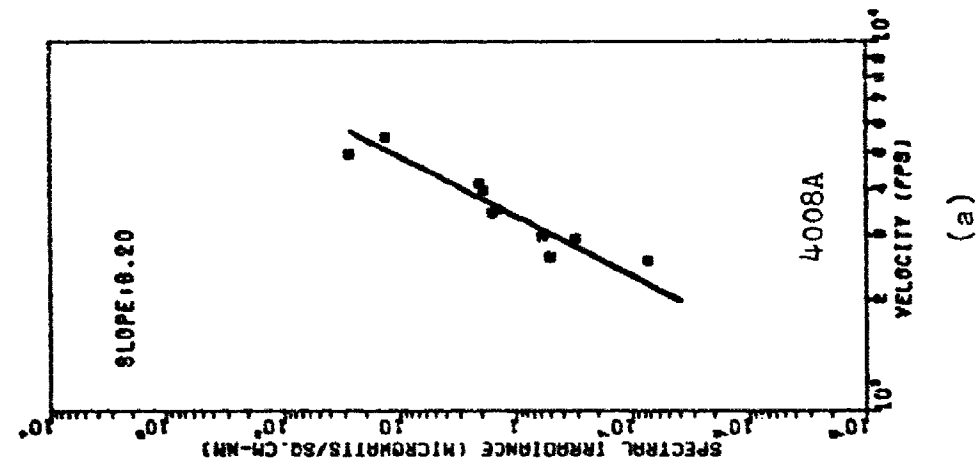
Table C-III

Spectral Irradiance for Uncoated
Aluminum Target Impacts

First Flash Maxima

Velocity (FPS)	Spectral Irradiance (Microwatts/cm^2-nm)		
	4008A	7010A	9025A
2108.2	n	n	n
2536.5	0.0732	0.3830	0.2477
2612.7	0.5124	n	4.9546
2911.2	0.3111	1.5320	0.7432
2943.3	0.5856	2.6810	2.7251
3427.6	1.6104	n	n
3514.9	1.4224	4.7724	n
3944.8	1.9304	6.3632	7.9277
4140.8	2.0320	7.1586	12.3870
4938.3	26.8128	n	n
5464.5	13.4064	n	n

Second Flash Maxima

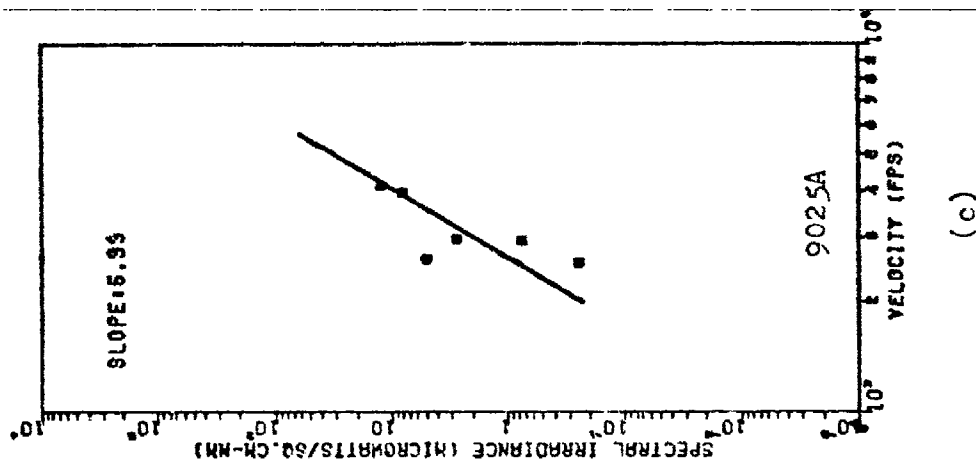| Velocity (FPS)	4008A	7010A	9025A
2108.2	0.1281	0.9575	0.4335
2536.5	0.1464	0.7660	0.6194
2612.7	0.3294	0.3830	2.4774
2911.2	0.4392	2.1065	1.2387
2943.3	0.6222	3.0640	3.2206
3427.6	1.9764	n	n
3514.9	2.5400	9.5448	13.8734
3944.8	3.2512	11.1356	14.8644
4140.8	2.7432	12.7264	29.7288
4938.3	49.1568	25.8476	61.9359
5464.5	26.8128	25.8476	82.5812

n - no data

92
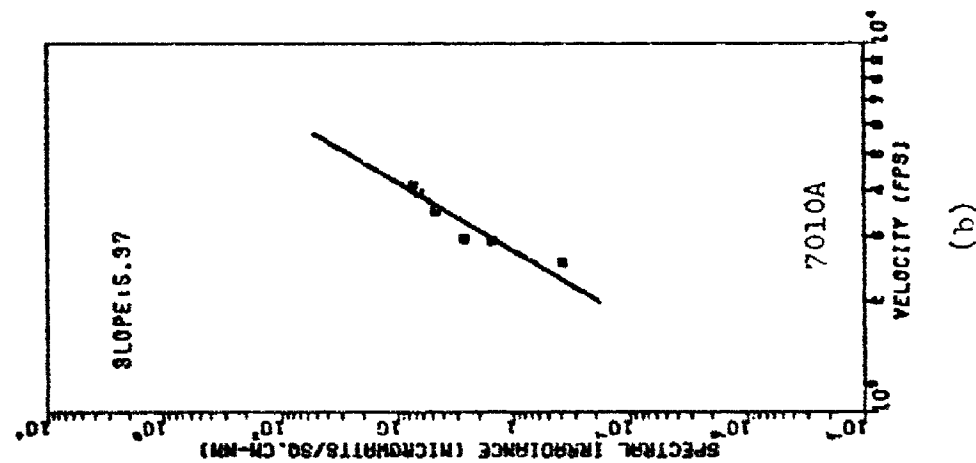
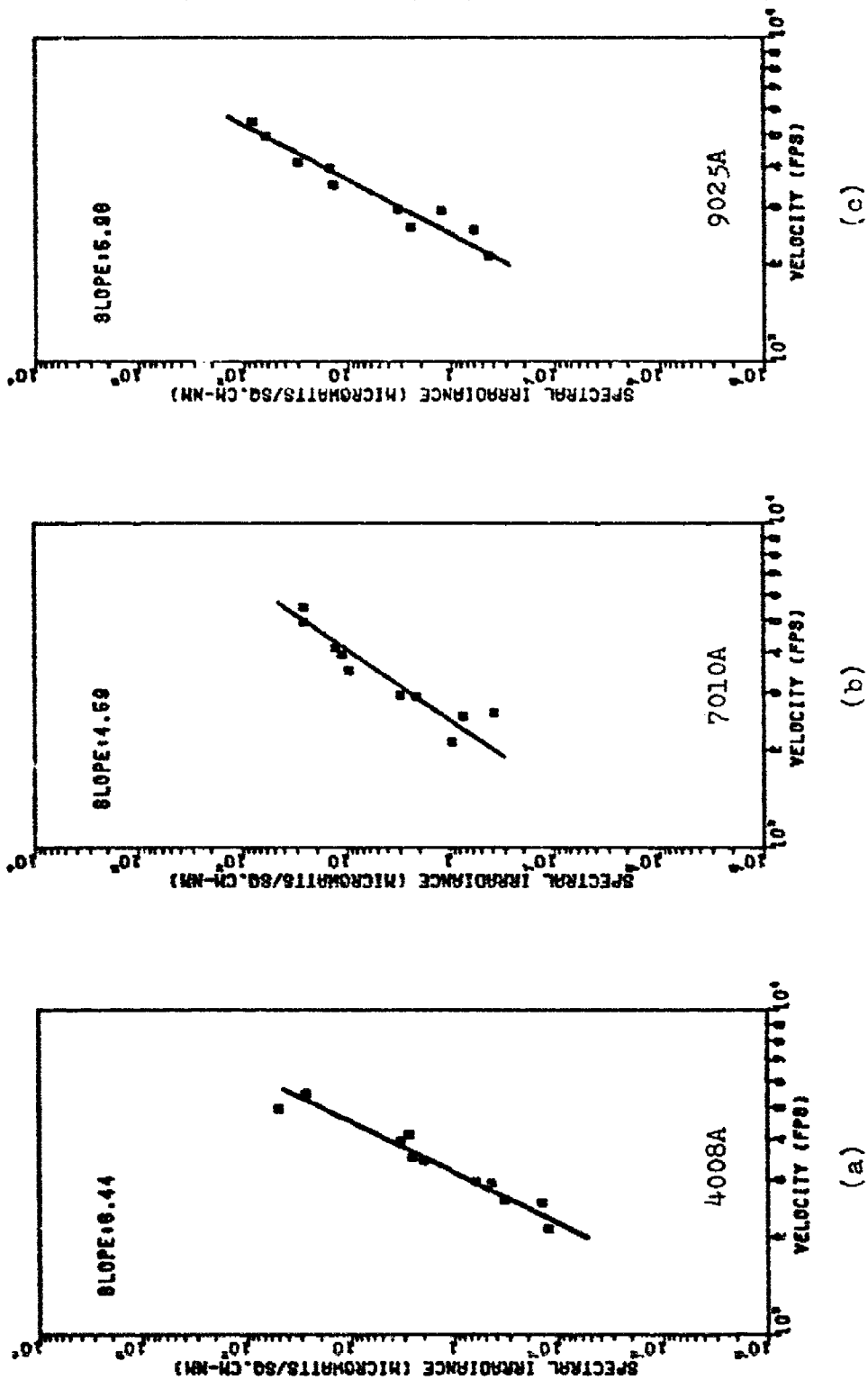Figure C-3. Uncoated Aluminum First Flash Maxima vs Velocity

Figure C-4. Uncoated Aluminum Second Flash Maxima vs Velocity

Table C-IV

Spectral Irradiance for White Polyurethane Paint Coated Titanium Target
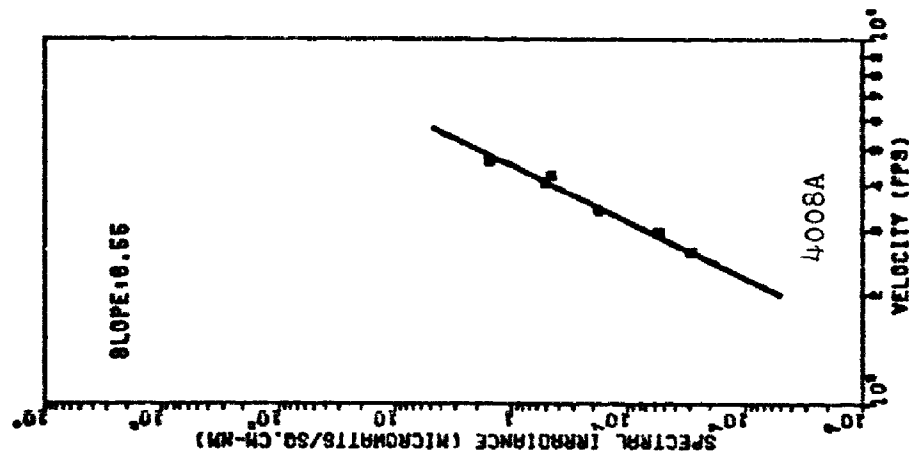### (Coating on Up Range Side)

First Flash Maxima

Velocity (FPS)	Spectral Irradiance (Microwatts/cm^2-nm)		
	4008A	7010A	9025A
2151.7	n	n	n
2585.6	0.0293	0.4405	0.6194
2943.3	0.0549	0.9575	0.7432
3389.8	0.1830	3.4470	n
4028.2	0.5080	10.7379	17.3418
4201.7	0.4572	5.5678	19.8192
4629.6	1.5408	10.3424	28.5882
5256.2	n	n	n
5509.5	n	n	n

Second Flash Maxima

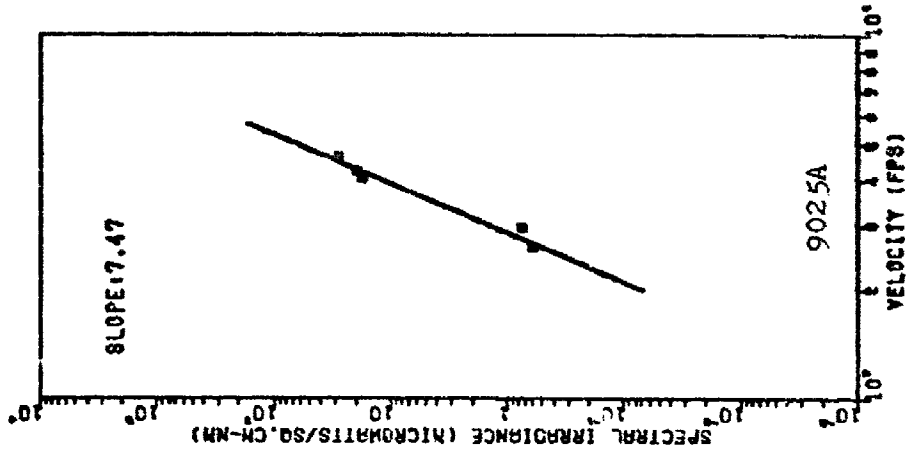| Velocity (FPS)	4008A	7010A	9025A
2151.7	0.0109	0.2298	0.2477
2585.6	0.0384	0.4022	0.5572
2943.3	0.0915	1.1490	0.8671
3389.8	0.2562	3.8300	n
4028.2	0.6096	8.7494	15.3598
4201.7	1.5240	12.7264	39.6384
4629.6	3.8520	24.5632	57.1716
5256.2	31.2800	77.5428	123.8718
5509.5	44.6880	77.5428	165.1624

n - no data
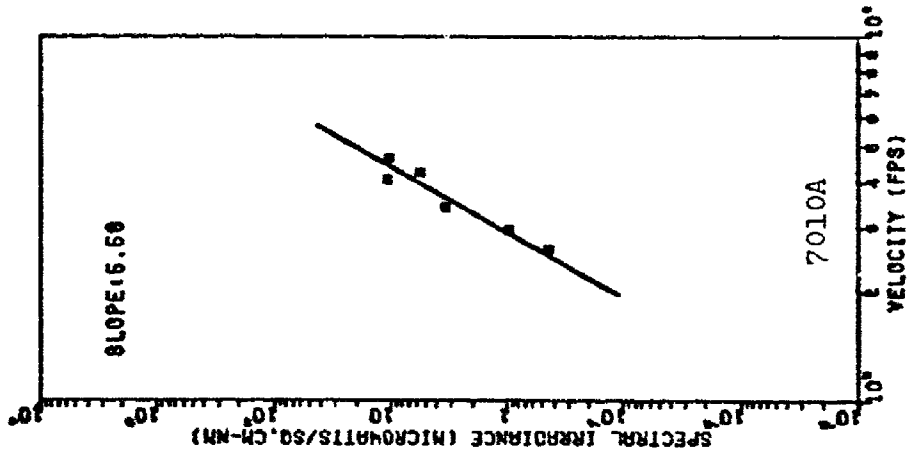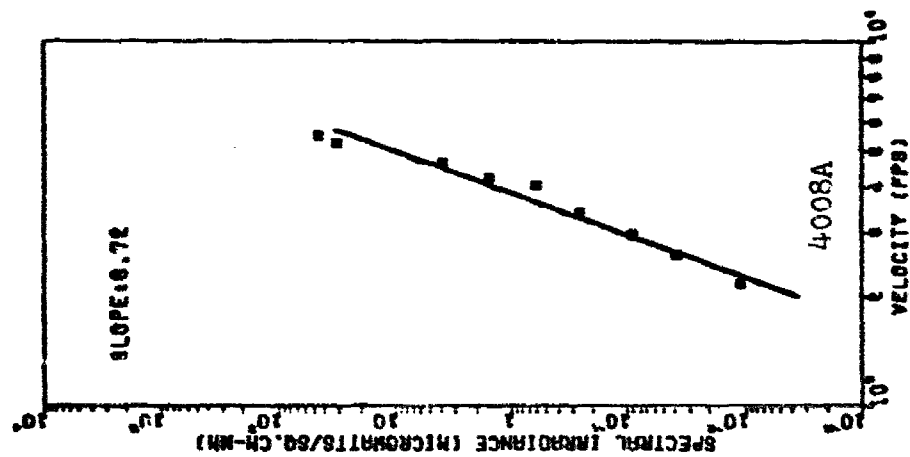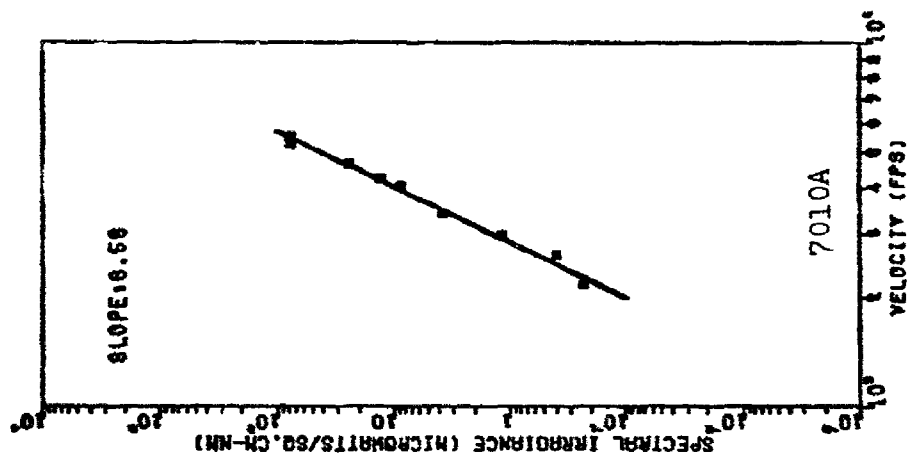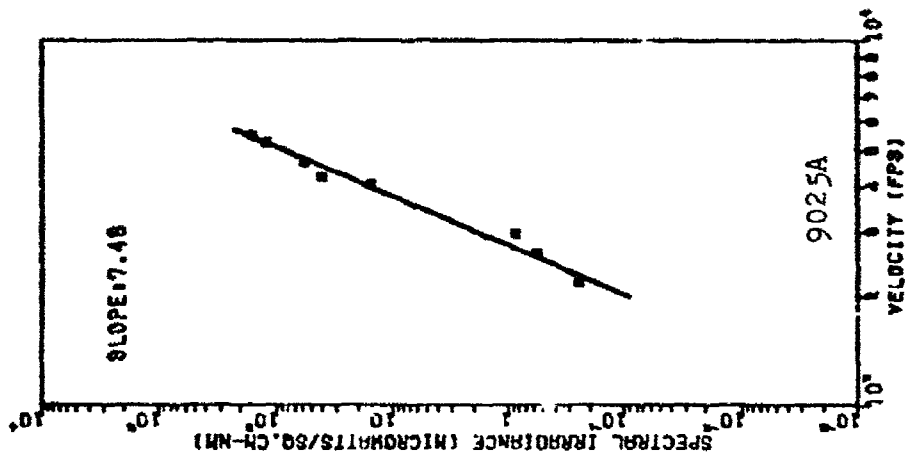
Figure C-5. Polyurethane Paint Coated Titanium First Flash Maxima vs Velocity
(Coating on Up Range Side)

Figure C-6. Polyurethane Paint Coated Titanium Second Flash Maxima vs Velocity
(Coating on Up Range Side)

Table C-V

Spectral Irradiance for White Polyurethane
Paint Coated Titanium Target
(Coating on Down Range Side)

First Flash Maxima

Velocity (FPS)	Spectral Irradiance (Microwatts/cm^2-nm)		
	4008A	7010A	9025A
2115.3	n	n	0.1486
2580.6	0.0549	0.7660	0.6193
2909.1	0.0732	1.5320	n
2949.9	0.1464	3.0640	n
3472.2	0.1464	3.8300	4.9548
3976.1	n	4.7724	n
4535.1	n	n	n
4896.0	17.8750	77.5428	n
5449.6	26.8128	155.0850	n

Second Flash Maxima

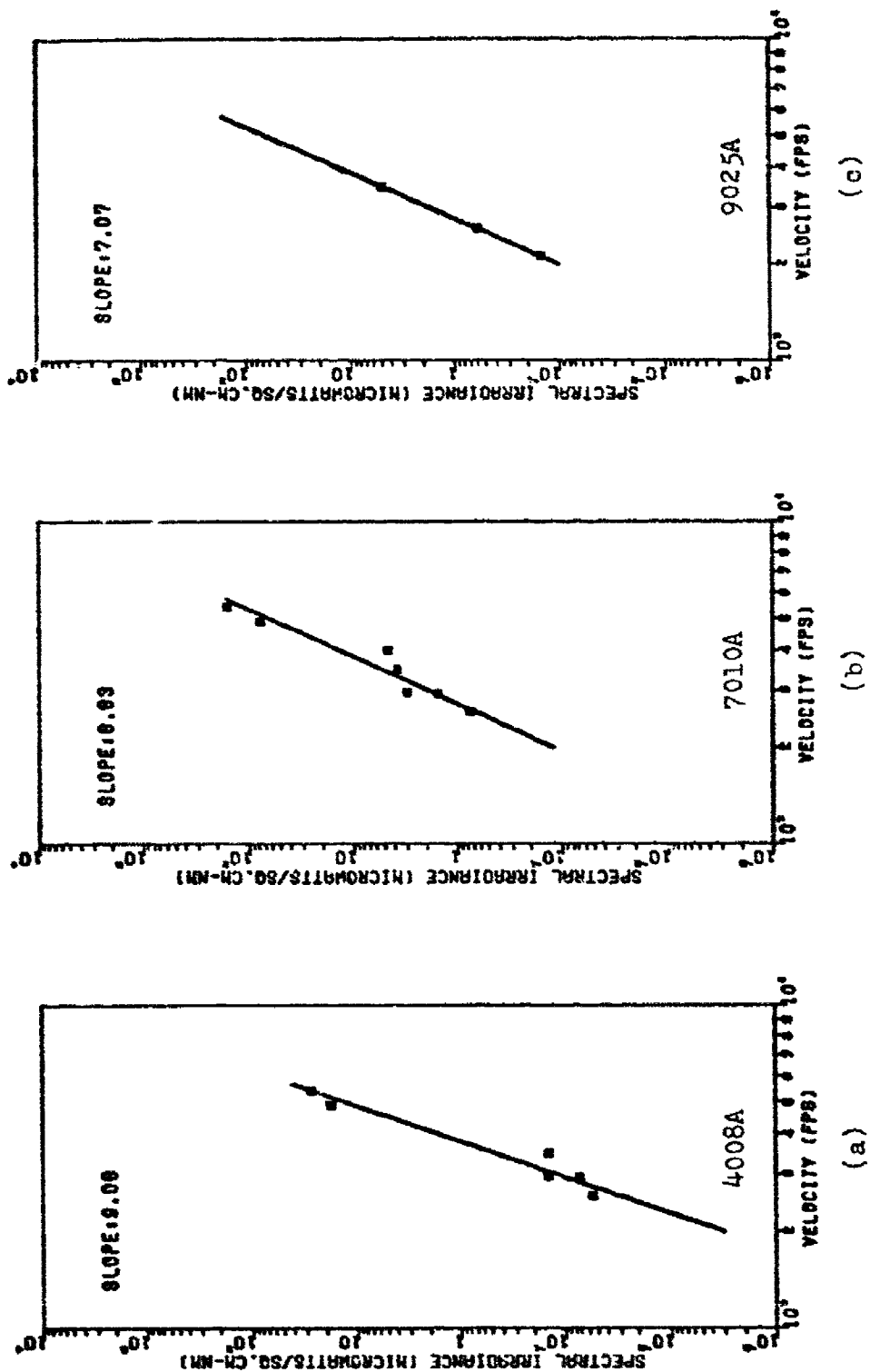| Velocity (FPS)	4008A	7010A	9025A
2115.3	0.0256	0.2681	0.1982
2580.6	0.0732	1.0533	0.9989
2909.1	0.1093	2.2980	n
2949.9	0.4209	5.5535	n
3472.2	0.4392	5.3620	7.4322
3976.1	1.3208	16.7034	n
4535.1	7.7040	n	214.3900
4896.0	71.5008	168.0090	516.1300
5449.6	71.5008	413.5600	743.2300

n - no data

98

Figure C-7. Polyurethane Paint Coated Titanium First Flash Maxima vs Velocity
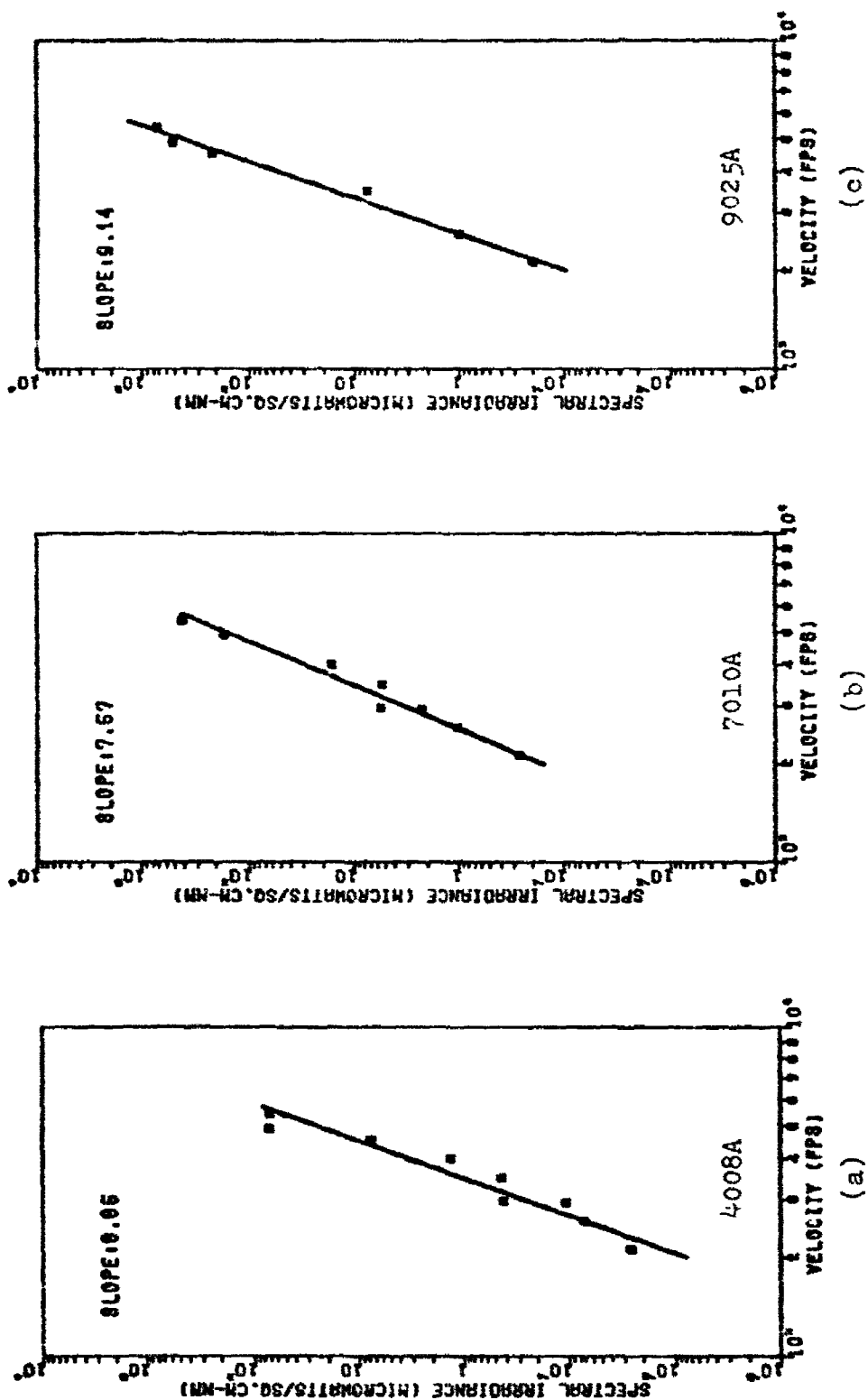(Coating on Down Range Side)

99

Figure C-8. Polyurethane Paint Coated Titanium Second Flash Maxima vs Velocity

(Coating on Down Range Side)

Table C-VI

Spectral Irradiance for Barium Titanate
Paint Coated Titanium Target
(Coating on Up Range Side)

First Flash Maxima

Velocity (FPS)	Spectral Irradiance (Microwatts/cm^2-nm)		
	4008A	7010A	5025A
2123.2	n	n	n
2560.8	0.0183	0.1915	0.1238
2902.8	0.0549	0.7660	n
2936.6	0.0732	0.9575	0.7433
3454.2	0.3660	3.8300	6.9367
3988.0	1.5240	14.3172	n
4028.2	n	n	n
4241.8	3.9770	3.9770	n
4592.4	n	n	n
5263.2	n	n	n
5509.6	n	n	n

Second Flash Maxima

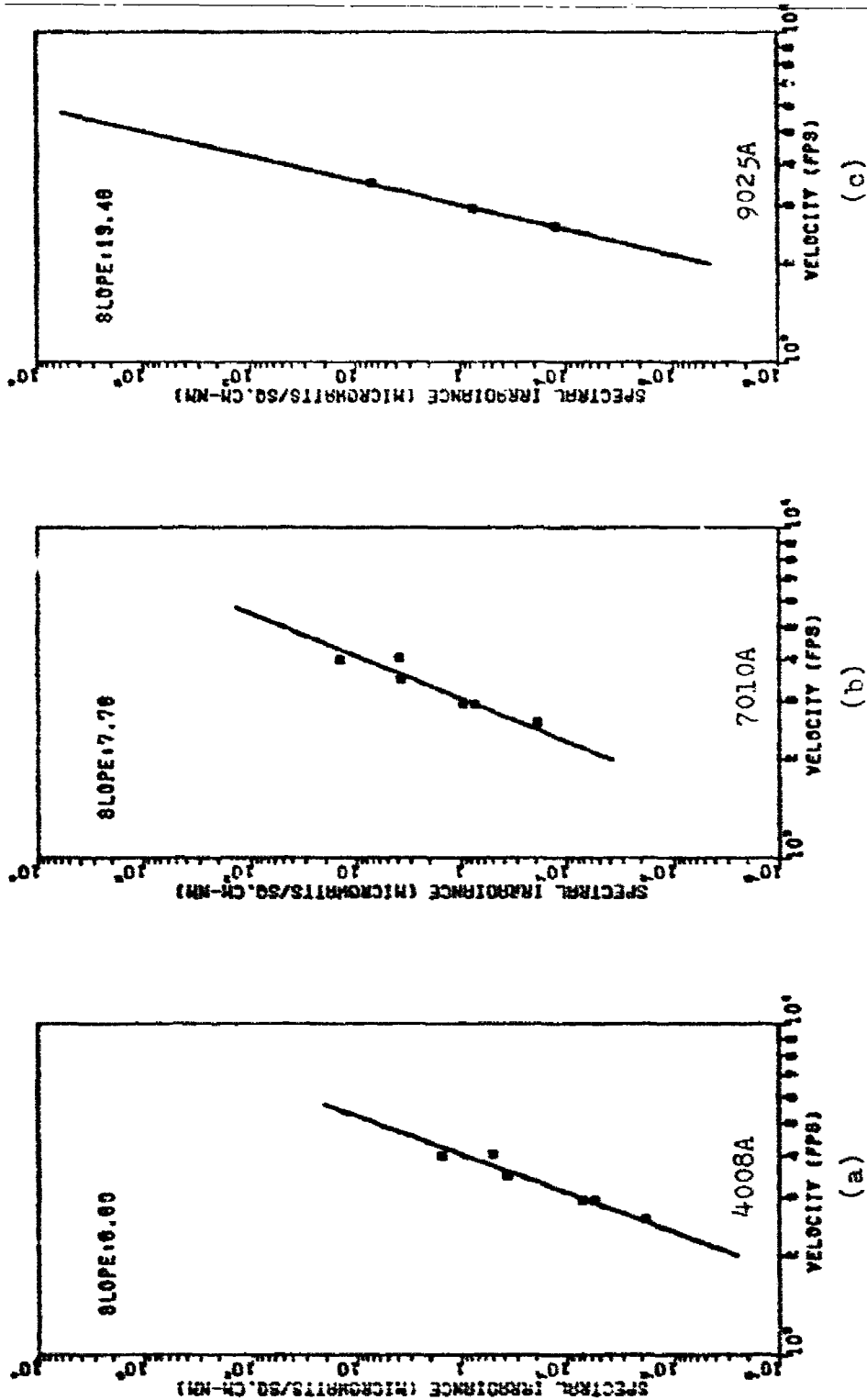| Velocity (FPS)	4008A	7010A	5025A
2123.2	n	0.0383	0.0495
2560.8	0.0366	0.3830	0.1858
2902.8	0.1281	1.1490	n
2932.6	0.1464	1.2447	1.1148
3454.2	0.5124	6.1280	8.4231
3988.0	1.6256	14.3172	n
4028.2	1.1176	11.1356	
4241.8	1.7272	14.3172	42.1158
4592.4	3.4668	25.8560	76.2288
5263.2	53.6256	64.6190	206.4530
5509.6	35.7500	77.5428	247.7400

n - no data

Figure C-9. Barium Titanate Silicone Paint Coated Titanium First Flash Maxima vs Velocity (Coating on Up Range Side)
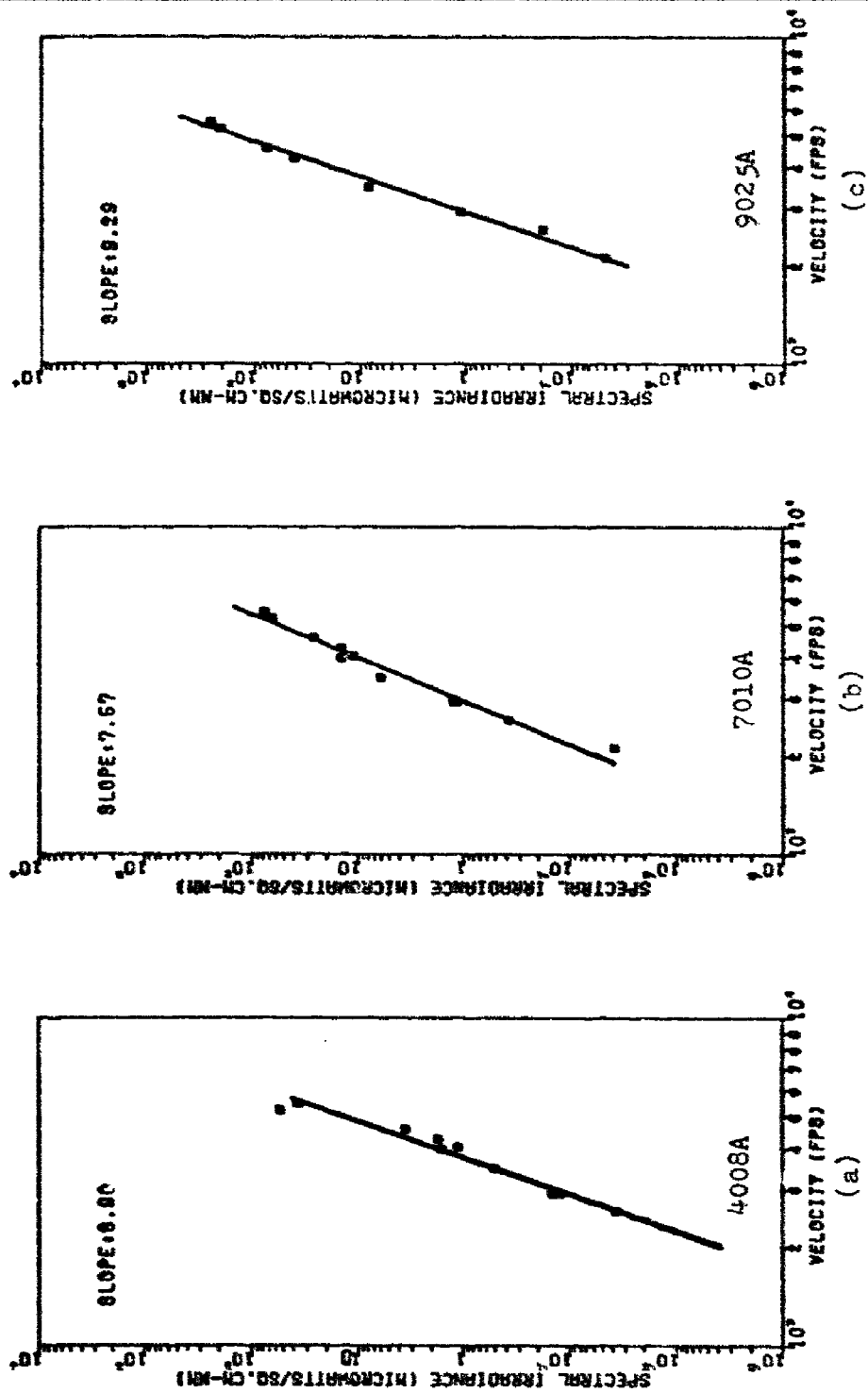
Figure C-10. Barium Titanate Silicone Paint Coated Titanium Second Flash Maxima vs Velocity (Coating on Up Range Side)

103

Table C-VII

Spectral Irradiance for Barium Titanate
Paint Coated Titanium Target
(Coating on Down Range Side)

First Flash Maxima

Velocity (FPS)	Spectral Irradiance (Microwatts/cm^2-nm)		
	4008A	7010A	9025A
2594.0	0.0732	0.7660	0.6813
2960.8	0.1098	1.7235	1.7342
3445.3	0.2928	3.0640	3.2206
4008.0	0.6096	6.3632	12.3870
4514.7	0.7704	5.1712	n
4842.6	88.5200	64.6190	n
5464.4	n	n	n

Second Flash Maxima

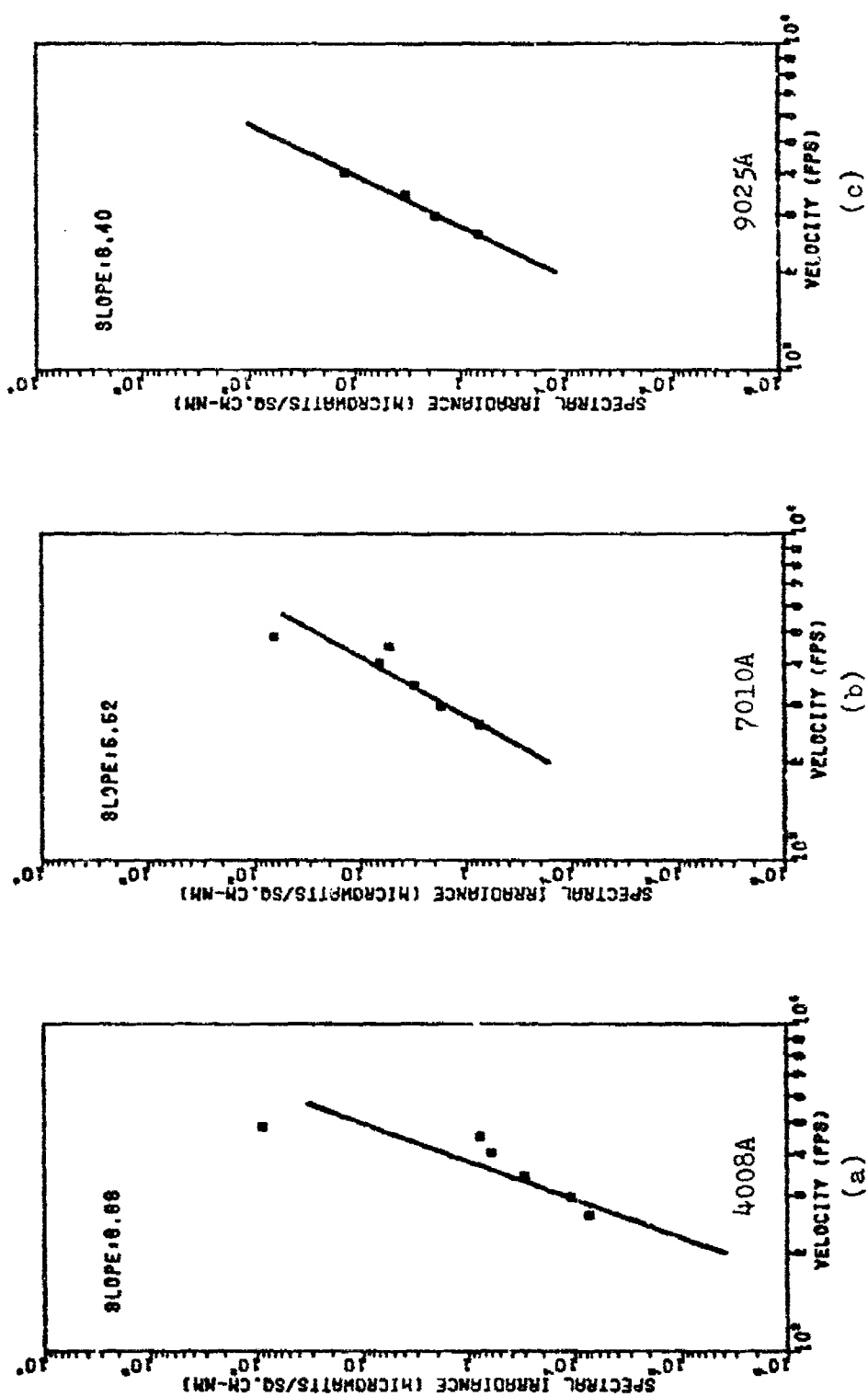| Velocity (FPS)	4008A	7010A	9025A
2594.0	0.0732	0.8617	0.7432
2960.8	0.2562	2.2980	1.9819
3445.3	0.6588	5.7415	7.9278
4008.0	1.6256	15.1126	34.6836
4514.7	7.7040	33.6128	199.6800
4842.6	61.9640	168.0094	722.5800
5464.4	177.0400	387.7140	1156.1360

n - no data

Figure C-11. Barium Titanate Silicone Paint Coated Titanium First Flash Maxima vs Velocity (Coating on Down Range Side)
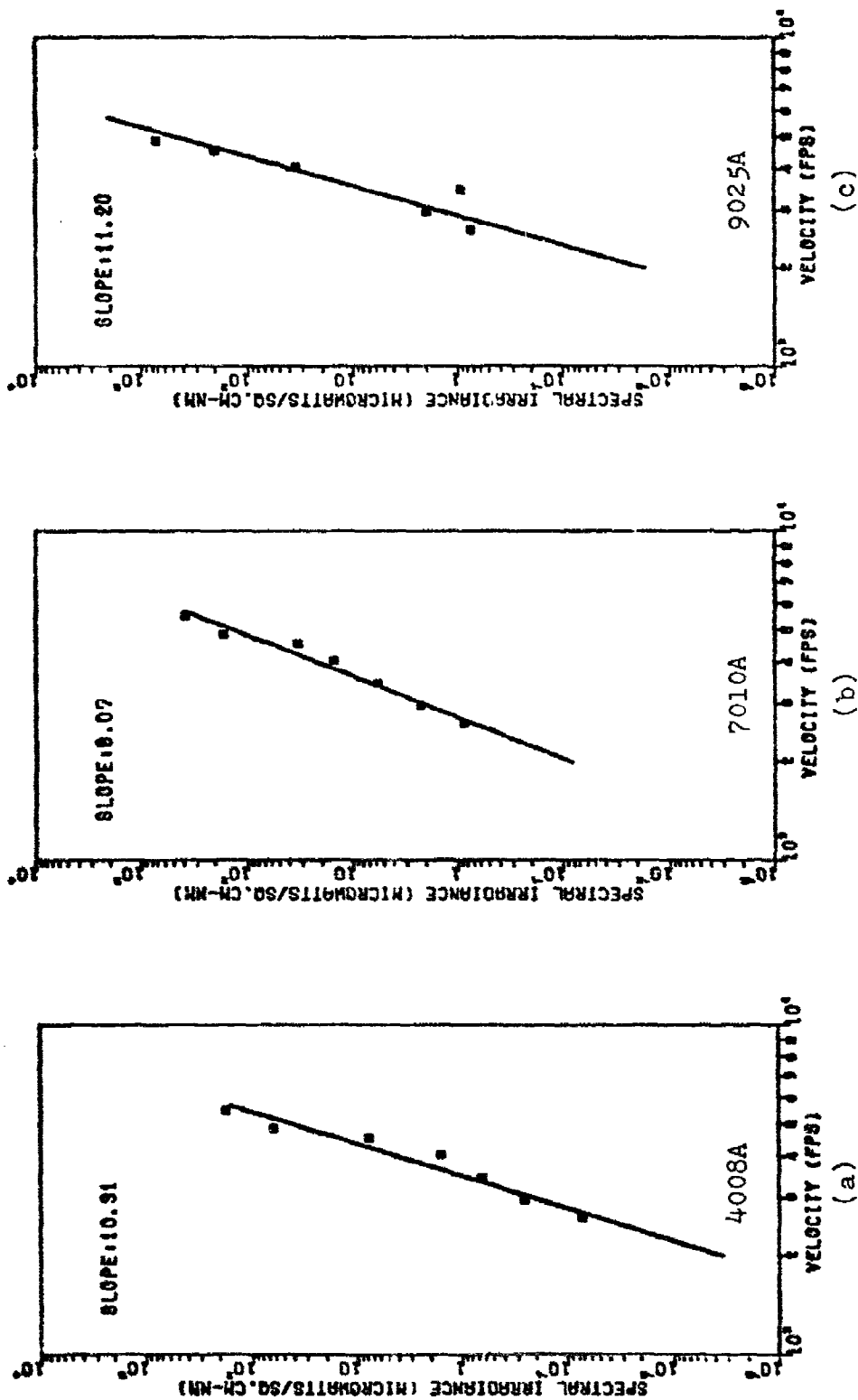
Figure C-12. Barium Titanate Silicone Paint Coated Titanium Second Flash Maxima vs Velocity (Coating on Down Range Side)

Table C-VIII

Spectral Irradiance for Flurocarbon
Paint Coated Titanium Target
(Coating on Up Range Side)

First Flash Maxima

Velocity (FPS)	Spectral Irradiance (Microwatts/cm^2-nm) 4008A	7010A	9025A
2584.0	n	0.1532	n
2605.9	n	0.1915	n
2928.3	0.1281	1.3405	0.9909
3493.4	0.3294	4.0215	4.4593
4028.2	1.1176	11.9310	19.8192
4597.7	1.5408	15.5136	38.1144
5256.2	13.4064	25.8476	82.5812
5524.8	13.4064	38.7714	n

Second Flash Maxima

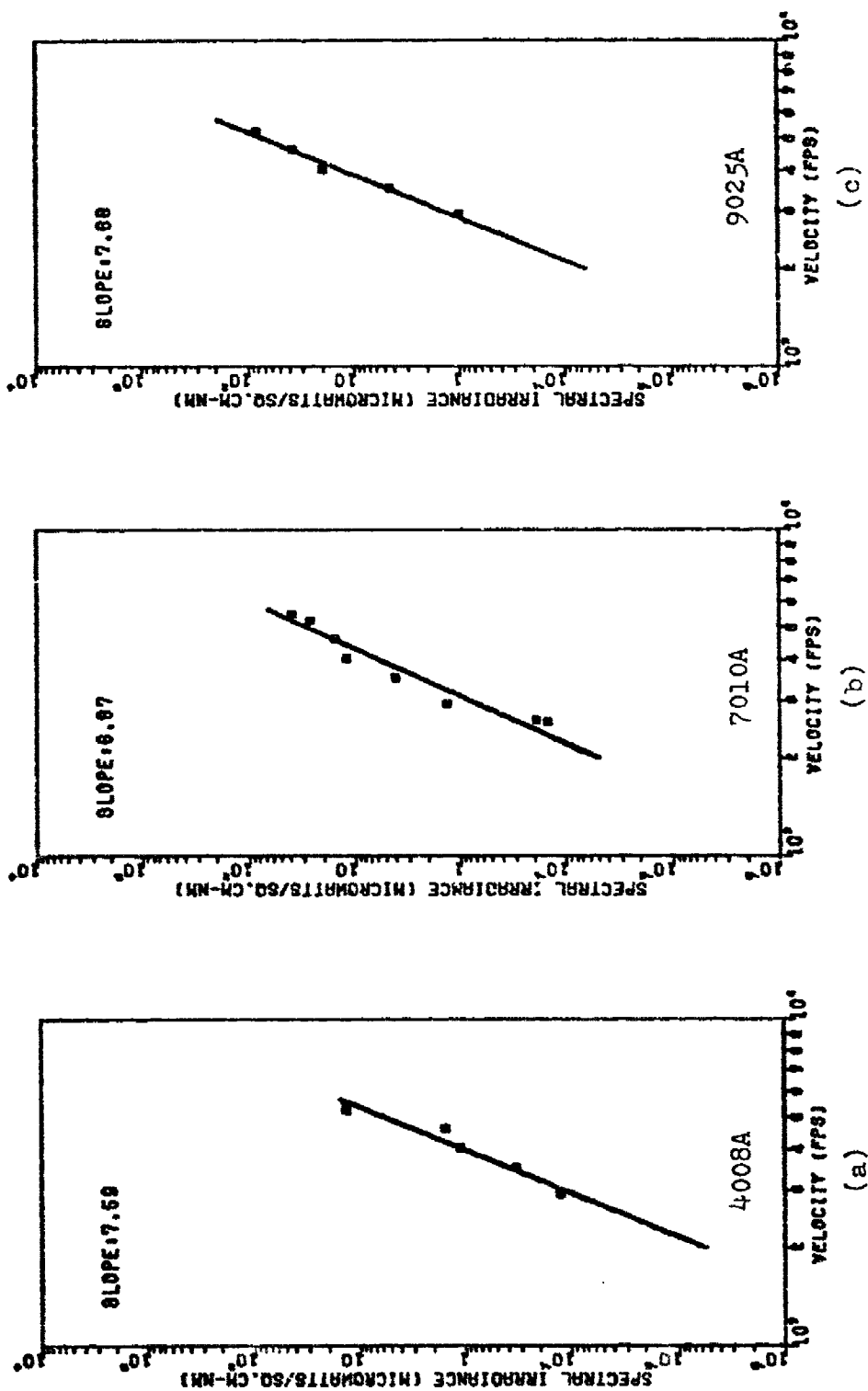| Velocity (FPS)	4008A	7010A	9025A
2584.0	0.0292	0.3064	n
2605.9	0.0228	0.3830	0.1238
2928.3	0.1464	1.3405	1.1148
3493.4	0.4375	4.4045	4.9548
4028.2	1.0160	10.3402	23.7830
4597.7	2.3120	23.2704	66.7022
5256.2	44.6880	129.2380	330.3248
5524.8	53.6256	180.9332	495.4872

n - no data

Figure C-13. Flurocarbon Paint Coated Titanium First Flash Maxima vs Velocity
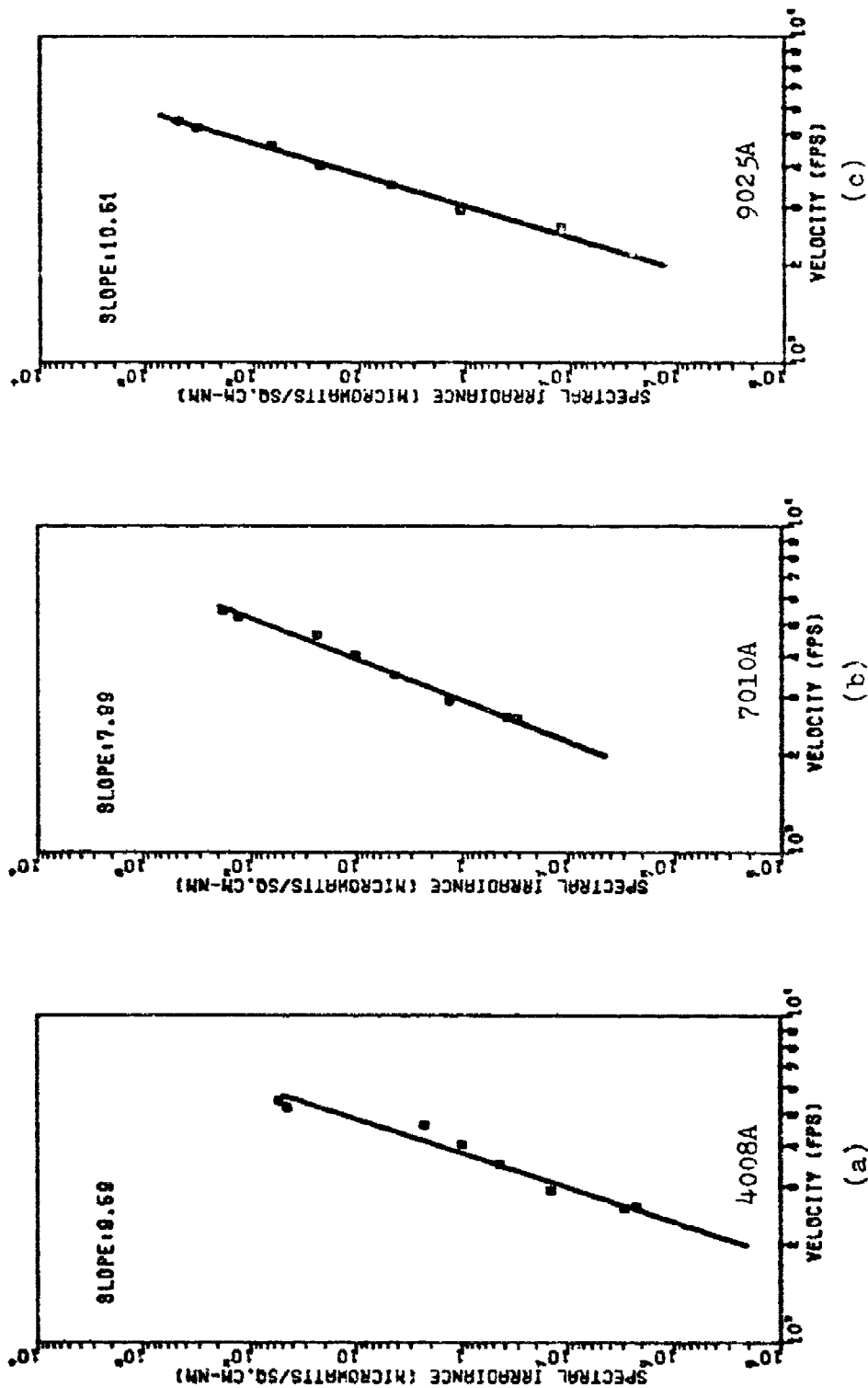(Coating on Up Range Side)

Figure C-14. Flurocarbon Paint Coated Titanium Second Flash Maxima vs Velocity
(Coating on Up Range Side)

109

Table C-IX

Spectral Irradiance for Flurocarbon Paint Coated Titanium Target (Coating on Down Range Side)

First Flash Maxima

Velocity (FPS)	Spectral Irradiance (Microwatts/cm^2-nm)		
	4008A	7010A	9025A
2594.0	0.0732	0.9728	n
2941.2	0.0915	0.4064	1.4864
3490.4	0.2562	1.4732	5.6980
4028.2	0.9144	9.5448	19.8192
4494.4	1.1556	15.5136	n
4842.6	62.5632	51.6952	n
5509.6	107.2512	103.3904	n

Second Flash Maxima

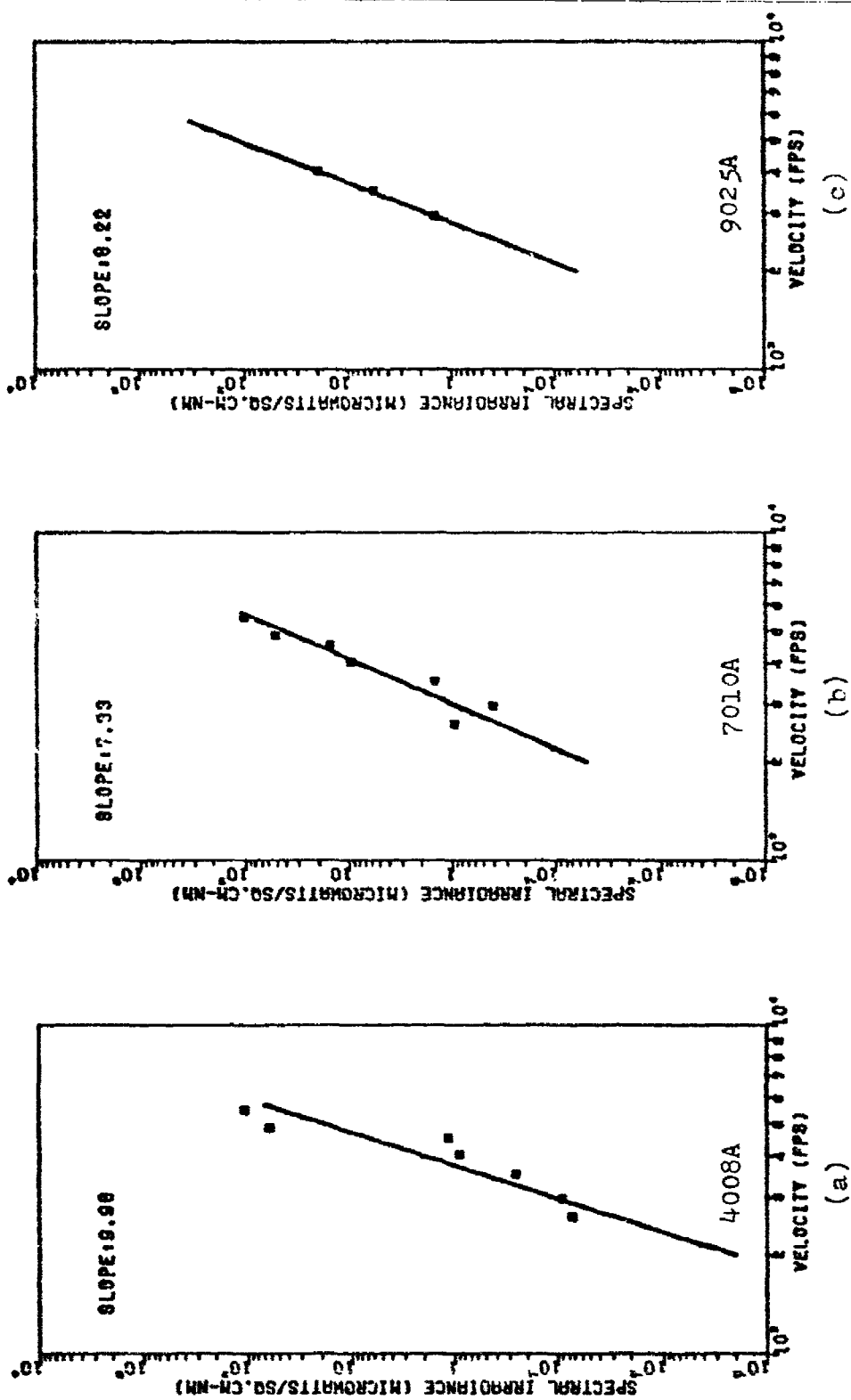|	4008A	7010A	9025A
2594.0	0.0915	0.2794	n
2941.2	0.1098	0.4572	1.6103
3490.4	0.3294	1.4224	6.1935
4028.2	1.8288	17.4788	34.6836
4494.4	6.9336	54.2976	190.5720
4842.6	102.7824	155.0856	578.0684
5509.6	321.7536	413.5616	n

n - no data

Figure C-15. Flurocarbon Paint Coated Titanium First Flash Maxima vs Velocity

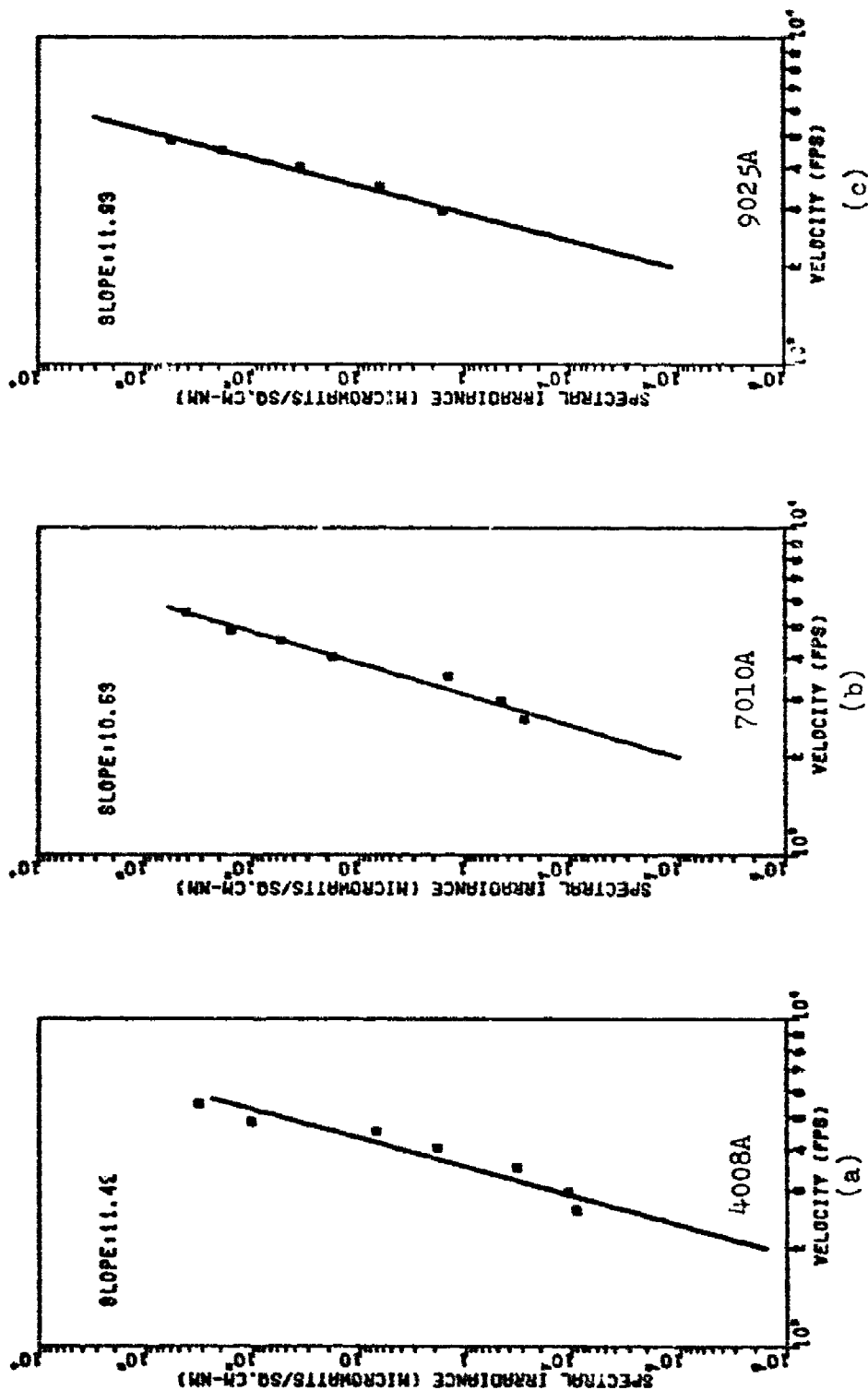(Coating on Down Range Side)

111

Figure C-16. Flurocarbon Paint Coated Titanium Second Flash Maxima vs Velocity

(Coating on Down Range Side)

Table C-X

Flash Energy for Uncoated
Titanium Target Impacts

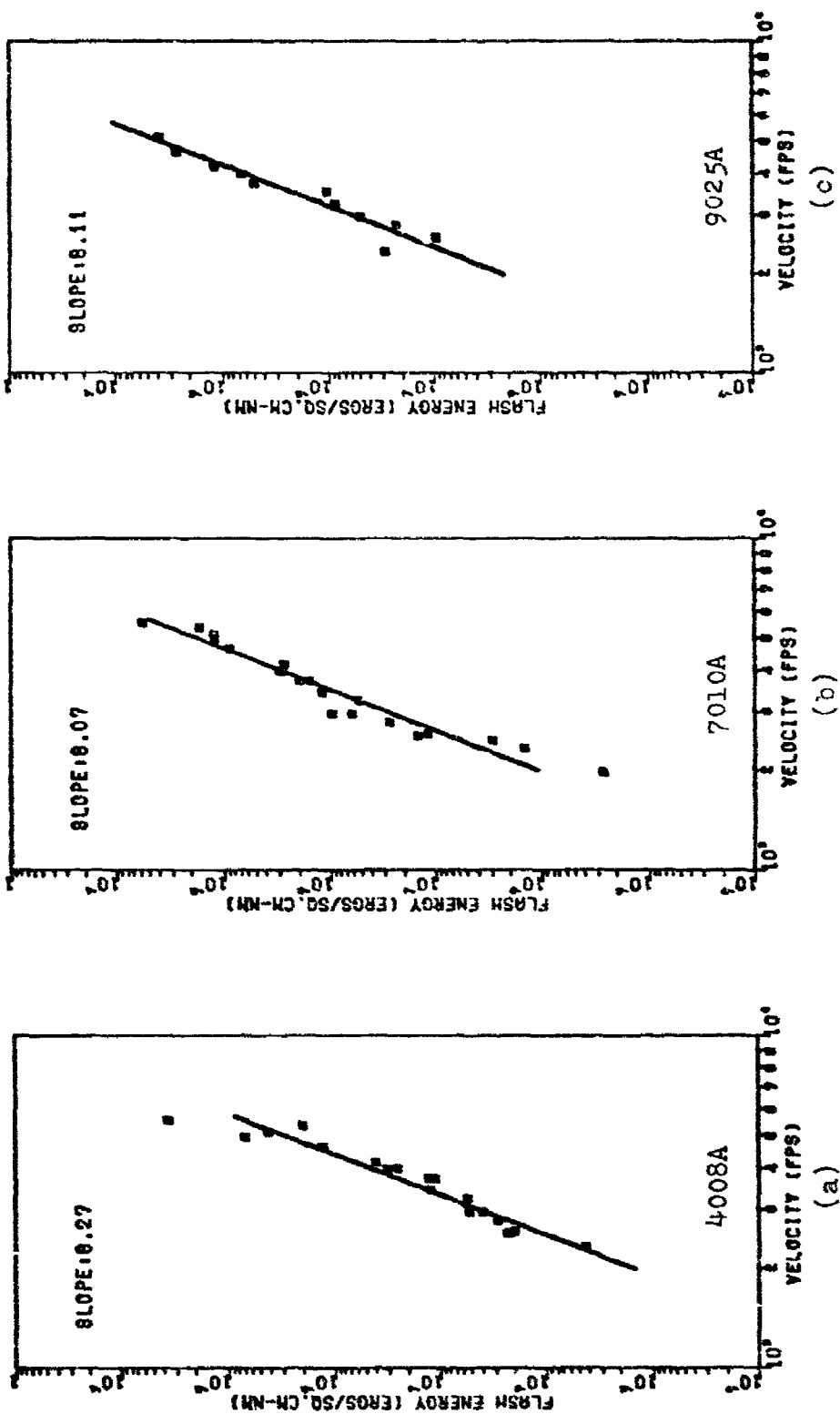| Velocity (FPS)	Total Energy (Ergs/cm^2-nm)		
	4008A	7010A	9025A
1971.4	n	2.68E-6	4.29E-7
2320.2	4.29E-6	1.50E-5	2.91E-4
2466.1	n	3.00E-5	n
2548.0	2.28E-5	1.50E-4	9.70E-5
2564.7	2.00E-5	1.20E-4	9.70E-5
2801.1	2.86E-5	2.70E-4	2.32E-4
2954.2	4.01E-5	9.60E-4	5.04E-4
2956.3	5.29E-5	6.30E-4	n
3246.8	5.43E-5	5.40E-4	8.73E-4
3439.4	1.26E-4	1.20E-3	n
3508.8	n	n	1.04E-3
3707.1	1.27E-4	1.61E-3	5.04E-3
3714.0	1.11E-4	1.98E-3	n
3964.3	2.54E-4	2.85E-3	6.59E-3
4000.0	3.21E-4	3.00E-3	n
4153.7	4.13E-4	2.73E-3	1.16E-2
4618.9	1.28E-3	8.91E-3	2.69E-2
4926.1	7.00E-3	1.22E-2	n
5115.1	4.20E-3	1.21E-2	3.88E-2
5390.8	1.97E-3	1.70E-2	n
5578.8	3.64E-2	5.67E-2	n

n - no data

Figure C-17. Uncoated Titanium Flash Energy vs Velocity

Table C-XI

Flash Energy for Uncoated
Aluminum Target Impacts

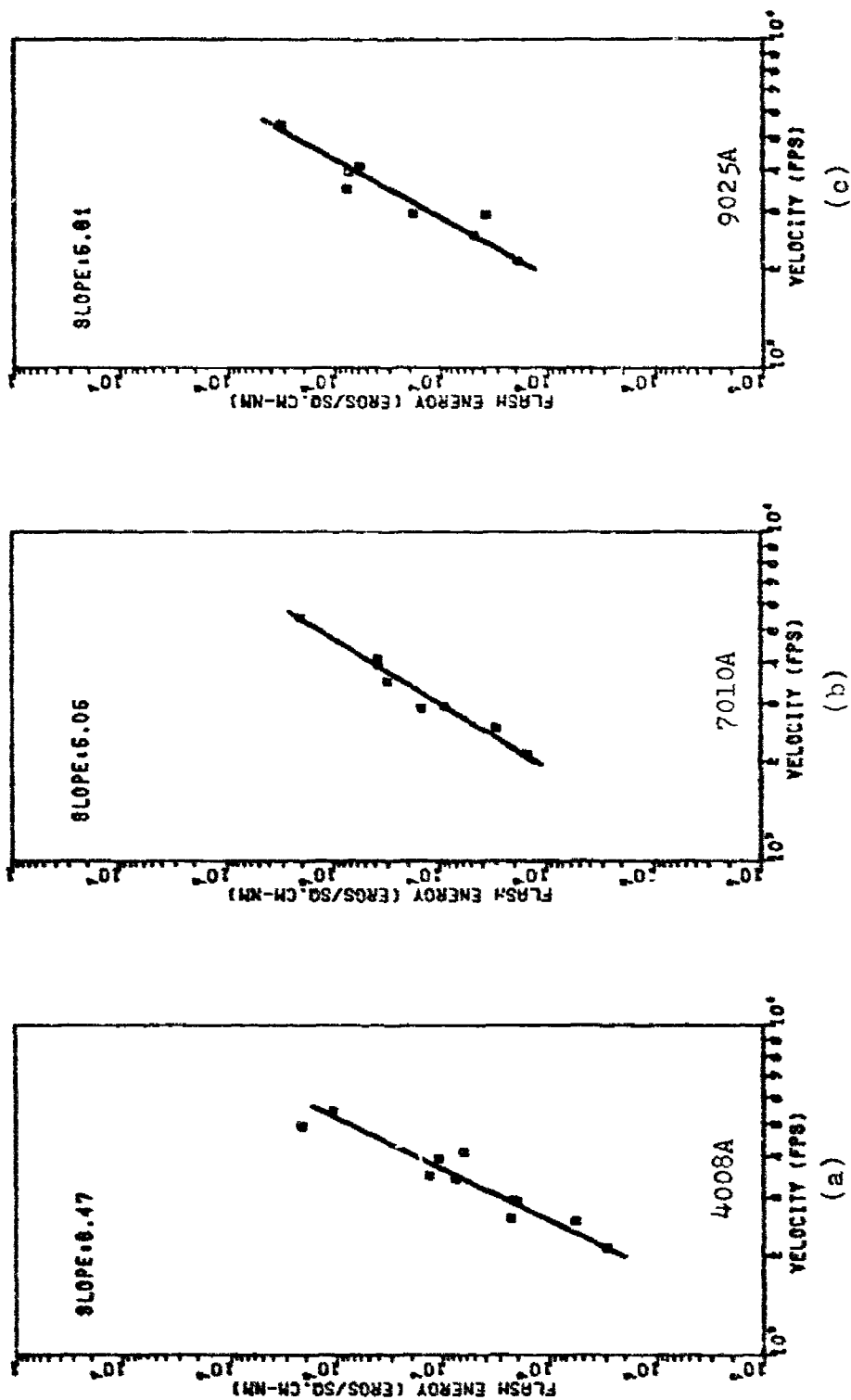| Velocity (FPS)	Total Energy (Ergs/cm^2-nm)		
	4008A	7010A	9025A
2108.2	2.86E-6	1.50E-5	1.94E-5
2536.5	5.70E-6	3.00E-5	4.85E-5
2612.7	2.29E-5	n	n
2911.2	2.00E-5	1.50E-4	3.88E-5
2943.3	2.14E-5	9.00E-5	1.84E-4
3427.6	7.45E-5	n	n
3514.9	1.33E-4	3.10E-4	7.75E-4
3944.8	1.09E-4	3.72E-4	7.35E-4
4140.8	6.30E-5	3.72E-4	5.80E-4
4938.3	2.10E-3	n	n
5464.5	1.05E-3	2.02E-3	3.23E-3

n - no data

Figure C-18. Uncoated Aluminum Flash Energy vs Velocity

Table C-XII

Flash Energy for White Polyurethane Paint Coated Titanium Target Impacts

(Coating on Up Range Side)

Velocity (FPS)	Total Energy (Ergs/cm^2-nm)		
	4008A	7010A	9025A
2151.7	1.15E-6	6.00E-5	n
2585.6	1.55E-5	1.20E-4	n
2943.3	2.00E-5	1.80E-4	9.70E-5
3389.8	5.73E-5	8.40E-4	n
4028.2	1.57E-4	6.69E-3	4.19E-3
4201.7	2.98E-4	2.23E-3	6.98E-3
4629.6	6.38E-4	4.86E-3	1.12E-2
5256.2	5.60E-3	6.06E-3	3.55E-2
5509.5	7.00E-3	1.01E-2	4.84E-2

(Coating on Down Range Side)

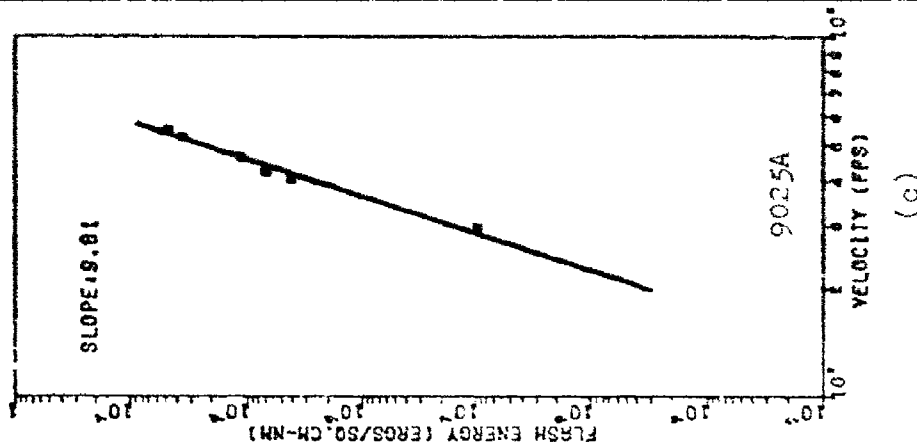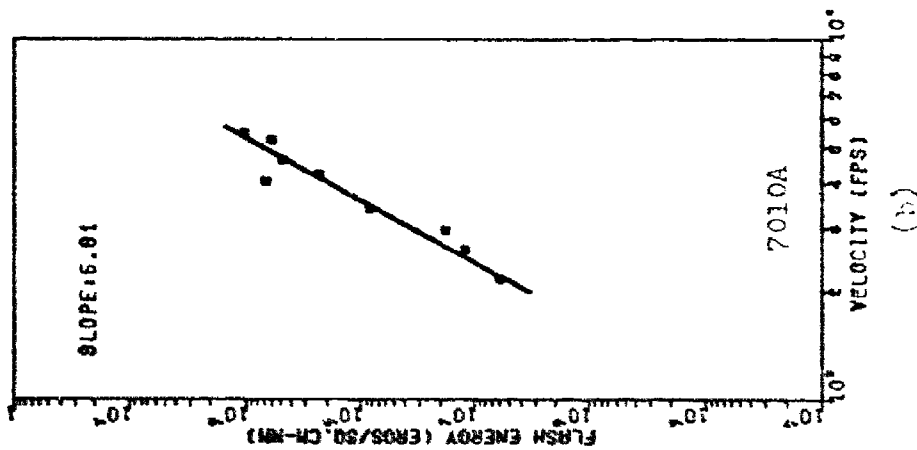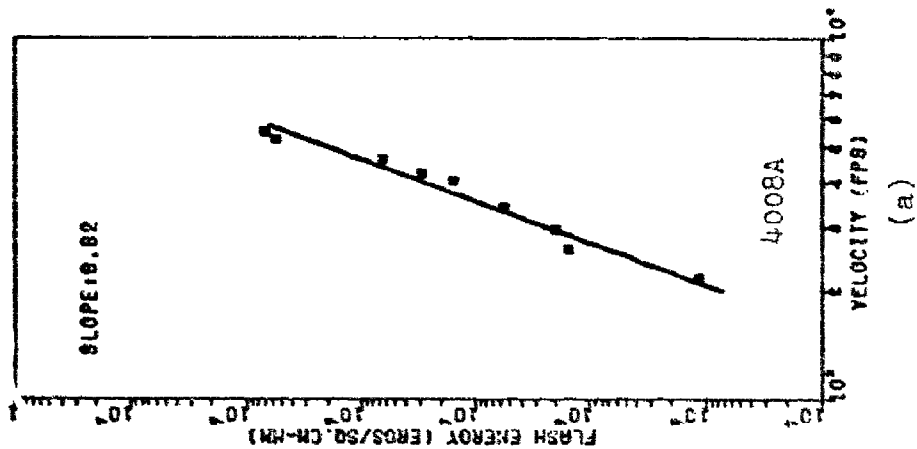| Velocity (FPS)	4008A	7010A	9025A
2580.6	1.86E-5	7.50E-5	1.36E-4
2909.1	2.86E-5	2.10E-4	n
2949.9	9.15E-5	9.00E-4	n
3442.6	1.26E-4	1.38E-3	1.90E-3
3976.1	1.88E-4	2.23E-3	n
4535.1	9.63E-4	n	3.14E-2
4896.0	5.63E-3	1.81E-2	6.46E-2
5449.6	7.00E-3	3.24E-2	1.61E-1

n - no data

Figure C-19.   Polyurethane Paint Coated Titanium Flash Energy vs Velocity
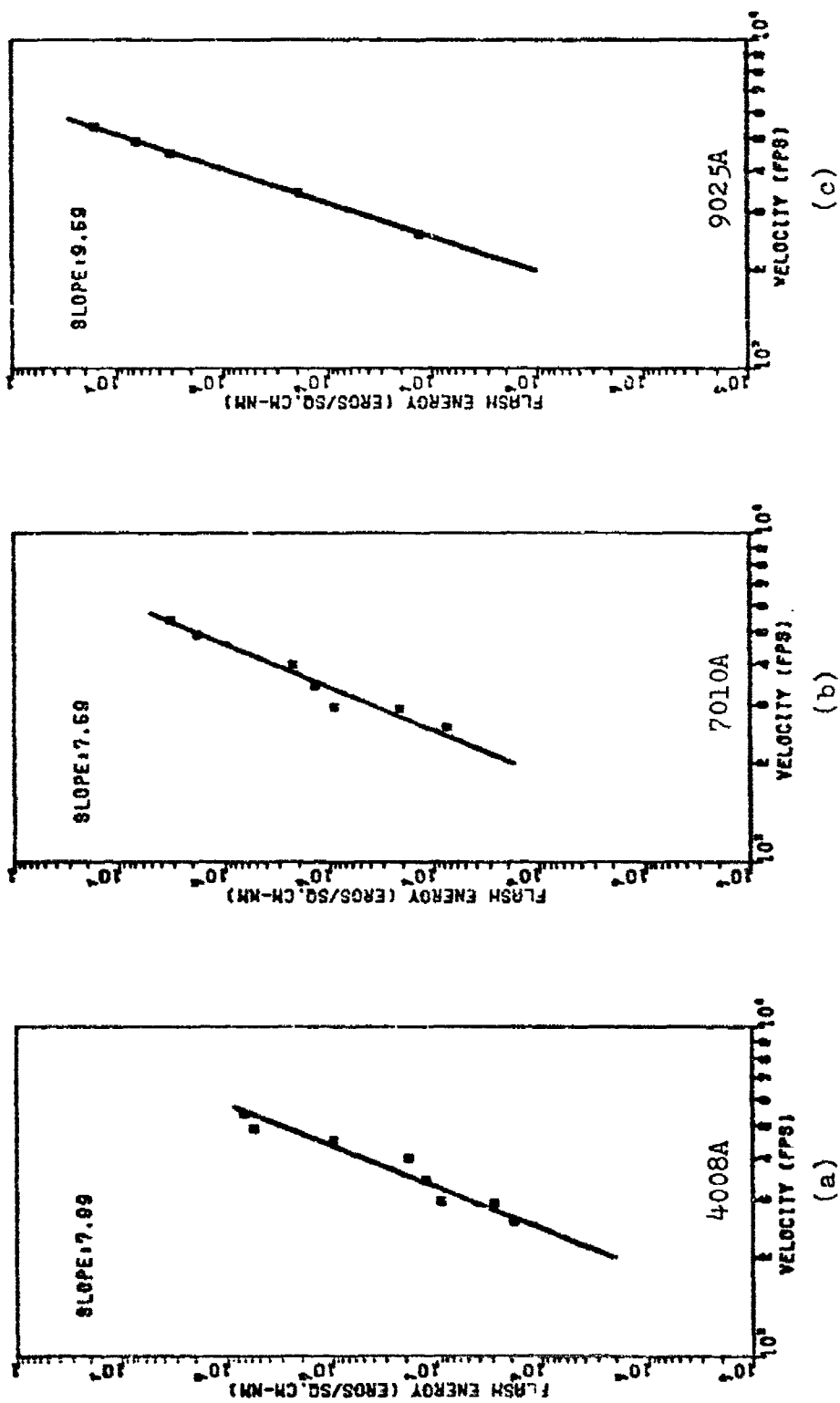
(Coating on Up Range Side)

Figure C-20. Polyurethane Paint Coated Titanium Flash Energy vs Velocity
(Coating on Down Range Side)

Table C-XIII

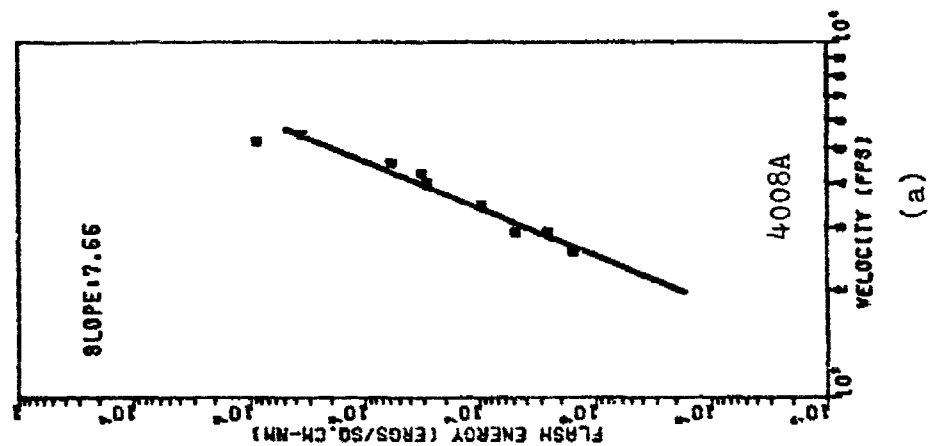### Flash Energy for Barium Titanate Paint Coated Titanium Target Impacts

(Coating on Up Range Side)

Velocity (FPS)	Total Energy (Ergs/cm^2-nm)		
	4008A	7010A	9025A
2560.8	1.57E-5	1.80E-4	5.83E-5
2902.8	2.57E-5	2.70E-4	n
2932.6	4.86E-5	3.90E-4	2.91E-4
3454.2	9.74E-5	1.26E-3	1.70E-3
3988.0	2.82E-4	2.23E-3	n
4028.2	2.83E-4	1.98E-3	n
4241.8	3.14E-4	2.85E-3	1.06E-2
4592.4	5.74E-4	4.45E-3	9.71E-3
5263.2	8.40E-3	8.08E-3	4.19E-2
5509.6	3.50E-3	1.41E-2	3.87E-2

(Coating on Down Range Side)

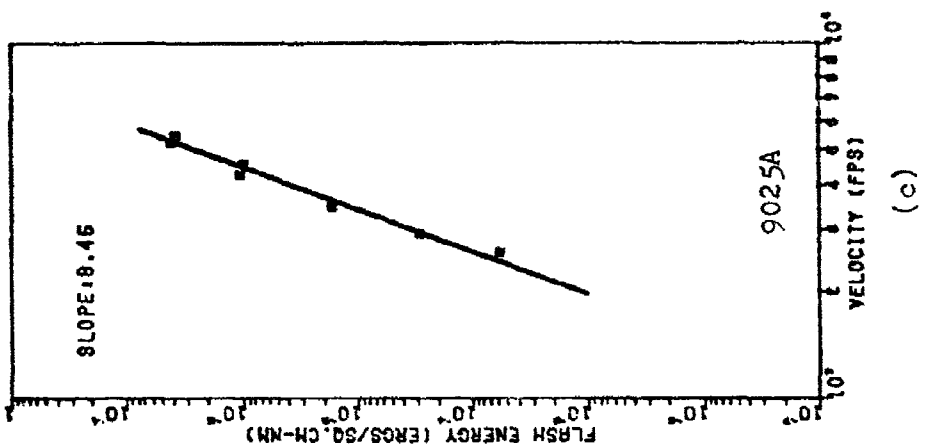| Velocity (FPS)	4008A	7010A	9025A
2594.0	1.57E-5	1.35E-4	1.55E-4
2960.8	8.00E-5	5.70E-4	6.59E-4
3445.3	2.06E-4	1.86E-3	2.52E-3
4008.0	2.35E-4	2.48E-3	5.62E-3
4514.7	7.66E-4	6.88E-3	3.14E-2
4842.6	4.90E-3	1.41E-2	5.16E-2
5464.4	2.52E-2	4.45E-2	1.55E-1

n - no data
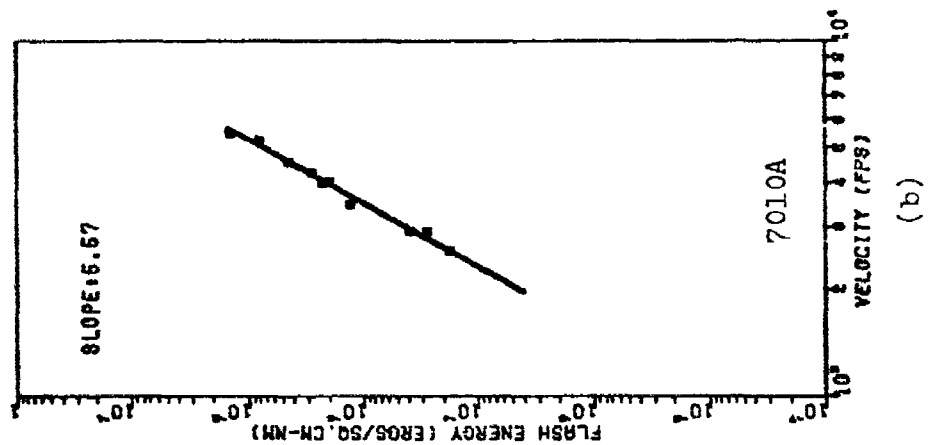
Figure C-21. Barium Titanate Silicone Paint Coated Titanium Flash Energy vs Velocity
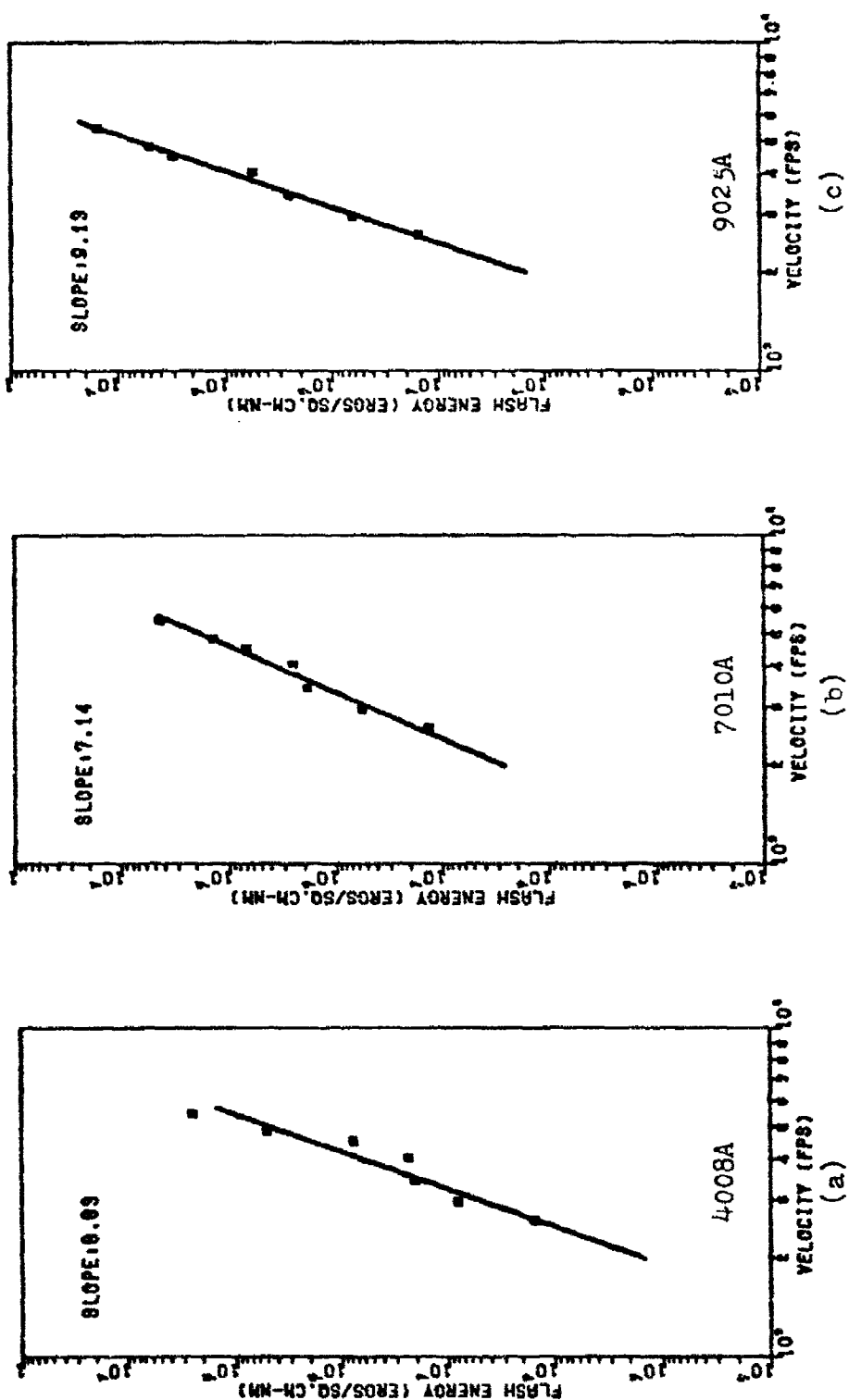(Coating on Up Range Side)

Figure C-22. Barium Titanate Silicone Paint Coated Titanium Flash Energy vs Velocity
(Coating on Down Range Side)

122

Table C-XIV

Flash Energy for Flurocarbon Paint Coated Titanium Target Impacts

(Coating on Up Range Side)

Velocity (FPS)	Total Energy (Ergs/cm^2-nm)		
	4008A	7010A	9025A
2584.0	9.16E-6	8.40E-5	n
2928.3	4.57E-5	1.50E-4	1.94E-4
3493.4	1.17E-4	1.08E-3	1.35E-3
4028.2	3.92E-4	3.22E-4	7.76E-3
4597.7	2.55E-4	2.83E-3	1.49E-2
5256.2	4.90E-3	1.41E-2	2.90E-2
5524.8	4.20E-3	1.41E-2	5.49E-2

(Coating on Down Range Side)

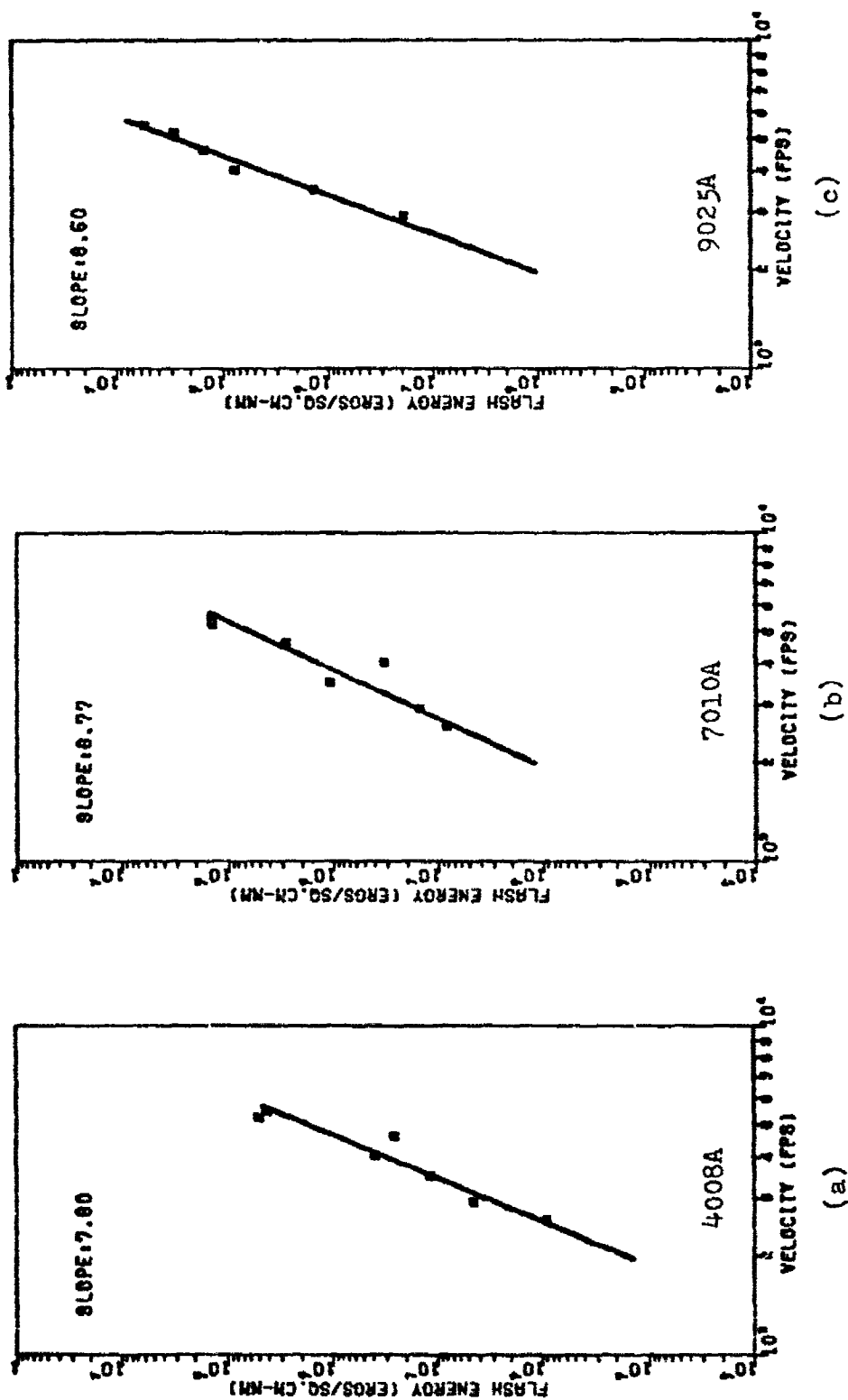| Velocity (FPS)	4008A	7010A	9025A
2941.2	6.57E-5	5.10E-4	5.04E-4
3490.4	8.58E-5	1.32E-3	1.41E-3
4028.2	2.82E-4	3.22E-3	6.01E-3
4494.4	7.01E-4	8.10E-3	2.98E-2
4842.6	1.05E-2	1.61E-2	9.69E-2
5509.6	4.76E-2	6.07E-2	n

n - no data

Figure C-23. Flurocarbon Paint Coated Titanium Flash Energy vs Velocity

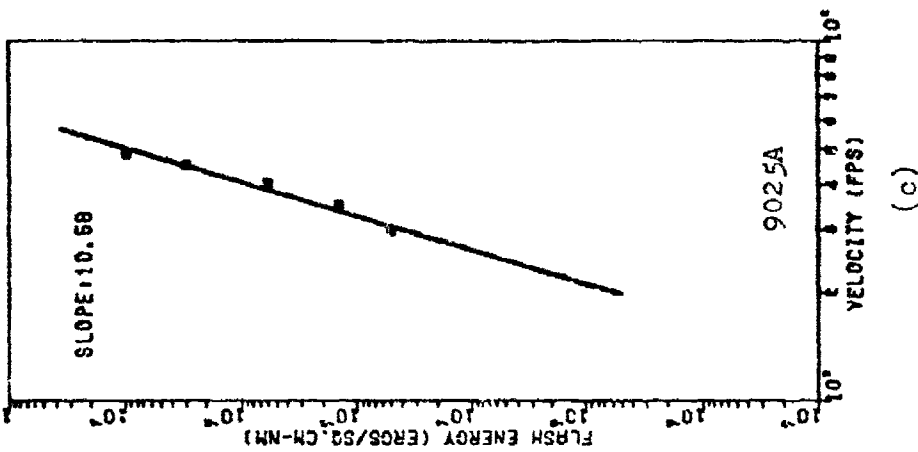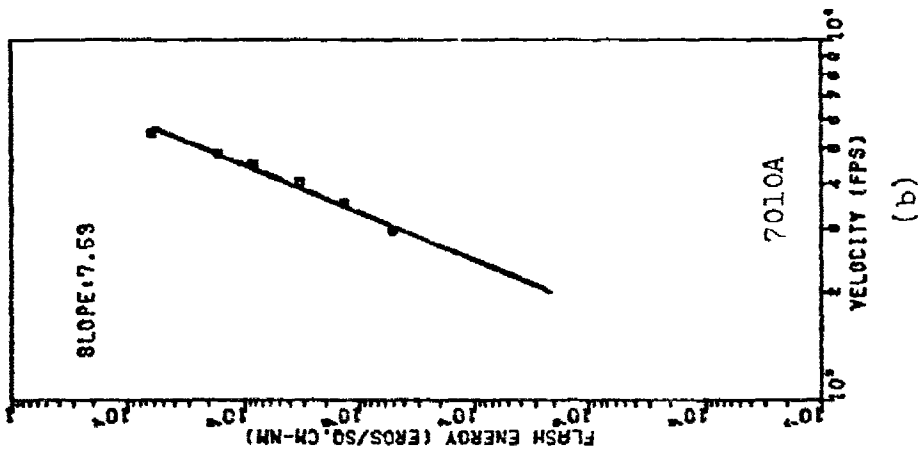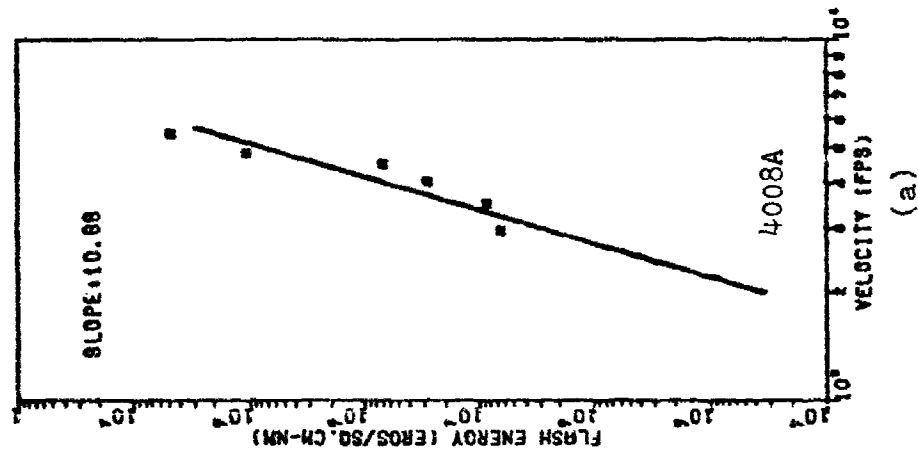(Coating on Up Range Side)

124

Figure C-24. Flurocarbon Paint Coated Titanium Flash Energy vs Velocity
(Coating on Down Range Side)

125

VITA

Joseph Gonzalo Aja was born on 6 January 1945 in Montpilier, Vermont. He attended Northeastern University where he was elected to membership in Phi Tau Sigma National Honorary Mechanical Engineering Fraternity. In June 1968, he received the degree of Bachelor of Science in Mechanical Engineering. Upon graduation, he was employed as a design engineer for the General Electric Company's Avionic Design Division, Binghamton, New York until he enlisted in the United States Air Force in December 1968. He attended Officer Training School and was commissioned in June 1969. He served as a Weapons Loading Officer at Cam Ranh Bay AB, RVN and as Officer in Charge of the Weapons Loading Section at Phu Cat AB, RVN. After he received his Explosive Ordnance Disposal (EOD) Badge in September 1971, he served as Officer in Charge of an EOD Team until entering the School of Engineering, Air Force Institute of Technology, in June 1974, majoring in the Air Weapons Option in Aeronautical Engineering.

> Permanent Address: 16 Railroad Street
> Essex Junction, Vermont 05452